A Thesis for the Degree of Doctor of Philosophy

Implication of Arginine Deiminase Pathway in Pathogenesis and a Novel Phage Infection Mechanism in *Salmonella enterica* serovar Typhimurium

Salmonella enterica serovar Typhimurium에서의 Arginine Deiminase Pathway의 병원성 조절과 새로운 박테리오파지 감염 기작 연구

February 2013

Younho Choi

Department of Agricultural Biotechnology

College of Agriculture and Life Science

Seoul National University

농학박사학위논문

Implication of Arginine Deiminase Pathway in Pathogenesis and a Novel Phage Infection Mechanism in *Salmonella enterica* serovar Typhimurium

Salmonella enterica serovar Typhimurium에서의 Arginine deiminase pathway의 병원성 조절과 새로운 박테리오파지 감염 기작 연구

지도교수 유 상 렬

이 논문을 박사학위논문으로 제출함

2013년 2월

서울대학교 대학원
농생명공학부
최 윤 호

최윤호의 박사학위논문을 인준함

2013년 2월

위원장	최 상 호 (인)
부위원장	유 상 렬 (인)
위 원	강 동 현 (인)
위 원	신 동 우 (인)
위 원	이 주 훈 (인)

ABSTRACT

Younho Choi
Department of Agricultural Biotechnology
The Graduate School
Seoul National University

Salmonella is responsible for a wide variety of cases of food-borne illness and typhoid fever in human. Various virulence factors and their regulation mechanisms have been identified in *Salmonella*, but the function and mammalian targets of only a few are known. I found a new gene cluster related to the virulence of *Salmonella enterica* serovar Typhimurium (*S.* Typhimurium) by comparative analysis. Arginine deiminase (ADI), ornithine carbamoyltransferase (OTC), and carbamate kinase (CK) constitute the ADI system. In addition to metabolic functions, the ADI system has been implicated in virulence of certain pathogens. To study on the ADI pathway, I determined the regulation of gene expression and the role of ADI in the *Salmonella* virulence.

S. Typhimurium possesses the *STM4467*, *STM4466*, and *STM4465* genes, which are predicted to encode ADI, CK, and OTC, respectively. There are also two genes in the downstream of ADI: *STM4464* encoding arginine

transporter and *STM4463* encoding arginine regulator. PCR revealed that ADI operon consists of 4 genes from *STM4467* to *STM4464* and *STM4463* is transcribed separately. PE analysis presented that there are two transcription initiation sites in the promoter of ADI. Among two regions, upper promoter was identified to be a regulatory region for ADI expression. Moreover, in the promoter region, I found a CRP-binding site and revealed the direct interaction between CRP and upper promoter region by gel shift assay. In the transcriptional analysis, three conditions, anaerobicity, polyamine, and the addition of L-arginine as a substrate for ADI, increased the expression. I also determined that a regulatory protein encoded by the *STM4463* gene functions as an activator for *STM4467* expression. The regulation of ADI by STM4463 was dependent on CRP. Interestingly, the expression of *STM4463* showed almost same pattern with *STM4467* suggesting that *STM4463* is a signal transducer and directly regulates the expression of ADI. In the regulation of *STM4463*, CRP also works by binding to the promoter of *STM4463*. A DNA-binding protein, Fis regulates *STM4463* negatively and this regulation is connected to the ADI expression. Moreover, a global regulator, ArcA positively regulates *STM4463* in anaerobic condition using polyamines as a signal.

Here, I also report that ADI activity plays a role for *S*. Typhimurium to

successfully infect a mammalian host. An *STM4467* deletion mutant was defective for replication inside murine macrophages and attenuated for virulence in mice. Expression of the ADI pathway genes was enhanced inside macrophages in a process that required STM4463. Lack of STM4463 impaired the ability of *S*. Typhimurium to replicate within macrophages. A mutant defective in the *STM4467*-encoded ADI displayed normal production of nitric oxide by macrophages.

A novel flagellatropic phage, iEPS5, infecting *Salmonella* was isolated and characterized. iEPS5 has an icosahedral head and a long, non-contractile tail with tail fiber, and specific for *S.* Typhimurium. Genome sequencing revealed a linear double-strand DNA of 59,254 bps with 75 ORFs. To identify the receptor for iEPS5, transposon insertion mutants of *S*. Typhimurium SL1344 resistant to the phage were isolated and all of the resistant mutants were found to have mutations in the genes involved in the flagellar formation, suggesting that the flagellum is an adsorption target of the phage. Analysis of phage infection against the *motA* mutant, which is flagellated but non-motile, showed a requirement of flagellar rotation for iEPS5 infection.

Further analysis of phage infection against the chemotaxis gene mutants (*ΔcheY*, SJW2811, and SJW3076) revealed that iEPS5 could infect host

bacteria having flagella rotating CCW more efficiently. The polyhook strain (*ΔfliK*) was resistant to iEPS5 both in plaque and adsorption analysis implying that the flagellar filament itself is essential for phage infection. Finally, fluorescently labeled phage and its gene transfer provide insight into mechanisms of infection: iEPS5 actively interacts with the flagellum and subsequently injects its DNA into the flagellar filament.

Key words: *Salmonella* Typhimurium, Arginine deiminase pathway, virulence, bacteriophage, receptor, flagella, and phage biocontrol

Student Number: 2007-21394

CONTENTS

LIST OF FIGURES

LIST OF TABLES

General introduction

Salmonella enterica serovar Typhimurium

Salmonella is one of the most extensively studied bacterial pathogens in terms of its physiology, genetics, cell structure, and development. The bacterial genus *Salmonella* was named following the discovery of this pathogen by the United States Department of Agriculture (USDA) veterinary bacteriologist Dr. Daniel E. Salmon. This microorganism is a Gram-negative, motile, rod-shaped, and non-spore forming bacterium belonging to the *Enterobacteriaceae* family and is capable of infecting a wide range of animals resulting in several symptoms (salmonellosis, an infection with *Salmonella*) of disease including enteric fever, bacteremia, enterocolitis, and focal infection. The current classification of *Salmonella* is complex: based on the DNA-DNA hybridization the genus *Salmonella* is divided into two species: *Salmonella enterica* and *Salmonella bongori*. *S. enterica* can be subdivided into the six subspecies (*enterica*, *salamae*, *arizonae*, *diarizonae*, *houtenae*, and *indica*) based on biochemical differences (27) and more than 2,500 serovars (serotypes) using the Kauffman and White Scheme (60). *S. enterica* subspecies *enterica* is mainly associated with infection of warm

blooded animals, while the other subspecies and *S. bongori* rarely cause infection in these animals (107, 162). It is generally accepted that there is a single species of *Salmonella* (*S. enterica*) and most investigators continue to designate "*S.* Typhimurium" rather than "*S. enterica* serovar Typhimurium" for a convenience. Thus, in this study, the *Salmonella* serotypes are referred to by their "species" name.

According to host specificities and disease manifestation, there are two serotypes. Firstly, *S.* Typhi and *S.* Paratyphi are exclusively human pathogens causing typhoid fever. Typhoid fever is a protracted systemic illness including fever, abdominal pain, transient diarrhea, or constipation. The pathological hallmark is mononuclear cell infiltration and hypertrophy of the reticuloendothelial system including the intestinal Peyer's patches, mesenteric lymph nodes (MLNs), spleen, and bone marrow. Without treatment, mortality is 10-15%. On the other side of the spectrum, non-typhoidal *Salmonella* strains, such as *S.* Typhimurium and *S.* Enteritidis have broad host range including poultry, cattle, and pigs and usually cause self-limited gastroenteritis: abdominal pain, vomiting, and inflammatory diarrhea in humans. *S.* Typhimurium also gives rise to the systemic disease in susceptible mouse strains similar to that of human *S.* Typhi infections (9, 149). Therefore, murine typhoid is widely accepted as an animal model for human typhoid fever (33, 68).

Typhoid fevers are most common in the developing world; the highest incidence of typhoid is found in Southeast and Central Asia where it is endemic, and is a frequent disease in Africa, the Middle East. As of the year 2000, there were an estimated 22 million cases globally of typhoid fever each year, and roughly 10% of these cases were fatal. Estimates for numbers of non-typhoidal salmonellosis (NTS) cases worldwide vastly exceed those for enteric fevers. Every year, approximately 42,000 cases of NTS are reported in the United States (Centers for Disease Control and Prevention, 2012). Because many milder cases are not diagnosed or reported, the actual number of infections may be twenty-nine or more times greater. In Korea, the case of food poisoning of pathogenic bacteria has been increased and the scale of incidence was also increasing because of the increased group food service and deterioration of the public health infrastructures (KFDA reports).

Salmonella grows between 8°C and 45°C and pH 4-8. It is highly resistant towards dehydration in the environment and thus can survive in soil and water for a long period of time. Animals that are known to carry *Salmonella* include poultry, swine, cattle, rodents, and pets. Human with mild and unrecognized cases are carriers as well. In the environment, *Salmonella* also exists in feces and contaminated food, which is the primary source of human infections, either directly or indirectly. Food sources that are known

to spread *Salmonella* include: contaminated raw and undercooked eggs/egg products, raw milk/milk products, meat, poultry products, contaminated water, and raw fruits and vegetables (112, 175, 201). Most people infected with *Salmonella* develop diarrhea, fever, and abdominal cramps 12 to 74 h after infection. The illness usually lasts 4 to 7 days and most persons recover without treatment. However, in some persons, the diarrhea may be so severe that the patient needs to be hospitalized.

Salmonella food poisoning treatment includes: Antibiotics in moderate to severe cases of *Salmonella* food poisoning, or when it occurs in a person who is at risk for complications, such as people with weakened immune systems due to such conditions as HIV/AIDS, cancer, diabetes, or taking steroid medications or undergoing chemotherapy. Avoiding solid food until symptoms subside. Drinking plenty of fluids to prevent dehydration: fluids include water or an oral rehydrating fluid. Hospitalization and rehydration with intravenous fluids would be required, if *Salmonella* food poisoning does not resolve quickly or lead to dehydration or other complications.

Salmonella pathogenesis and its virulence mechanisms

S. Typhimurium thrives in a variety of locations, including the gastrointestinal tract and the intracellular milieu of eukaryotic cells. About 10^5 to 10^6 bacteria are estimated to be required for the initial infection (22), but the exact amount needed varies with the strain and the physiological state of the host (32, 37). During the early stages of infection, *S*. Typhimurium should survive the acid barrier of the stomach to reach small intestine. *S*. Typhimurium has an adaptive acid-tolerance response that might promote their survival in the low pH milieu of the stomach (73).

After passage through the upper gastrointestinal tract, *Salmonella* traverse the intestinal mucous layer before encountering and evade being killed by digestive enzymes, bile salts, secretory IgA, antimicrobial peptides, and other innate immune defenses in order to gain access to the underlying epithelium (138, 180). *S*. Typhimurium has the ability to invade the non-phagocytic enterocytes of the intestinal epithelium, preferentially microfold (M) cell in the Peyer's patches by a morphologically distinct process termed bacterial-mediated active endocytosis (69, 105). Shortly after bacteria adhere to the apical epithelial surface, profound cytoskeletal rearrangements occur in the host cell. Bacterial-mediated endocytosis requires coordinated synthesis of multiple bacterial proteins. Once the

epithelial barrier has been breached, *S*. Typhimurium can across the intestinal epithelium and encounters another obstacle, the submucosal macrophage. *S*. Typhimurium enters intestinal macrophages by inducing macropinocytosis and subsequently activates virulence mechanisms that allow evasion of the microbicidal functions of the phagocyte allowing survival and replication in the intracellular environment (10). Migration of infected phagocytes to other organs of the reticuloendothelial system facilitates dissemination of bacteria in the host.

After *Salmonella* has been taken up by macrophages, it does not enter into the cytoplasm but resides inside the phagosomal vacuole. In the phagosome, *Salmonella* has to be able to cope with environmental changes such as rapid decrease in pH and nutritional deprivation that are restrictive for the growth of bacteria. In addition, phagosomes containing ingested particles usually enter the degradative pathway of the cells. After fusion with lysosomes to form a phagolysosome, engulfed *Salmonella* will encounter toxic substances such as hydrolytic enzymes (protease, lysozyme), small cationic proteins (defensins), and enzymes that produce reactive forms of oxygen to cause the oxidative burst, as well as reactive nitrogen intermediates (NO□, NO^{2-}, NO^{3-}). Adapting to the nutrient limitation encountered within the phagosome requires induction of multiple biosynthetic genes necessary for de novo synthesis of essential

metabolites, including aromatic amino acids and purines. Therefore, *Salmonella* activates various virulence mechanisms in order to survive and replicate (15, 140, 152, 199).

Studies performed by various groups have established that the function of a large number of virulence genes is required for the successful pathogenesis of *Salmonella* infections. Many of these virulence genes have defensive functions: protection of *Salmonella* against defense mechanisms of the innate and adaptive immune system of the infected host. However, recent studies revealed that *Salmonella* has developed two complex virulence functions to actively interact with the host and to modify host cell functions (78). Therefore, two interactions during infection: invasion into non-phagocytic cells and the intracellular survival within phagocytes had been hallmarks of *Salmonella* pathogenesis.

A specialized apparatus, named the type III secretion system (T3SS), is essential to *Salmonella* pathogenesis and the colonization of host tissues. The T3SS mediates the transfer of bacterial virulence proteins, known as effectors, from the bacterial cell into the host-cell cytoplasm. *Salmonella* encodes two distinct virulence-associated T3SSs within *Salmonella* pathogenicity islands 1 and 2 (SPI1 and SPI2) that function at different times during infection (197). Whereas the SPI1-encoded T3SS is active on contact with the host cell and translocates bacterial proteins across the

plasma membrane (178), the SPI2 T3SS is expressed within the phagosome and translocate effectors across the vacuolar membrane. The SPI1 system has been shown to be required for invasion of non-phagocytic cells, induction of intestinal inflammatory responses and diarrhea, as well as colonization of the intestine. The SPI1 T3SS apparatus is also required to kill the M cells that sample antigens and occlude access to gut-associated lymphoid tissue (105). The SPI2 T3SS, by contrast, confers an important role in bacterial survival in the macrophages and is required for establishment of systemic disease in the mouse infection model (53, 83, 111). The genetic locus of SPI2 comprises 40 genes, of which 25 have been shown to contribute to the intracellular phenotypes. Mutants deficient in the SPI2 T3SS cannot replicate efficiently in tissue-culture cells and are highly attenuated in animal models of infection. Current hypotheses for the function of the SPI2 T3SS propose the promotion of intracellular replication by altering host vesicular trafficking, so that useful metabolic molecules, such as amino acids and lipids, are routed to the SCV and the vesicular compartment membrane is expanded (28-30, 65, 165). Induction of SPI2 genes depends on a two-component regulatory system, SsrA/SsrB, encoded within the SPI2 region (74, 194). Expression of SsrAB is also mediated by two-component regulatory systems, OmpR/EnvZ and PhoP/PhoQ, which sense osmotic stress and cation limitation, respectively (116, 137, 208).

Salmonella has evolved these two elaborate virulence systems for different kinds of interactions with eukaryotic cells. However, the strategy by which *Salmonella* modifies the host cells to survive and cause symptoms is not yet fully understood. Despite this wealth of information, the known effector repertoire of the host-pathogen interactions is incomplete; therefore many reports place an emphasis on discovery of new effectors by using highly advanced technologies.

Bacteriophage

Bacteriophages (phages) are viruses that specifically infect bacteria. They are like complex spaceships, each carrying its genome from one susceptible bacterial cell to another in which it can direct the production of more phages. As such, their basic life cycle involves cooption of cellular metabolism toward production of new virus particles, release of those particles from their cellular confines, and then acquisition of new host bacterial cells (96, 98, 120). Phages, like all viruses, are absolute parasites. Although they carry all the information to direct their own reproduction in an appropriate host, they have no machinery for generating energy and no ribosomes for making proteins.

Phages are thought to be the most abundant "organisms" in Earth's biosphere (about 10^{31} phages on earth) (4). They are widespread in nature and universally observed in very large numbers wherever their hosts live - open and coastal waters, marine sediments, terrestrial ecosystems such as soil, and the bodies of humans, animals, and insect (3, 14, 20, 26). Even, it is thought that for each individual bacterial cell there are 10 bacteriophage particles (183). Their high level of specificity, long-term survivability, and ability to reproduce rapidly in appropriate hosts contribute to their maintenance of a dynamic balance among the wide variety of bacterial species in any natural ecosystem (1, 104).

The International Committee on Taxonomy of Viruses (ICTV) classifies phages into 1 order, 13 families, and 31 genera according to their morphological characteristics, types of nucleic acid, and presence or absence of envelope or lipid. Most of reported phages are 'tailed phages', which are composed of an icosahedral head and tail. All those tailed phage have linear double-stranded DNA (dsDNA) as genome (3). These phages are also classified into three families according to the morphological features of the tail: *Myoviridae* (contractile tails consisting of a sheath and a central tube, e.g. T4), *Siphoviridae* (long non-contractile tails, e.g. λ), and *Podoviridae* (extremely short non-contractile tails, e.g. T7) (5, 136, 186).

Upon infection of the bacterial host, different phages can have quite different fates. Some phages follow the lytic infection cycle (or lytic pathway) whereby they multiply in the bacterial cell and lyse the cell wall caused by the endolysin-holin system or the single lytic factor at the end of the cycle to release newly formed phage particles (67). A typical lytic bacteriophage will produce 100-300 new phage particles from an infected bacterial cell in a matter of times (132). On the other way, some phages may use the lysogenic pathway where the phage genome will integrate as part of the host genome, replicate as part of the host genome and stay in a dormant state as a prophage for extended periods of time. If the host bacteria encounter adverse environmental conditions, the prophage may become activated and turn on the lytic cycle at the end of which the newly formed phage particles will lyse the host cell. In both life cycles, the ability of the phages to kill bacteria at the end of the infectious cycle is the cornerstone of the idea using phages as therapeutic agents (132, 183).

Bacteriophage therapy for bacterial infection is a concept with an extensive but controversial history. Phages have been explored as means to eliminate pathogens like *Campylobacter* in raw food and *Listeria* in fresh food or to reduce food spoilage bacteria. In agricultural practice phages were also used to control pathogens like *Escherichia* and *Salmonella* in farm animal, *Vibrio* and *Lactococcus* in fish from aquaculture and *Erwinia* in

plants. However, the oldest use was in human medicine. After discovery of bacteriophage particles that seems to 'eat bacteria' by Twort (196) and d'Herelle (46) in the early 20th century, the therapeutic potential of phages was recognizes and applied for several decades before the discovery and widespread adoption of antibiotics (189). Phages were used against diarrheal diseases caused by *E. coli*, *Shigella,* or *Vibrio* and against wound infections caused by facultative pathogens like *staphylococci* and *streptococci* in human medicine. However, mixed therapeutic results, poor understanding of phage biology, and the advent of broad-spectrum antibiotics led to the decline of phage therapy in the Western world (86, 189). There has been a recent resurgence of interest into bacteriophages as an alternative antimicrobial treatment owing to the increasing incidence of antibiotic resistance and virulent bacterial pathogen. The reintroduction of phage therapy into modern-day Western medicine faces numerous hurdles including skepticism about the prior phage therapy studies, strict regulatory constrains placed on new clinical therapeutics, limited phage host ranges, the evolution of bacterial resistance to phages, manufacturing challenges, systemic side effects of phage therapy, and delivery (114, 190).

Objectives of this study

Salmonella is a leading cause of bacterial gastroenteritis and systemic infection. The increasing numbers of infection with *Salmonella* and the rapid growth in antimicrobial resistance have become a global problem. Thus, the development of efficient controlling methods and antimicrobial therapy to control *Salmonella* is crucial to address current issues in public health. These studies were performed to provide molecular-based information in the *Salmonella* pathogenesis and to elucidate a novel phage infection mechanism, which can be applied for controlling of *Salmonella* as follows:

Discovery of new target gene for *Salmonella* virulence and characterization of its function and regulation.

A comparative analysis has discovered a possible gene related to *Salmonella* infection. Several experiments identified the function of ADI and its regulation in molecular level.

Investigation of the role of ADI in *Salmonella* pathogenesis.

The effect of ADI on *Salmonella* survival during infection was assessed.

Evaluation of the interaction between bacteriophage and its host.

A new phage was isolated and elucidated its infection mechanism.

PART I:

Molecular analysis of the ADI regulation in *Salmonella* Typhimurium

Introduction

Although *Mycobacterium tuberculosis* and *Salmonella enterica* are very different microorganisms and produce distinct pathologies in humans, both proliferate within the phagosomal environment of the macrophage. In contrast to intracellular pathogens that escape to the nutrient rich cytosol of the host cell, pathogens that remain within a phagosome must resist or avoid killing by microbicidal products contained in host granules and lysosomes and must acquire or manufacture nutrients not available in the phagosome. Thus, growth of intracellular pathogens within the unique environment of the phagosome requires specialized gene products.

The biosynthesis and metabolism of arginine have attracted the interest of researchers because of the complexity and variety of the metabolic pathways used. Arginine and its precursors are involved in the biosynthesis of several metabolites such as polyamines and some antibiotics. Arginine metabolism is also linked to the pyrimidine biosynthetic pathway through carbamoyl phosphate. Multiple pathways for arginine degradation have been described in microorganisms and, occasionally, several of them are simultaneously present in the same organism. Among these pathways, the arginine deiminase (ADI) is the most widespread anaerobic route for arginine degradation.

The arginine deiminase pathway comprises three reactions, catalyzed by arginine deiminase (ADI, EC 3.5.3.5), ornithine carbamoyltransferase (OTC, EC 2.1.3.3), and carbamate kinase (CK, EC 2.7.2.2) (Fig. 3), and performs the conversion of arginine to ornithine, ammonia, and CO_2, generating one mol of ATP per mol of arginine consumed (195). The ADI pathway is wildly distributed among prokaryotic organisms and constitutes a major source of energy for these microorganisms (195). ADI catalyzes the first step of the pathway, the deimination of arginine, yielding citrulline and ammonium. ADI genes have been sequenced from Bacteria, Archaea, and anaerobic eukaryotes such as *Giardia intestinalis*. The OTC can also catalyze the reverse reaction, the synthesis of citrulline from ornithine and carbamoyl phosphate, one of the steps of the arginine biosynthetic pathway and the first step of the urea cycle. CK catalyzes the hydrolysis of the carbamoyl phosphate to CO_2 and NH_4^+, while the phosphate group is used to phosphorylate ADP. Apart from these three genes encoding the catalytic activities, a number of additional genes can be found associated to ADI gene clusters. These genes include regulatory genes belonging to different families of transcriptional regulators, genes encoding a number of enzymatic activities, some not yet characterized, and genes encoding putative transport proteins.

Materials and methods

Bacterial strains, plasmids, and growth conditions

The bacterial strains and plasmids used in this study are listed in Table 1. *S*. Typhimurium strains were derived from strain 14028s. Phage P22-mediated transductions were performed as described previously (96). Bacteria were grown at 37°C in Luria-Bertani (LB; 1% Bacto-tryptone, 0.5% yeast extract, 1% NaCl) (Difco, Detroit, MI) medium in the aerobic or anaerobic conditions as has been described (139). A stationary-phase culture that has been grown overnight with shaking (220 rpm) was inoculated into fresh LB broth at a 1:100 dilution. Ampicillin, chloramphenicol, kanamycin, and isopropyl-β-D-thio-galactopyranoside (IPTG) were used at 50 μg/ml, 25 μg/ml, 50 μg/ml, and up to 0.5 mM, respectively.

Construction of strains

To generate a nonpolar mutation (CH102) of *STM4467* gene, the one-step gene inactivation method, i.e., *λ*-red and FLP-mediated site-specific recombination system was used (48, 55). Briefly, the Km^r cassette from the plasmid pKD13 (48) was amplified using the primers STM67-lamb-F (5'-

ACTCCTTCTTTATTCTTGTAATTATGTAAAAGGTATAATGTGTAGGCT
GGAGCTGCTTCG-3′) and STM67-lamb-R (5′-CGCGACGACCAGTGTGC
GTTTGTTTTCCATAACGTCTCCTATTCCGGGGATCCGTCGACC-3′).
The resulting PCR product was integrated into the *STM4467* region in the strain 14028s, and the Km^r cassette was removed by using the plasmid pCP20 (48). The strain CH201 carries a deletion of the *STM4463* gene. For its construction, the Cm^r cassette of pKD3 (48) was amplified using the primers STM63-lamb-F (5′-CGTTGATATCAATAATAAAGATAAGGTGC
ATTTATGAAGGTGTAGGCTGGAGCTGCTTCG-3′) and STM63-lamb-R
(5′-ATTAATGCATGATTTACTCATCGCAAACGGTTCTTATGAAATATG
AATATCCTCCTTAGTTC-3′), which was integrated into the *STM4463* region in the strain 14028s. The strain CH302 carries a deletion of the *crp* gene. For its construction, the Km^r cassette of pKD13 (48) was amplified using the primers crp-lamb-F (5′- TCTGGCTCTGGAGACAGCTTATAACA
GAGGATAACCGCGCTGTAGGCTGGAGCTGCTTCG-3′) and crp-lamb-R
(5′- ACTTTTTCAGAGGTGACTTGTAAGCGACGAGCCATCTGGGATTC
CGGGGATCCGTCGACC -3′), which integrated into the *crp* region in the strain 14028s. Deletion of the corresponding genes was verified by colony PCR. The strain CH110 carrying a transcriptional *STM4467-lacZ* fusion was constructed as described previously (55). The *lacZY* genes were introduced into the FRT site in the strain CH102 using the plasmid pCE70 (134).

Double and triple deletion strains were constructed by using P22-mediated transduction (96).

Construction of plasmids

To construct the plasmid p4463, in which the *STM4463* gene is expressed from the *lac* promoter, the *STM4463* gene was amplified using primers STM4463-pUHE-F (5′-AAATGTGATGAATTCCGCCAGTCC-3′) and STM4463-pUHE-R (5′- TGAACCATGGATCCTCCCGGC-3′). The PCR product was introduced between the EcoRI and BamHI restriction sites of pUHE21-2*lacI*^{q} (184). To construct the plasmid pfis, in which the *fis* gene is expressed from the *lac* promoter, same experiment was performed using pUHE21-2*lacI*^{q}(184). For protein expression, plasmid pCRP-His$_{6}$ encoding the CRP protein with a six-His tag at the N terminus was constructed. The *crp* coding region was amplified by PCR using primers crp-pET15b-F (5′-GATAACCGCATATGGTGCTTGG-3′) and crp-pET15b-R (5′-AAAATGGCGCTCGAGAAAACGC-3′) and chromosomal DNA from strain 14028s as a template. The product was introduced between the NdeI and XhoI restriction sites of pET15b vector. Sequence of the *STM4463* and *crp* coding regions on the recombinant plasmids were verified by nucleotide sequencing.

Determination of ADI activity

The ADI activity of cell-free extracts was measured using a chemical colorimetric method based on the production of L-citrulline from L-arginine (25) (Fig. 4). A total of 50 ml of bacterial culture grown in LB medium were harvested, and the cell pellet was suspended in 3 ml of lysis buffer [10 mM Tris (pH 8.0) containing 0.3 M NaCl] and disrupted by sonication. After removal of cellular debris by centrifugation, 0.4 ml of 10 mM L-arginine in 100 mM potassium phosphate buffer (pH 7.2) was added to 1 ml of cell-free extract. After 60 min incubation at 37°C, 250 μl of a 1:3 mixture (v/v) of 95% sulfuric acid and 85% phosphoric acid, and 250 μl of a 3% diacetyl monooxime solution (Sigma) were added, and the mixtures were boiled for 15 min. The development of an orange color was monitored at 490 nm.

β-galactosidase assay

β-galactosidase assays were carried out in duplicate and the activity was determined as described previously (139). In brief, 1 ml of culture was centrifuged at 14,500 rpm for 2 min and re-suspended to the Z buffer (60 mM $Na_2HPO_4 \cdot 7H_2O$, 40 mM $Na_2HPO_4 \cdot H_2O$, 10 mM KCl, 1 mM $MgSO_4 \cdot 7H_2O$), 50 mM β-mercaptoethanol, adjusted to pH 7.0). To disrupt the cell, 20 μl of 0.1% SDS and 40 μl of chloroform were treated for 10 min

at room temperature and then 200 μl of 4 mg/ml ortho-Nitrophenyl-β-galactoside (ONPG) was added as a substrate. After developing yellow color, 0.5 ml of 1 M Na_2CO_3 was added to stop the reaction and absorbance at 420 and 550 nm were determined by spectrophotometer (Ultrospec 6300 *pro*, Amersham). Activity was calculated with the following equation; $U = 1000 \times [OD_{420} - (1.75 \times OD_{550})] / t \times v \times OD_{660}$, where t = time of reaction (min); v = volume of culture used in assay (ml).

Primer extension (PE) analysis

Total RNA was isolated from cells grown in LB medium using a Trizol reagent (Molecular Research Center) according to the manufacturer's instruction. Purified RNA was re-suspended in sterile RNase free water and the RNA concentration was estimated using NanoVue (GE Healthcare Bio-Sciences). The oligonucleotide, STM67-PE-3, complementary to the *STM4467* was labeled with 80 μCi of [γ-^{32}P]-ATP (GE Healthcare) using T4 polynucleotide kinase (Invitrogen) at 37°C for 1 h. The labeled mixture was heated at 70°C for 10 min and purified with MicroSpin™ G-25 columns (GE Healthcare). The [γ-^{32}P] end-labeled primers (0.5 pmol) were co-precipitated with 30 μg of total RNA by the addition of sodium acetate and absolute ethanol. The pellet was washed with 75% ethanol, dried at room temperature and re-suspended in 20 μl of 250 mM KCl, 2 mM Tris (pH 7.9),

and 0.2 mM EDTA. The mixture was heated to 65°C and then allowed to cool at room temperature over a period of 1 h for annealing. Superscript reverse transcriptase (Invitrogen) was used to perform the primer extension reaction within mixture harboring 50 μl of reaction solution containing 5 μg of actinomycin D, 700 μM of dNTPs, 10 mM $MgCl_2$, 5 mM dithiothreitol, 20 mM Tris (pH 8.7), 30 units of RNasin (Promega, Madison). Then, the product was purified by ethanol precipitation, re-suspended in formamide loading dye, and denaturated at 90°C for 3 min. Samples were analyzed by electrophoresis on a 6% denaturing polyacrylamide-8M urea gels alongside sequencing reactions that were generated by double-stranded DNA cycle sequencing system (Invitrogen) using STM67-PE-3 and *STM4467* promoter region as template. Gel was dried in SLAB GEL DRYER (GD2000, Hoefer) and the radiolabeled DNA fragments were visualized using BAS2500 system (Fuji film).

Purification of the CRP protein

E. coli BL21 (DE3) cells harboring plasmid, pCRP-His_6 was grown to an OD_{600} of 0.5; then 1 mM IPTG was added to the culture for the induction of CRP-His_6 protein, and another 6 h of incubation followed. The N-terminal His-tagged CRP protein was purified by Ni^{2+}-affinity chromatography. The cell pellet was suspended in lysis buffer (10 mM Tris (pH 8.0) and 0.3 M

NaCl) and disrupted by sonication. After removal of cell debris by centrifugation, the cell-free extract was applied onto a column with 2 ml of Ni-nitrilotriacetic acid resin (QIAGEN). The column was washed two times, once with lysis buffer containing 20 mM imidazole and next with lysis buffer containing 30 mM imidazole, and the adsorbed His-tagged protein was eluted with elution buffer (i.e., lysis buffer containing 300 mM imidazole). Finally, the eluted protein was dialyzed with lysis buffer containing 25% glycerol and stored at -70°C.

Gel shift assay

Gel shift assays to measure the binding of CRP to the regulatory region of *STM4467* were performed as described (173). The 282-bp DNA fragments corresponding to the *STM4467* promoter region were generated by PCR amplification using primers STM67-EMSA-F1 (5′-CAAACCATATAGCTGC GTAGTAATTCAT-3′) and STM67-EMSA-R1 (5′-TAATTGACCGATTTCAG AACCGACAAAA-3′). The *STM4467* promoter DNA was labeled with [γ-^{32}P]-ATP (GE Healthcare), and unincorporated radioisotope was removed using a MicroSpin™ G-25 column (GE Healthcare). The ^{32}P-labeled DNA probe (0.3 ng) was incubated with the purified CRP-His_6 protein (100, 200, 500, and 1000 nM) at 37°C for 30 min in a 20 μl reaction mixture containing 1x binding buffer (100 mM Tris, 0.5 mM EDTA, 25 mM magnesium

chloride, 0.5 mM dithiothreitol (DTT) and 0.5 M potassium chloride), 200 μM 3′-5′-cyclic adenosine monophosphate (cAMP), and 1 μg of poly (dI-dC). For competition assay, various amounts of the unlabeled *STM4467* promoter DNA was added to the reaction mixture containing 0.3 ng of the labeled DNA prior to the addition of 1000 nM of CRP. The reaction mixtures were resolved on a 6% non-denaturing polyacrylamide gel, and the radiolabeled DNA fragments were visualized using BAS2500 system (Fuji film).

To confirm the binding of CRP to the regulatory region of *STM4463*, same experiments were performed using relevant primers. The sequences of the primers used in the gel shift assay are listed in Table 3.

RNA isolation and qRT-PCR analysis

RNA was extracted by using RNeasy Mini Kit (QIAGEN) from *S.* Typhimurium growing LB medium in different conditions. The RNA samples were then treated with RNase-free DNase (Ambion), and cDNA was synthesized using Omniscript reverse transcription reagents (QIAGEN) and random hexamers (Invitrogen). Quantification of cDNA was carried out using 2X iQ SYBR Green Supermix (Bio-Rad), and real-time amplification of the PCR products was performed using the iCycler iQ real-time detection system (Bio-Rad). The calculated threshold cycle (C_t)

corresponding to a target gene was normalized by the C_t of the control *rpoD* gene. The sigma factor *rpoD* gene was chosen as a control because no significant variation of *rpoD* expression. The sequences of primers used in the quantitative reverse transcription-PCR (qRT-PCR) analysis were listed in Table 4.

Determination of ADI operon

To identify the operon construct, inter region of two adjacent genes was amplified by PCR using genomic DNA and cDNA, which was reverse transcribed from RNA of wild-type 14028s. The existence of correct size of PCR product was confirmed by electrophoresis. The sequences of primers used in PCR were listed in Table 5.

Epifluorescence microscopy (EFM)

To assess the ADI expression in the eye, a plasmid, pFPV25-P_{STM67}-*gfp*, expressing GFP under the control of ADI promoter was constructed and acquired by Prof. Dongwoo Shin. WT harboring pFPV25-P_{STM67}-*gfp* was grown in different conditions and applied for microscopy observation (Axio Imager.A1 upright microscope, Carl Zeiss).

Statistical analysis

Statistical analyses were conducted using the GraphPad Prism program (version 5.0). Survival curves of animal experiments were analyzed by the log-rank test, and all other results were analyzed by the unpaired *t*-test. Data were represented as mean ± standard deviation. A P value of < 0.05 was considered statistically significant.

Table 1. The bacterial strains and plasmids used in PART I and II

Strain or plasmid	Description	Reference or source
***S.* Typhimurium**		
14028s	wild-type	(64)
CH102	*ΔSTM4467*	This study
CH103	*ΔSTM4467* / p4467	This study
CH104	*ΔSTM4467* / p4463	This study
CH110	$P_{STM4467}$::*lacZY* (Km^r)	This study
CH111	$P_{STM4467}$::*lacZY*(Km^r) *ΔSTM4463*	This study
CH112	CH111 pSTM63	This study
CH113	$P_{STM4467}$::*lacZY*(Km^r) *Δcrp*	This study
CH114	$P_{STM4467}$::*lacZY*(Km^r) *Δcrp ΔSTM4463*	This study
CH115	CH114 p4463	This study
CH003	p4463	This study
CH004	pFPV25-$P_{STM4467}$-*gfp*	This study
CH201	*ΔSTM4463*	This study
CH203	*ΔSTM4463* p4463	This study
CH302	*Δcrp*	This study
CH304	*Δcrp*, *ΔSTM4463*	This study
CH305	CH304 p4463	This study
CH401	*Δfis*::Km^r	This study
CH402	*Δfis*::Km^r pfis	This study
CH403	*Δfis*::Km^r *ΔSTM4463*	This study
CH404	CH403 pfis	This study
CH405	CH403 p4463	This study
CH601	*ΔarcA*	This study
E. coli		
DH5α	[F^-. *sup*E44, *Δlac*U169(*ΦlacZ*ΔM15)*hsd*R17, *relA*1, *emdA*1, *gyr*96, *thi*-1, *relA*1]	(82)
BL21(DE3)	[F-, *dcm*, *ompT*, *hsdS*(r_{B^-} m_{B^-}), *gal* λ(DE3)]	(142)
CH701	BL21(DE3), pCRP-His_6	This study
Plasmids		
pUHE21-2*lacI*^{q}	rep_{pMBI} Ap^r *lacI*^{q}	(184)
pACYC184	rep_{p15A} Cm^r Tet^r	(38)
pET15b	rep_{pMBI} Ap^r P_{T7}	Novagen
pKD13	$repR_{6K\gamma}$ Ap^r-FRT Km^r-FRT	(48)
pKD3	$repR_{6K\gamma}$ Ap^r-FRT Cm^r-FRT	(48)
pKD46	$rep_{pSC101(Ts)}$ Ap^r P_{araBAD} γ β *exo*	(48)
pCP20	$rep_{pSC101(Ts)}$ Ap^r Cm^r*cI*857 λ P_R*flp*	(48)
pCE70	$repR_{6K\gamma}$ Ap^r-FRT *lacZY*$^+$	(134)
p4467	pACYC184-*STM4467*	This study
p4463	pUHE21-2*lacI*^{q}-*STM4463*	This study
pPM4463	pACYC184-*STM4463*	This study
pfis	pUHE21-2*lacI*^{q}-*fis*	This study
pCRP-His_6	pET15b-*crp*-His_6	This study

Table 2. Oligonucleotides used for the construction of stains and plasmids in PART I and II

	Sequence (5′ → 3′)	Purpose
STM4467-lamb-F	ACTCCTTCTTTATTCTTGTAATTATGTAAAA GGTATAATG*TGTAGGCTGGAGCTGCTTCG*	λ Red deletion of ***STM4467***
STM4467-lamb-R	CGCGACGACCAGTGTGCGTTTGTTTTCCATA ACGTCTCCT*ATTCCGGGGATCCGTCGACC*	
STM4463-lamb-F	GCCAGTCCGTTGATATCAATAATAAAGATA AGGTGCATTT*TGTAGGCTGGAGCTGCTTCG*	λ Red deletion of ***STM4463***
STM4463-lamb-R	ATTAATGCATGATTTACTCATCGCAAACGG TTCTTATGAAAT*ATGAATATCCTCCTTAGTTC*	
crp-lamb-F	TCTGGCTCTGGAGACAGCTTATAACAGAGG ATAACCGCGC*TGTAGGCTGGAGCTGCTTCG*	λ Red deletion of ***crp***
crp-lamb-R	ACTTTTTCAGAGGTGACTTGTAAGCGACGA GCCATCTGGG*ATTCCGGGGATCCGTCGACC*	
fis-lamb-F	GAAAATTTTGCGTAAACAGAAATAAAGAGC TGACAGAACTTG*TAGGCTGGAGCTGCTTCG*	λ Red deletion of ***fis***
fis-lamb-R	CGAGTAGCGCCTTTTTAAACAAGCAGTTAG CTAATCGAAA*ATTCCGGGGATCCGTCGACC*	
arcA-lamb-F	GGGAAAAACGGTCTCCTGTTAGCGCGTGAA CTGCGTGAAC*TGTAGGCTGGAGCTGCTTCG*	λ Red deletion of ***arcA***
arcA-lamb-R	GGCCGGTCATTTTCTTCAACAGCTCTGCGC GCGACTGAAT*ATTCCGGGGATCCGTCGACC*	

Table 2. Oligonucleotides used for the construction of stains and plasmids in PART I and II (continued)

	Sequence (5′ → 3′)	Purpose
STM4467-pACYC-F	TTGTTTTTTGAAGCTTTCTGACCC	Complementation of ***STM4467*** gene in pACYC184
STM4467-pACYC-R	ACGACCAGCATGCGTTTGTTTT	
STM4463-pACYC-F	GAAAGTCTGAATTCCGGCCTCTC	Complementation of ***STM4463*** gene in pACYC184
STM4463-pACYC-R	TTTACTCATCGCATGCGGTTCTTATG	
STM4463-pUHE-F	AAATGTGATGAATTCCGCCAGTCC	Overexpression of ***STM4463*** gene in pUHE21-2*lacI*^{q}
STM4463-pUHE-R	TGAACCATGGATCCTCCCGGC	
fis-pUHE-F	CAGAAATAAAGAATTCACAGAACTATGTTCGAAC	Overexpression of ***fis*** gene in pUHE21-2*lacI*^{q}
fis-pUHE-R	GCGGATCCAAATTAGTTCATGCCGTATTT	
crp-pET15b-F	GATAACCGCATATGGTGCTTGG	Purification of ***crp*** gene in pET15b
crp-pET15b-R	AAAATGGCGCTCGAGAAAACGC	

Table 3. Primers used in primer extension and gel shift assay

Primer name	Sequence (5′ → 3′)	Purpose
STM4467-PE-label-3	TCGGTTAACAGCAACACTTCTATC	Primer extension
STM4467-EMSA-F2	CTCACGCATAGTTATGCAACCATTAA	Gel shift assay (w/ CBS)
STM4467-EMSA-R2	GTTTCAGTTAAATTCGGGAGCAATGA	
STM4467-EMSA-F3	ATTAACAACCCAAATAAAATTCAATCATTGCT	Gel shift assay (w/o CBS)
STM4467-EMSA-R3	GCTCTACGGATAATACATCGTCAAAAA	
STM4463-EMSA-F1	GGCTGGAAGTATTGCTCTCCTT	Gel shift assay (w/o CBS)
STM4463-EMSA-R1	AATCTCCTCCTGGGACAGGTAA	
STM4463-EMSA-F2	CGATGCTCAGTACCGCCATATT	Gel shift assay (w/ CBS)
STM4463-EMSA-R2	GCGATGATGTAACGAGCCAGAT	

Table 4. Primers for qRT-PCR analysis

Primers	Target genes	Sequences (5′ to 3′)
STM4467-RT-F	*STM4467*	CTGGCTACTGGATACGCAAA
STM4467-RT-R	*STM4467*	GACGCCGTTATATATCCAGC
STM4466-RT-F	*STM4466*	AACCGCTGGAGGCTGATATT
STM4466-RT-R	*STM4466*	ATGATTCTTCAGCGCCTGTT
STM4465-RT-F	*STM4465*	GGATGCGAAAAGCAAACACT
STM4465-RT-R	*STM4465*	GGACGCGAGCAGTATCTTTC
STM4463-RT-F	*STM4463*	TTGTCAGCGCCTGATTAGTG
STM4463-RT-R	*STM4463*	ACCATTTCGGCTATTGAACG
ssaG-RT-F	*ssaG*	AGTGGATATGCTCTCCCACA
ssaG-RT-R	*ssaG*	AGGCAAATTGCGCTTTAATC
rpoD-RT-F	*rpoD*	GATGAAGATGCGGAAGAAGC
rpoD-RT-R	*rpoD*	GGTAATGGCTTCCGGGTATT

Table 5. Primers for the determination of ADI operon

Primers	Target region	Sequences (5′ to 3′)
STM4467-66-F	*STM4467-66*	GTTCCTGGCGCAGGCATTGTTTAA
STM4467-66-R	*STM4467-66*	CCTGTTGCAGCATGTAGCCAATCA
STM4466-65-F	*STM4466-65*	TGCTTCGTGAAATGCAGTTCGACG
STM4466-65-R	*STM4466-65*	GCATGTTCCAGCATGGTCATCAGA
STM4465-64-F	*STM4465-64*	GGATTTCCTCTATACCGACGTCTG
STM4465-64-R	*STM4465-64*	GCCGTTGAGTTTGATAGTTACCCG
STM4464-63-F	*STM4464-63*	GTGGTGGTCATGGATAACGGTATG
STM4464-63-R	*STM4464-63*	GCCGCTGGGGATTTACGGAATAAA

Results

Protein homologues between *S.* Typhimurium and *M. tuberculosis*

Although *Salmonella enterica* and *Mycobacterium tuberculosis* are distantly related microorganisms and produce distinct pathologies in humans, both should proliferate within the phagosomal environment of macrophage (31, 153). Pathogens that remain within a phagosome must resist or avoid killing by microbicidal products contained in host granules and lysosomes and must acquire or manufacture nutrients not available in the phagosome.

Thus, based on the hypothesis that intracellular pathogens in the unique environment of the phagosome may require specialized gene product, I searched protein homologues by comparing whole genomes of *S.* Typhimurium and *M. tuberculosis*. Following the consecutive rounds of whole genome searches, I eliminated genes that are present in *Escherichia coli* K-12 (i.e., closely related to *S. enterica* but commensal to human), and then selected genes present in *Salmonella enterica* serovar Typhi (i.e., highly related to *S.* Typhimurium and causing systemic infection in human (Fig. 1)). Finally, this approach revealed seven protein homologues displaying 25~45% amino acid sequence identity in *S.* Typhimurium and *M. tuberculosis* (Table 6). Interestingly, six of seven gene candidates in

Salmonella were uncharacterized genes encoding putative enzymes involved in metabolic pathways (Table 6).

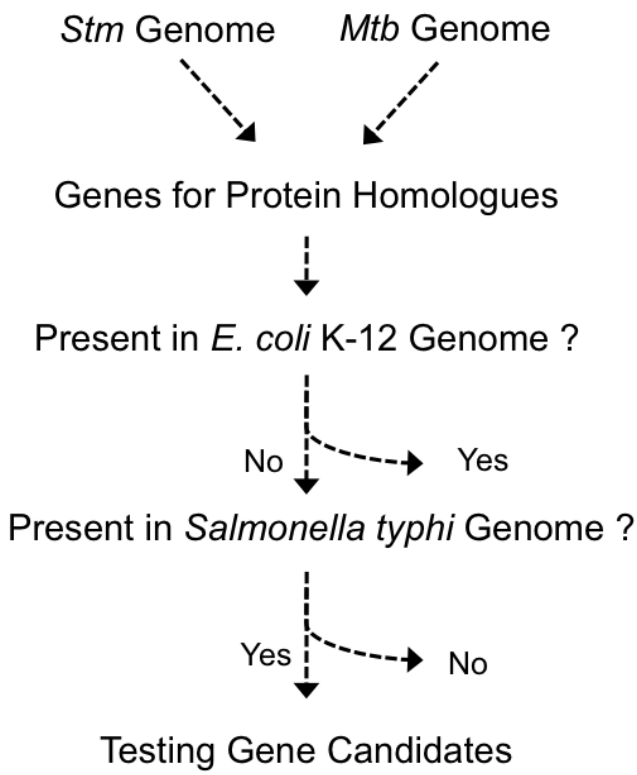

Figure 1. A strategy for discovery of genes that might be involved in proliferation of *Salmonella* inside host cell. Protein homologues by comparing whole genomes of *S.* Typhimurium and *M. tuberculosis*. Following the consecutive rounds of whole genome searches, genes that are present in *E. coli* K-12 were eliminated, and then candidate genes present in *S*. Typhi, were selected genes.

Table 6. Gene homologues specific to *S.* Typhimurium and *M. tuberculosis*

***S.* Typhimurium**	***M. tuberculosis***	**Product**	**Identity**
STM1269	Rv1885c	chorismate mutase	24%
STM1623	*lipT*	carboxylesterase	27.6%
STM2405	Pdc	indolepyruvate decarboxylase	45.2%
nixA	*nicT*	nickel transporter	38.2%
STM3651	Rv0919	acetyltransferase	46.4%
STM4318	Rv0919	acetyltransferase	43.7%
STM4467	***arcA***	**arginine deiminase**	**44%**

The *STM4467* gene encodes ADI in *S*. Typhimurium

In *S*. Typhimurium genome, the *STM4467*, *STM4466*, and *STM4465* genes are clustered into an operon-like structure (Fig. 2) and are predicted to encode enzymes of the ADI system, ADI, CK, and OTC, respectively (Fig. 2). It has been reported that, when *Salmonella* is grown in LB medium containing 0.4 M NaCl without agitation, expression of this gene cluster is induced to promote OTC activity (185). Although this finding suggests that the ADI pathway might be functional in *S*. Typhimurium, the genes responsible for enzymatic activities of the ADI pathway have remained unknown. Therefore, I compared the ADI activity between wild-type *Salmonella* and its isogenic *STM4467* deletion mutant. When ADI activity assay (Fig. 4) was conducted using a cell extract prepared from the wild-type strain, orange color was developed (Fig. 5), which indicated the ADI-catalyzed production of citrulline from arginine (25, 170). However, in the *STM4467* deletion mutant, the enzyme activity was poorly detected (Fig. 5A) and was only ~40% compared with that present in the wild-type strain (Fig. 5B). This phenotypic defect was due to the function of STM4467 because expression of the *STM4467* gene from a plasmid enabled the *STM4467* deletion mutant to produce citrulline at levels even higher than the wild-type strain (Fig. 5A and 5B). Thus, these results indicate that the *STM4467* gene encodes ADI or that is required for full ADI activity.

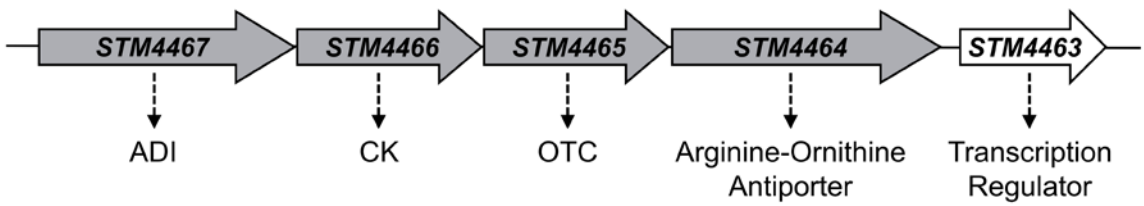

Figure 2. Schematic representation of the ADI pathway gene cluster in *S.* Typhimurium.

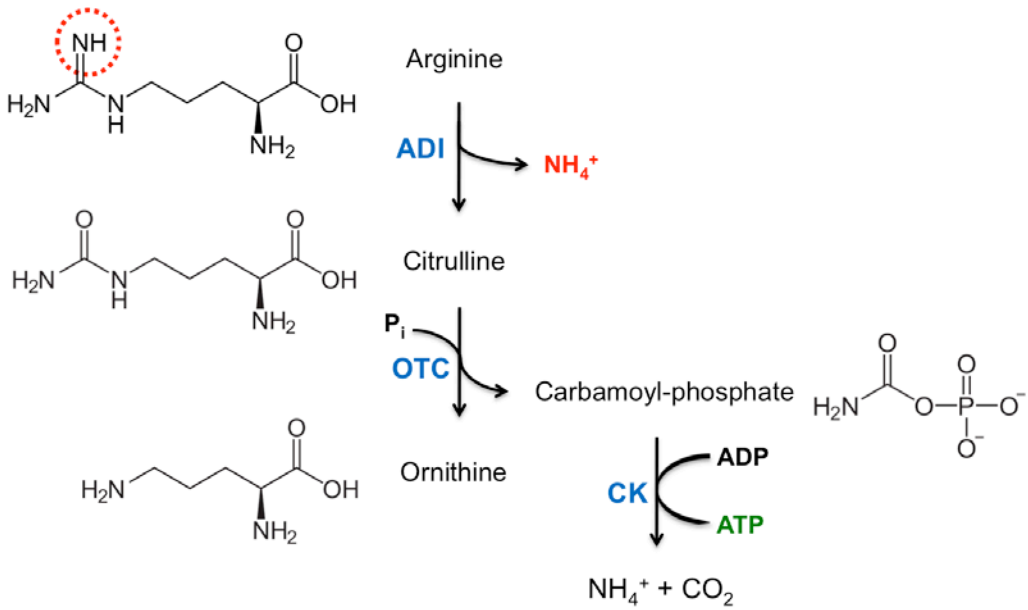

Figure 3. The Arginine Deiminase (ADI) pathway

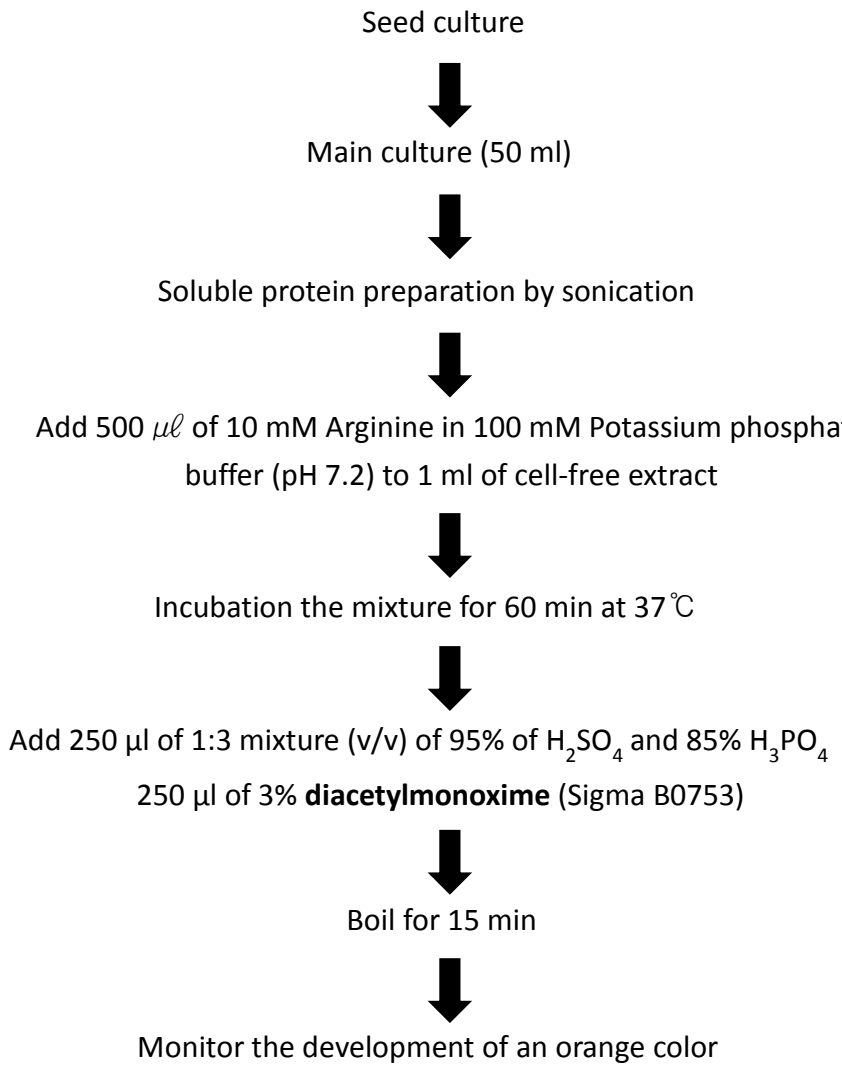

Figure 4. Procedure for ADI activity determination (colorimetric method)

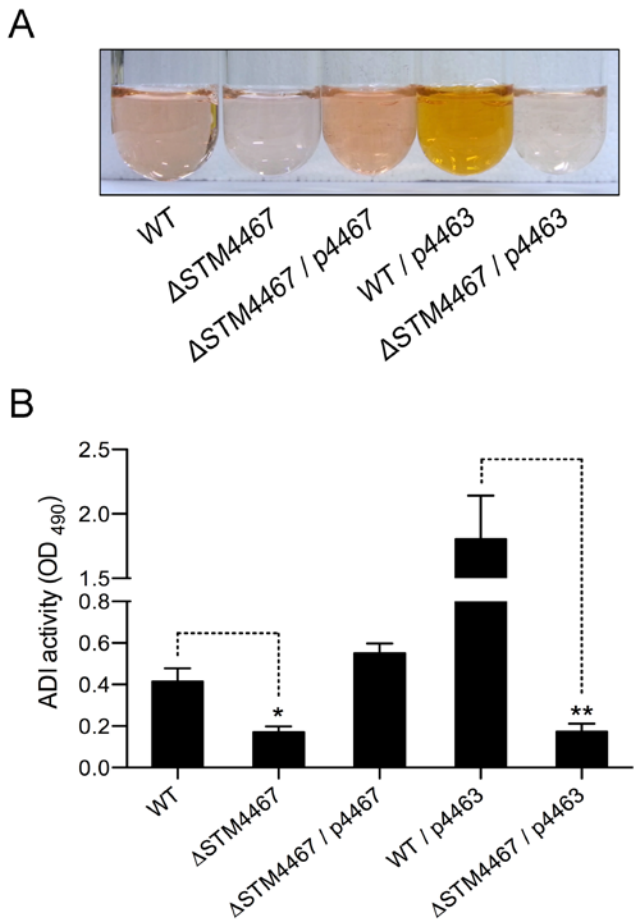

Figure 5. ADI activity was measured using a colorimetric method based on the production of citrulline from arginine. (A) The ADI activities of the wild-type (WT) strain (14028s), the *STM4467* deletion mutant (CH102, *ΔSTM4467*), strain CH102 carrying plasmid p4467 (*ΔSTM4467*/p4467), the WT strain carrying plasmid p4463, and strain CH102 plasmid p4463 (*ΔSTM4467*/p4463) were determined by using cell extracts grown in LB medium. The development of an orange color indicates the ADI-catalyzed production of L-citrulline from L-arginine. (B) Quantification of the ADI activity displayed by the *S*. Typhimurium strains described for panel for B. Means and standard deviations from three independent experiments are shown (**, $P < 0.01$). OD_{490}, optical density at 490 nm.

Expression of STM4467 in different conditions

As low pH, anaerobicity and the addition of arginine have been shown to regulate the expression of ADI genes differently in other bacteria, the expressions of *Salmonella* ADI genes were examined by qRT-PCR. In the anaerobic condition, the expression of *STM4467* was increased more than 10-fold compared to that of aerobic condition in the LB (Fig. 6A). The arginine, as a substrate for ADI pathway, also induced the ADI expression (Fig. 6A). In EFM analysis, I could identify the ADI expression in the eyes by using a plasmid, which expresses GFP under control of ADI promoter (Fig. 6B).

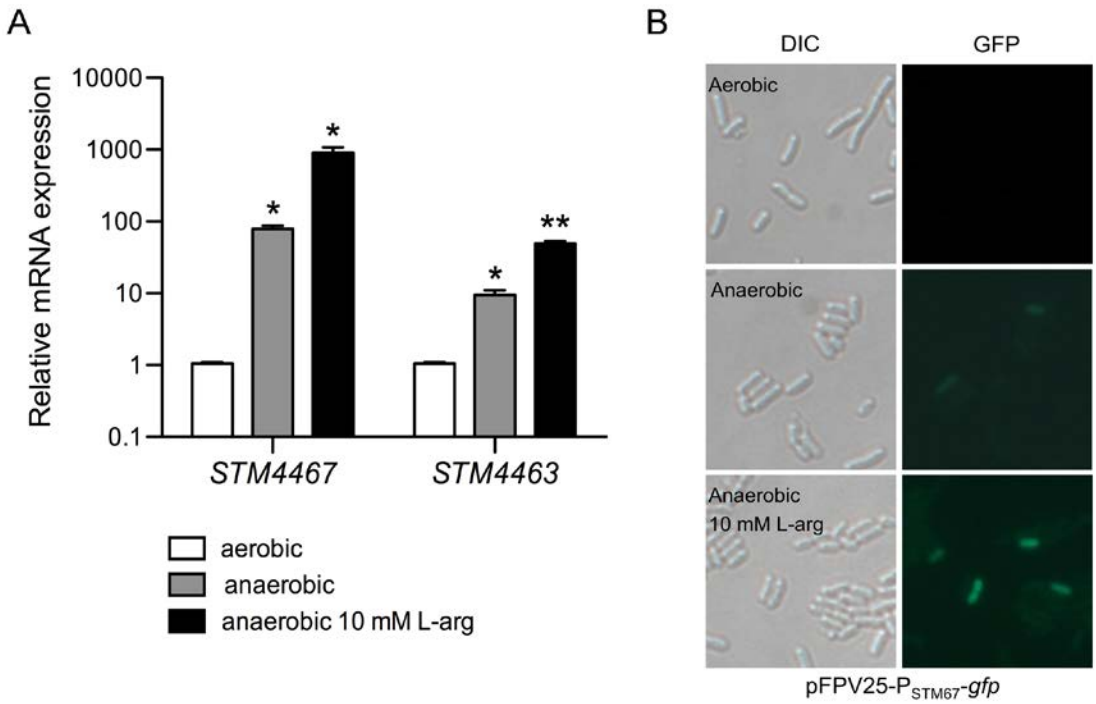

Figure 6. Anaerobic condition and L-arginine showed positive regulation of *STM4467* expression. The transcriptional levels of the *STM4467* gene were determined by conducting qRT-PCR (A) and EFM (B). (A) Each culture was harvested at 4 h after incubation. L-arginine was added into medium at 10 mM. Means and standard deviations from three independent experiments are shown (**, $P < 0.01$; *, $P < 0.05$). (B) The wild-type harboring pFPV25-P$_{STM4467}$-*gfp* strain (CH004) was grown in LB medium with or without 10 mM L-arginine. The ADI-expressing bacteria represented fluorescence in the microscope. DIC, differential interference contrast.

The STM4463 protein is a positive regulator of *STM4467* transcription

Next to the ADI operon, there was a gene, *STM4463* that was referred as *rosE* (40). The protein encoded by *STM4463* had homology to arginine repressor, ArgR and showed high sequence identity to the ArgR of *E. coli*. To assess the role of STM4463 in the ADI pathway, I constructed a deletion mutant of the *STM4463* gene and also made a complementary plasmid, p4463 as described (Fig. 7B). Transcription of ADI gene was determined in the anaerobic condition with 10 mM arginine by qRT-PCR. The expression of ADI was extremely reduced in the mutant and recovered up to 8 times in the complementary strain with increased concentration of inducer (IPTG) (Fig. 7A). These results suggested that a transcriptional regulator, STM4463 regulates the ADI expression positively.

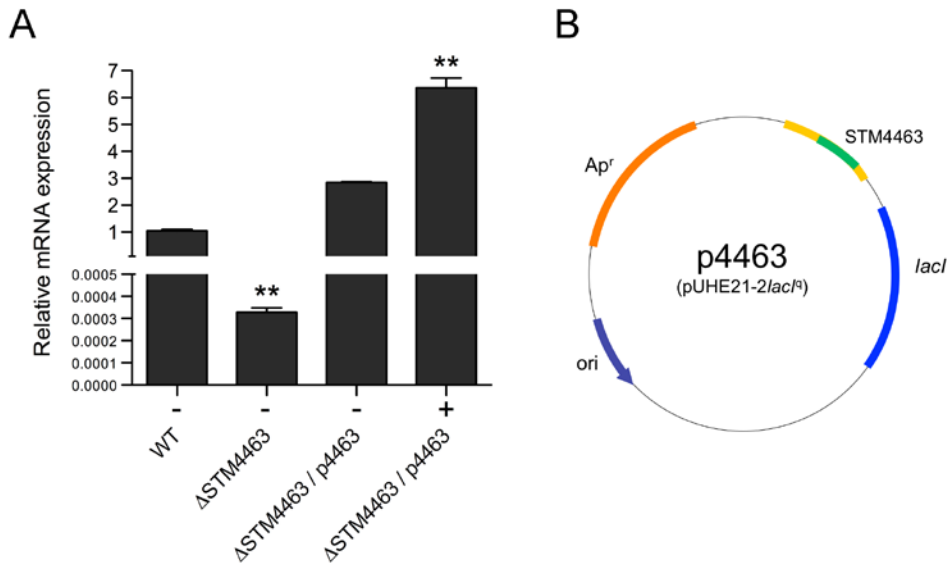

Figure 7. The STM4463 regulator activates transcription of the *STM4467* gene. (A) Transcription levels of the *STM4467* gene were determined by conducting qRT-PCR on *S*. Typhimurium strains. The 14028s strain (WT), its isogenic *STM4463* deletion mutant (CH201, *ΔSTM4463*) and CH203 strain harboring the p4463 plasmid (*ΔSTM4463*/p4463) were grown in LB medium with (+) or without (-) 0.5 mM IPTG. Means and standard deviations from three independent experiments are shown (**, $P < 0.01$). (B) Construction of *STM4463* overexpression plasmid, p4463.

Determination of the transcription initiation site of ADI and analysis of the 5′ region

Before determining the promoter region of ADI, I firstly decided the composition and orientation of the ADI operon by PCR. PCR products from the cDNA indicated that the ADI operon consists of 4 genes (*STM4467*, *STM4466*, *STM4465*, and *STM4464*) (Fig. 8). The ADI regulator, STM4463, was transcribed separately under its own promoter (Fig. 8) and the regulation of this promoter will be discussed later on.

The exact location of transcriptional initiation site of ADI was searched by primer extension. Total RNAs were isolated from aerobically incubated 14028s and its isogenic mutants in LB. the oligonucleotide STM67-PE-3 (underlined arrow), which was complementary to the 5′ end of the *STM4467* gene, was used for the primer extension reaction. Two adjacent start sites were detected at C90 (upper promoter) and A29 (bottom promoter) upstream regions from start codon (Fig. 9). The consensus promoter sites were located at -10 (TTCAAT) and -35 (ATCACA) from the transcriptional initiation site for upper promoter. But bottom promoter had poorly conserved -10 (GCCACT) and -35 (CAAGCA) sites suggesting that upper promoter is a putative regulatory region for ADI expression. The results of other two mutants (WT/pSTM63 and *ΔSTM4463*) proved that the induction of ADI expression by STM4463 was due to the transcription from

upper promoter. There were highly expressed band relevant to upper transcriptional initiation site along with normally expressed bottom band and fragmented upper band in the WT/pSTM63 strain. However, the upper band was gone in the *ΔSTM4463* strain supporting that the upper promoter is a regulatory region of ADI (Fig. 9).

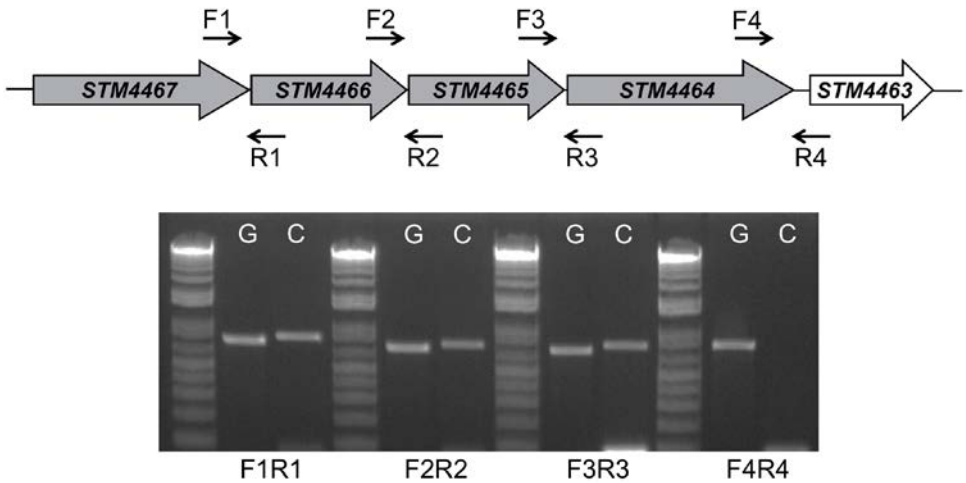

Figure 8. Determination of the *Salmonella* ADI operon. The organization of ADI operon is represented as gray arrows. Gel image represents the presence of PCR product from each region at the cDNA template. Primers are designated with a fine arrow. G, genomic DNA; C, cDNA.

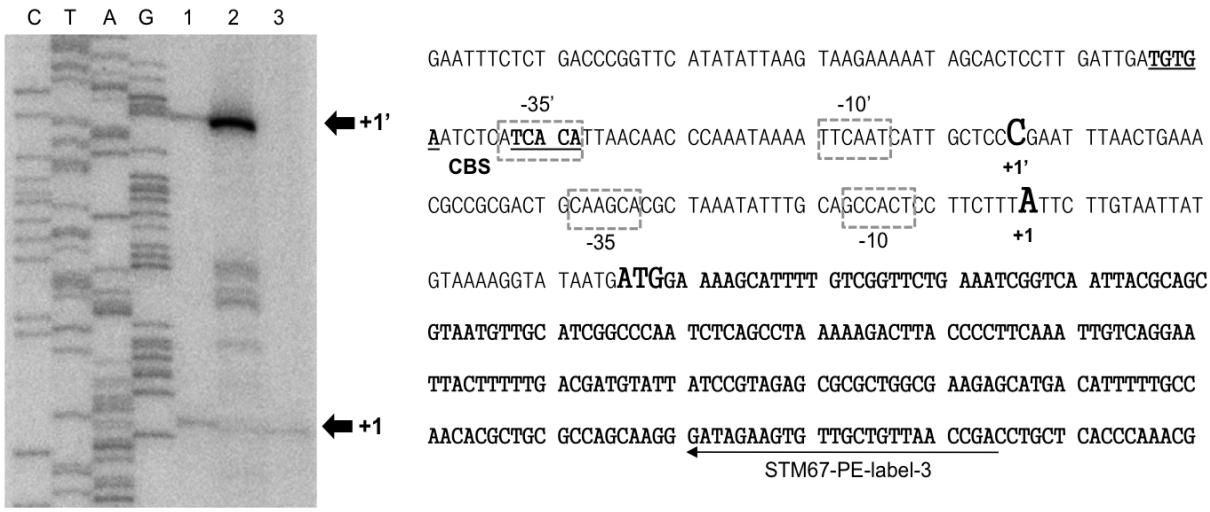

Figure 9. Identification of the *Salmonella* ADI promoter. Primer extension analysis was performed with end-labeled STM67-PE-label-3 primer (under lined arrow) using total RNA from the wild-type (1: 14028s, WT), wild-type strain carrying p4463 (2: CH003, WT/p4463), and *STM4463* deletion mutant (3: CH201, *ΔSTM4463*) strain grown in LB medium. The start sites (+1' and +1) are indicated by arrow and the promoter element that resemble the consensus -10 and -35 sites are boxed. CRP-binding site (CBS) is underlined.

Regulation of *STM4467* by CRP

From primer extension analysis and sequences of promoter regions, I found the well-preserved CRP-binding site (CBS, TGTGA-N_6-TCACA) located at upper promoter (Fig. 9). This conserved CBS prompted me to explore whether the CRP protein could directly interact with the ADI promoter. Therefore, I constructed a plasmid for purification of CRP protein using pET system, as described (Fig. 10) then performed gel shift assay. Incubation of the purified CRP protein and the 5′ end-labeled ADI promoter DNA resulted in electrophoretic mobility shifts of the DNA molecules (Fig. 11A and 12A). The CRP-ADI promoter interaction was specific because the addition of the unlabeled ADI promoter DNA competed with the labeled probe from the shifted band (Fig. 11B). In addition, the CRP protein could not gel shift the bottom promoter DNA, which lacks the CRP-binding sequence (Fig. 12B).

To elucidate the CRP effect on the ADI expression, I constructed several *crp* mutants as described and performed qRT-PCR. In anaerobic condition with 10 mM of L-arginine, *crp* mutant decreased ADI expression (Fig. 13). And *crp* mutant did not showed glucose effect on the ADI expression (Fig. 13) proving that the reduction of ADI expression by glucose was mediated to CRP regulation. Moreover, *crp* mutant affected the STM4463 regulation for ADI at transcriptional level. Without *crp*, over-expression of STM4463,

which showed positive regulation, did not induce the transcription of ADI compared with wild-type (Fig. 14A). This regulation was also confirmed from primer extension analysis. The wild-type showed two bands for transcriptional start sites as described before and STM4463 over-expression strain (CH003, p4463) appeared highly expressed band corresponded to upper transcriptional initiation site (Fig. 9). Interestingly, in *crp* deleted background, there was no band for the upper transcriptional initiation site even at the STM4463 over-expression condition, indicating that the activating effect of STM4463 on the ADI expression was through the CRP binding to the promoter region (Fig. 14B).

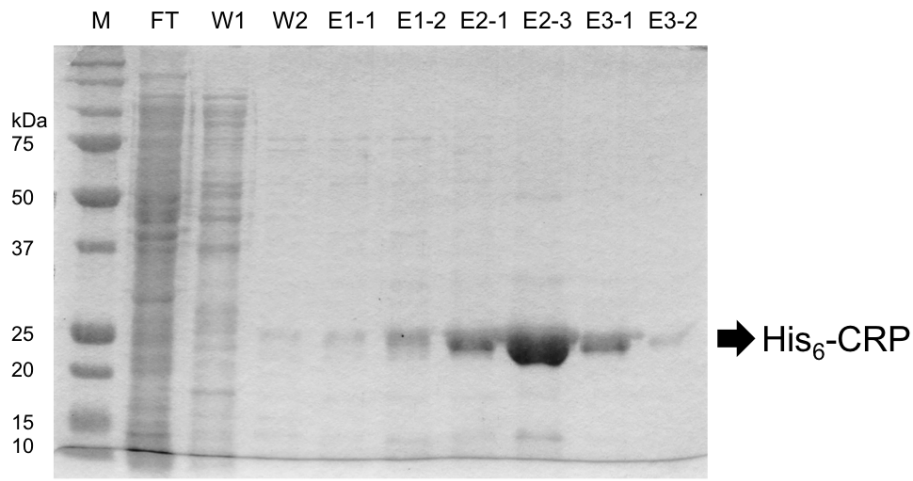

Figure 10. Purification of His_6-tagged CRP protein. A soluble protein from 1 mM IPTG-induced pCRP-His_6/BL21 (DE3) was applied onto the Ni^{2+}-affinity chromatography. The column was washed and eluted by lysis buffer (10 mM Tris (pH 8.0) and 0.3 M NaCl) with increasing concentration of imidazole. FT; follow through, W1; washing 1 (20 mM of imidazole), W2; washing 2 (50 mM), E1; elution 1 (100 mM), E2; elution 2 (300 mM), E3; elution 3 (500 mM).

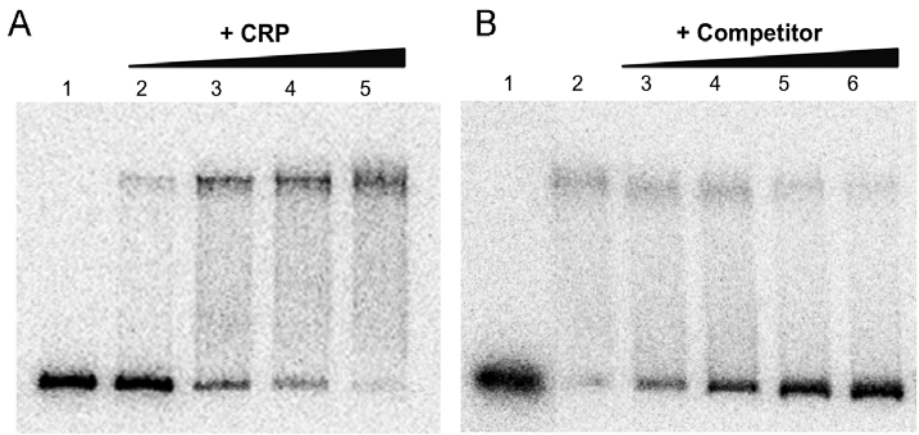

Figure 11. Specific binding of CRP protein to the ADI promoter. The 282-bp DNA fragment of the *STM4467* upstream region was radioactively labeled and then used as a probe DNA. (A) Increasing amounts of CRP (0, 100, 200, 500, 1000 nM in lanes 1-5 respectively) were added to the radiolabeled probe (0.3 ng). (B) For competition analysis, the same, but unlabeled, 282-bp DNA fragment was used as competitor DNA. Lane 1, probe DNA alone; lanes 2-6, probe DNA incubated with 1000 nM of CRP and 0, 100, 200, 300, 400 nM of competitor DNA, respectively.

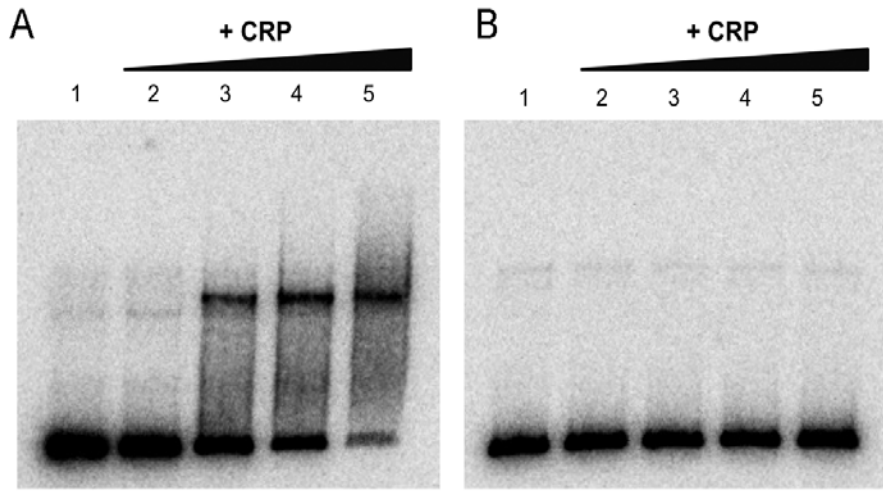

Figure 12. CRP protein only binds to upper promoter region of ADI. Two different DNA fragments of the *STM4467* upstream region were radioactively labeled and then used as a probe DNA. (A) The radio-labeled 282 bp size DNA probe (0.3 ng), which harbors CBS indicated up-shift along with the increasing amounts of CRP (0, 100, 200, 500, 1000 nM in lanes 1-5, respectively). (B) Increasing amounts of CRP (0, 100, 200, 500, 1000 nM in lanes 1-5, respectively) were added to another radiolabeled probe (260 bp, 0.3 ng, no CBS).

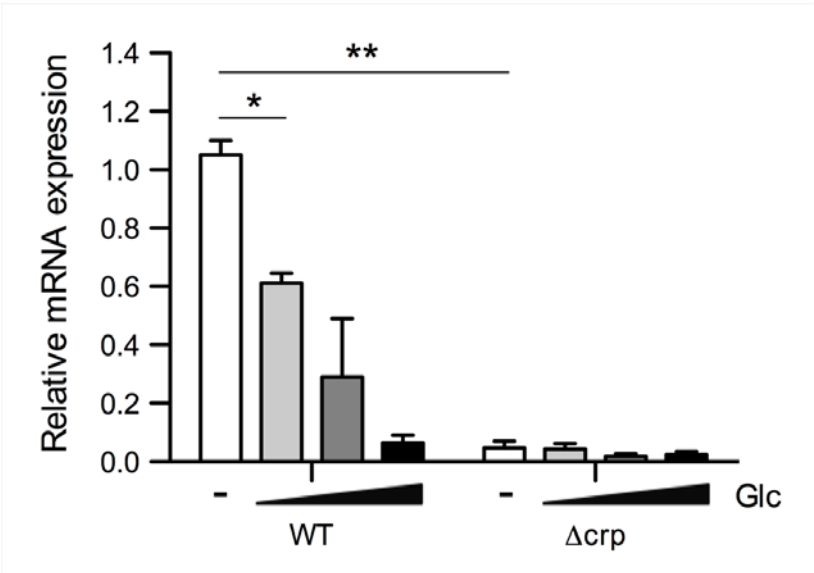

Figure 13. Glucose had an effect on the expression of *STM4467* via CRP regulation. The transcriptional levels of the *STM4467* gene were determined by qRT-PCR. Each culture was harvested at 4 h after incubation. Glucose was added into medium at 1, 5, and 10 mM. Means and standard deviations from three independent experiments are shown (**, $P < 0.01$; *, $P < 0.05$).

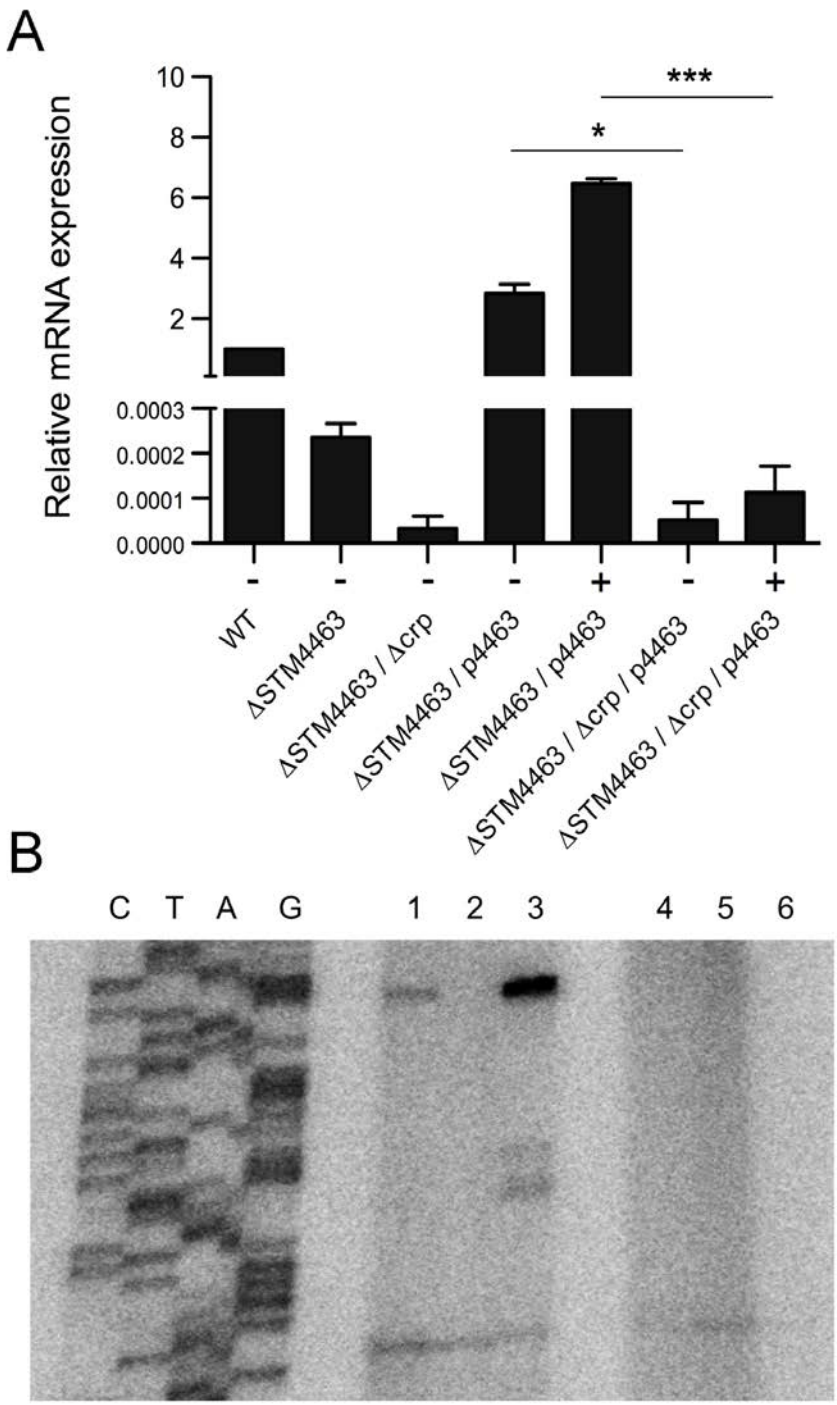
A
Relative mRNA expression
10
8
6
4
2
0.0003
0.0002
0.0001
0.0000
*
***
- - - - + - +
WT
ΔSTM4463
ΔSTM4463 / Δcrp
ΔSTM4463 / p4463
ΔSTM4463 / p4463
ΔSTM4463 / Δcrp / p4463
ΔSTM4463 / Δcrp / p4463
B
C T A G
1 2 3
4 5 6

Figure.14 CRP mediates the ADI regulation of STM4463. The transcriptional levels of the *STM4467* gene were determined by conducting qRT-PCR (A) and PE (B). (A) Each culture was harvested at 4 h after anaerobic incubation. L-arginine was added into medium at 10 mM. Means and standard deviations from three independent experiments are shown (***, $P < 0.001$; *, $P < 0.05$). (B) PE analysis was performed with end-labeled STM67-PE-label-3 primer using total RNA from the wild-type (1: 14028s, WT), wild-type strain carrying p4463 (2: CH003, WT/p4463), *STM4463* deletion mutant (3: CH201, *ΔSTM4463*), *crp* deletion mutant (4: CH302, *Δcrp*), *crp*/*STM4463* double deletion mutant (5: CH304, *Δcrp*/*ΔSTM4463*), CH304 harboring p4463 (6: CH504, *Δcrp*/*ΔSTM4463*/p4463) strains.

CRP also regulates *STM4463*

In the previous result, the expression of *STM4463* was also increased in the anaerobic condition with L-arginine (Fig. 6). This result made me think that the ADI-inducing signals might pass through regulator, STM4463. Therefore, I assessed the expression of *STM4463* in the same condition, which was used for *STM4467*. Interestingly, CRP regulated the expression of *STM4463* expression. Glucose could down-regulate the expression of *STM4463* via CRP in like manner of *STM4467* (Fig. 15). Without CRP, there was no *STM4463* resulting in halting ADI expression. Then, I confirmed whether CRP regulates *STM4463* directly or indirectly by performing gel shift assay. Because I did not know the promoter region of *STM4463*, I firstly selected a ~500 bp upstream from the start codon of *STM4463* as a DNA probe (Fig. 16A). Expectedly, incubation of the purified CRP protein and the 5′ end-labeled *STM4463* promoter DNA resulted in electrophoretic mobility shifts of the DNA molecules (Fig. 16C). Then I narrowed down the promoter region dividing two segments (Fig. 16A). Using these two DNA probes, gel shift assay revealed that CRP only bound to the region ~200 bp upstream from the start codon. This interaction was confirmed by competition assay using the unlabeled DNA probe (Fig. 17). Moreover, I could find a preserved CBS (TGTGA-N_6-TCGCC) in this region supporting the interaction between CRP and *STM4463* promoter (Fig. 16B).

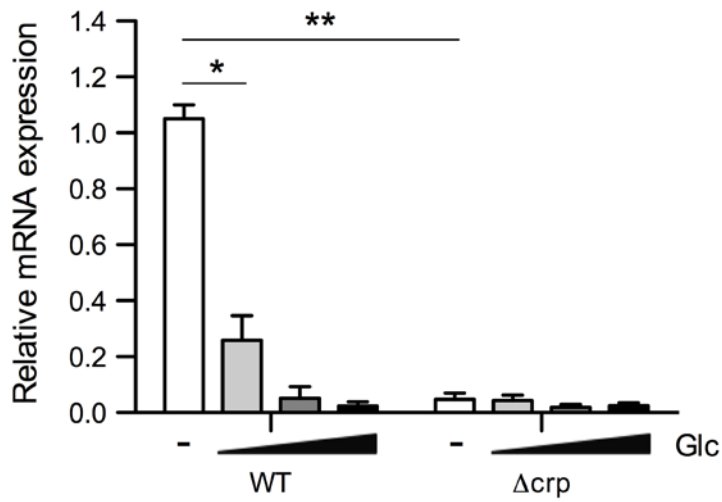

Figure 15. Glucose also affected the expression of *STM4463* via CRP regulation. The transcriptional levels of the *STM4463* gene were determined by qRT-PCR. Each culture was harvested at 4 h after incubation. Glucose was added into medium at 1, 5, and 10 mM. Means and standard deviations from three independent experiments are shown (**, $P < 0.01$; *, $P < 0.05$).

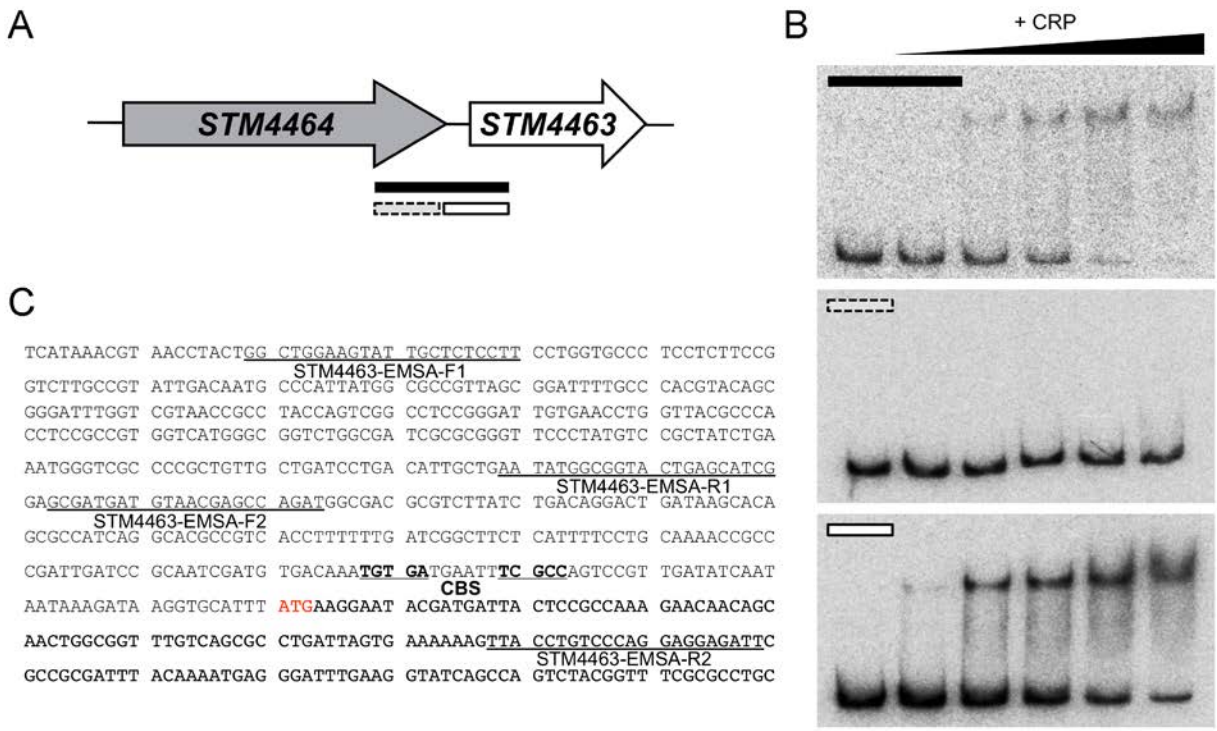

Figure 16. Specific binding of CRP to the *STM4463* promoter (1). (A) Three different DNA fragments of the STM4463 upstream region were radioactively labeled and then used as a probe DNA. (B) Increasing amounts of CRP (0, 100, 200, 500, 700, and 1000 nM, respectively) were added to the radiolabeled probe (0.3 ng). (C) The promoter region in the nucleotide sequences; start codon (ATG in red), CBS (CRP-binding site with under bar and bold), and relevant primer sequences (labels with under bar) are designated, respectively.

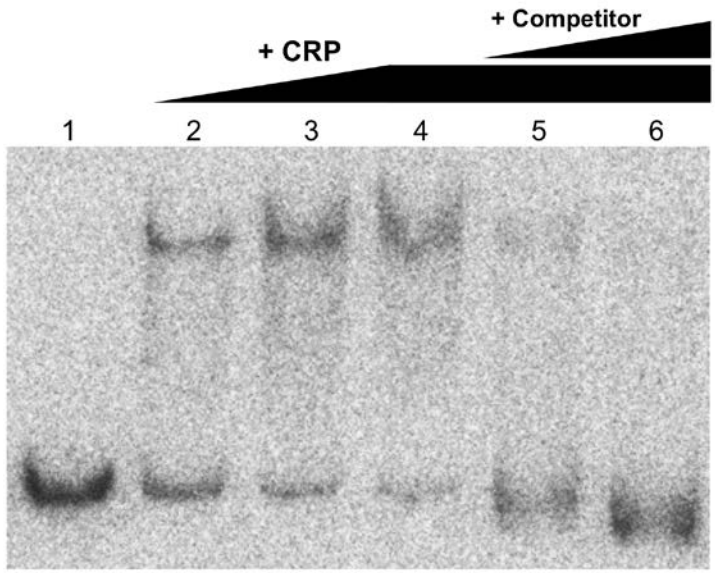

Figure 17. Specific binding of CRP to the *STM4463* promoter (2). The 297-bp DNA fragment of the *STM4463* upstream region was radioactively labeled and then used as a probe DNA. For competition analysis, the same, but unlabeled, 297-bp DNA fragment was used as competitor DNA. Lane 1-3, labeled probe DNA alone with 200, 500 nM of CRP; lanes 4-6, probe DNA incubated with 1000 nM of CRP and 0, 200, 400 nM of competitor DNA, respectively.

Fis regulates ADI via the STM4463

Fis is a global regulator of transcription involved in the adjustment of cellular metabolism to varying growth conditions. To test the effect of Fis on the expression of ADI, I constructed a deletion mutant of the *fis* gene and also made a complementary plasmid, pfis. Transcription of ADI gene was determined by qRT-PCR. The expression of ADI was increased extremely in the mutant and recovered in the complementary strain with increased concentration of inducer (IPTG) (Fig. 18A).

Interestingly, the expression of *STM4463* was also negatively regulated by Fis in transcriptional level like as *STM4467* (Fig. 18B). To determine whether Fis regulates ADI or its regulator, STM4463, I made a double deletion mutant of *STM4463* and *fis* genes. Without *STM4463*, Fis could not regulate the expression of ADI (Fig. 18A). These results suggested that a global regulator, Fis negatively regulated ADI regulator, STM4463.

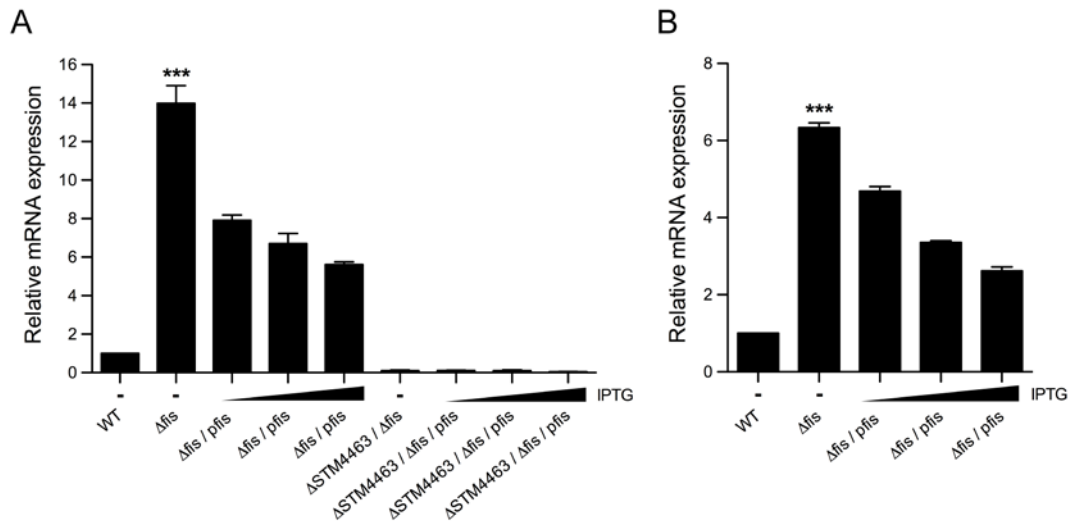

Figure 18. Fis negatively regulates the *STM4467* expression via STM4463. The transcriptional levels of the *STM4467* (A) and *STM4463* (B) were determined by conducting qRT-PCR. Each culture was harvested at 4 h after incubation. Means and standard deviations from three independent experiments are shown (***, $P < 0.001$).

ArcA regulates the ADI expression sensing polyamines

The Arc two-component signal transduction system is major regulatory system mediating adaptive responses of *Salmonella* in changing respiratory conditions of growth. In *arcA* deletion mutant, ADI expression was abruptly decreased in anaerobic condition, which was a signal for ADI induction (Fig. 20A). ArcA also regulated the expression of STM4463 supporting the STM4463-mediated regulation of ADI (Fig. 20A).

In *E. coli*, polyamine stimulates the expression of *arcA* (167). Therefore, I tested the effect of several polyamines on ADI expression. Putrescine and spermidine increased the expression of ADI, but spermine did not (Fig. 19). Spermidine is synthesized from putrescine and L-methionine by SpeE and SpeD (99). Therefore, spermidine increased the expression of ADI more than putrescine (Fig. 20A) indicating that final product; spermidine is a signal for the regulation of ADI expression by ArcA. Expectedly, there was no increase of ADI expression in *ΔarcA* mutant with putrescine and spermidine indicating that polyamines are signal for ADI activation by ArcA (Fig. 20B).

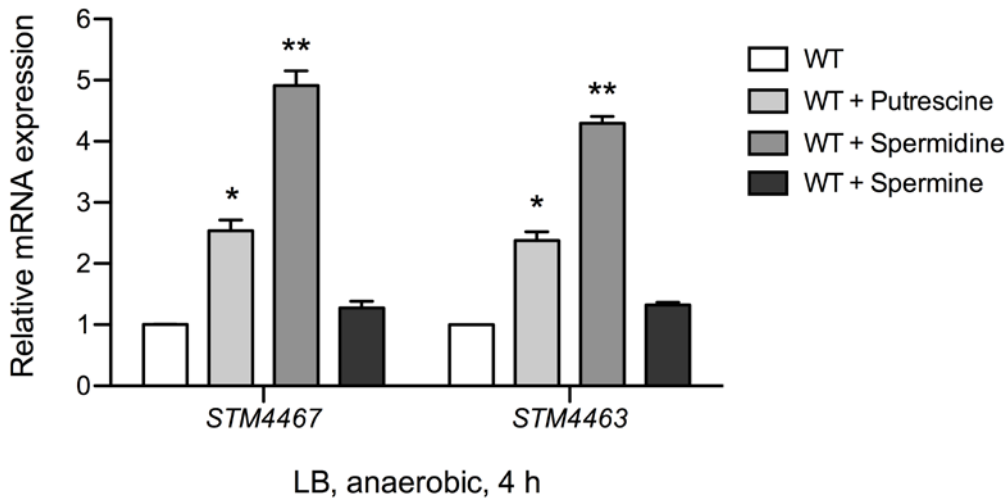

Figure 19. Polyamines increase the expression of ADI. The transcriptional levels of the *STM4467* and *STM4463* were determined by conducting qRT-PCR. Each culture was harvested at 4 h after anaerobic incubation. Putrescine, spermidine, and spermine were added to LB medium at 3 mM. Means and standard deviations from three independent experiments are shown (**, $P < 0.01$; *, $P < 0.05$).

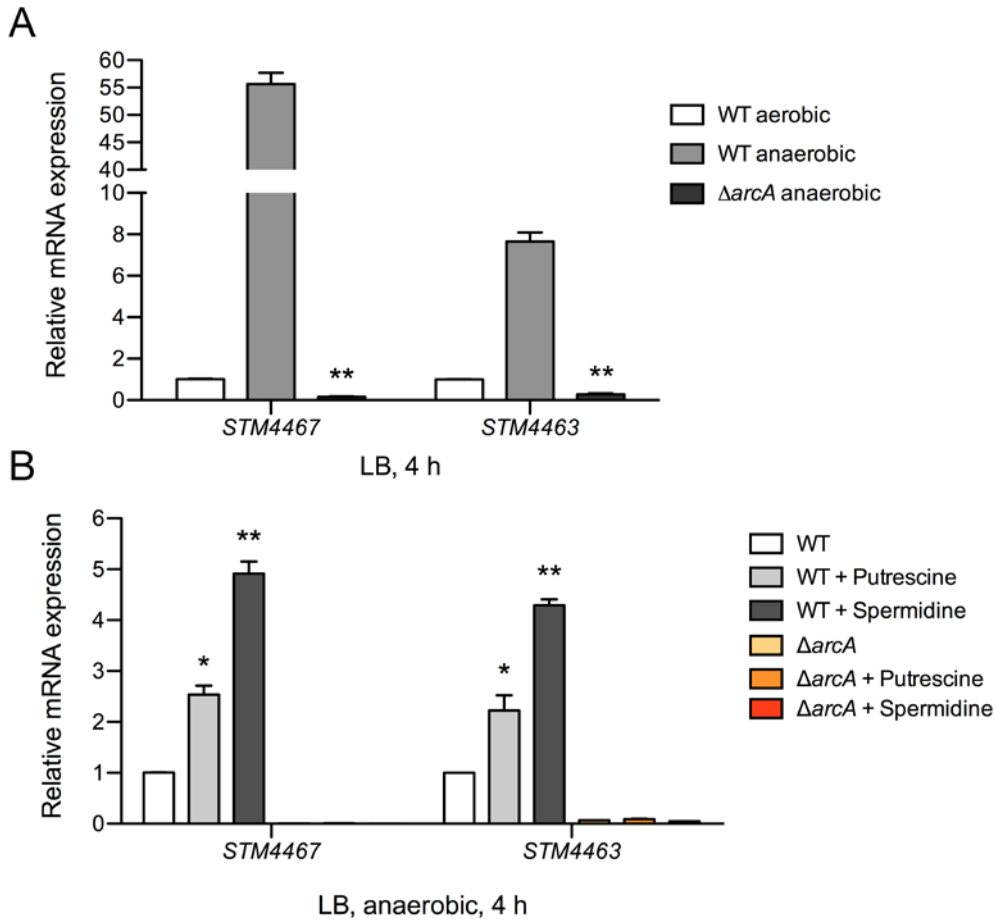

Figure 20. AcrA activates the ADI expression in anaerobic condition by sensing polyamines. The transcriptional levels of the *STM4467* and *STM4463* in both wild-type and *ΔarcA* mutant were determined by conducting qRT-PCR. Each culture was harvested at 4 h after anaerobic incubation. Putrescine and spermidine were added to LB medium at 3 mM. Means and standard deviations from three independent experiments are shown (**, $P < 0.01$; *, $P < 0.05$).

Discussion

The ability to replicate and survive in the macrophage vacuole is crucial for *Salmonella* pathogenesis. Already, many virulence genes (e.g. SPI-2 locus) required for survival in intracellular region has been identified and well known for their actions (197). Therefore, it was required that more wide but specific screen. Previous studies demonstrated that *Salmonella mgtC* gene encoding a putative Mg^{2+} transporter is required for its growth within macrophages and for virulence *in vivo* (21). Although *M. tuberculosis* is a phylogenetically distant pathogen, it harbors an ORF displaying 38% amino acid identity with the *Salmonella* MgtC protein (31). Interestingly, *M. tuberculosis* mutant lacking the *mgtC* gene also exhibited a growth defect within macrophages and attenuation of virulence for mice (31). These studies suggest that growth of intracellular pathogens in the unique environment of the phagosome may require specialized gene products, and that I may identify such genes by searching protein homologues in the genome sequence data. The availability of several complete genome sequences of *Salmonella enterica* and *M. tuberculosis* aided in the identification of novel genes for virulence. In the comparative analysis, the rational was to find genes of *S*. Typhimurium existing both in *M. tuberculosis* and *S*. Typhi but not in the commensal bacteria *E. coli* K-12.

Target genes have to be connected with phagosomal survival for *M. tuberculosis* and related to typhoid fever for *S*. Typhi. As a result, I obtained the *STM4467* gene that meets the criteria. The *STM4467* is annotated as a putative L-arginine deiminase and is clustered with other three genes, *STM4466*, *STM4465*, *STM4464*, which respectively encodes a putative carbamate kinase (CK), a putative ornithine carbamoyltransferase (OTC), and a putative arginine/ornithine antiporter (212). In addition, *STM4463* is also associated with this gene cluster encoding a putative regulatory protein (Fig. 3).

An initial biochemical assay established that the predicted *S*. Typhimurium ADI gene product is functional in producing citrulline from arginine (Fig. 5). Although I could confirm the production of citrulline by comparing wild-type and *STM4467* mutant, the density of orange color by wild-type was not much strong. Therefore, I tested the wild-type strain carrying p4463 plasmid, which showed over-expression of *STM4467* in the qRT-PCR, and expectedly it produced much amount of citrulline with dark orange (Fig. 5A). Finally, the *STM4467* deletion made the p4463 no use of producing orange color confirming that the *STM4467* gene encodes ADI in *S*. Typhimurium.

In several bacteria, arginine-responsive transcriptional regulator binds DNA at its amino end to repress arginine biosynthesis or activate arginine

catabolism (149, 156). And it has been identified that ArgR controlled expression of the ADI operon positively or negatively in the many other strains (50, 122, 127). In *Lactobacillus sakei*, ArcR is essential for expression of the ADI pathway (212) and *Staphylococcus aureus* ArcR binds to a conserved CRP–like sequence motif present in the *arc* promoter region and thereby activates the expression of the ADI pathway genes (128). Therefore, I also constructed *STM4463* mutant and assessed the effect of putative regulator on the ADI expression. In the transcriptional assay, *STM4463* deletion resulted in decreasing the expression of ADI but highly activated the expression when it was over-expressed (data not shown). Interestingly, slight increase of regulator (*STM4463*) from the inducible-*lac*-promoter with little amount of inducer, it could up-regulate the ADI expression up to 8 times higher than the wild-type indicating the importance of STM4463 for the ADI regulation.

Actually, the expression levels of ADI in several media cultures were relatively lower; Miller units of ADI in the wild-type were just under 200. Therefore, I speculated that there might be a repressor strongly binding to the ADI promoter. With this hypothesis, I constructed random mutant using EZ:Tn transposon in the *STM4467-lacZ* fusion strain. In this experiment, most random mutants presented white colonies in the LB agar containing X-gal reflecting the low level of Miller units in wild-type (data

not shown). After several selections of mutants, I got a mutant, which showed a dark blue colony in the X-gal plate and higher Miller unit in the β-galactosidase assay. This mutant revealed that the transposon was inserted in the *STM4464* gene. However, there was no effect of *STM4464* on the ADI expression in the previous qRT-PCR result. These results made me ambiguous about the ADI regulation. Then I questioned that *lacZ*-fusion into the *STM4467* gene had a polar effect on the *STM4463* expression because *STM4463* has its own promoter (Fig. 8). I compared the expression level of *STM4463* in both wild-type and *STM4467-lacZ* fusion strains by qRT-PCR. Expectedly, the expression of *STM4463* was suppressed in the *lacZ*-fusion strain concluding that the low level of Miller units in the wild-type was due to the suppression of *STM4463*. Therefore, I changed the method for the ADI expression from β-galactosidase assay to qRT-PCR for accuracy, even though two experiments resulted in same patterns of the ADI expression.

To manipulate the ADI operon in detail, I decided to identify the transcriptional start site and characterize promoter region. At first time, I purified RNA samples for PE analysis at the normal growth condition, like exponential phase in LB medium with aeration. At that time, I could get a transcriptional start site band (+1, bottom promoter), which locates 29 bp upstream from the start codon. But the intensity of band was too low

reflecting the β-galactosidase results that the expression levels of the ADI represent low Miller units. Therefore, I obtained again the RNA from ADI overexpression condition (WT/p4463) and then found another transcriptional start site (+1', upper promoter), which showed thicker band at the PE results. There was also a low intensity band, which is relevant to the bottom promoter (Fig. 6). Interestingly, the expression of transcript from upper promoter was dependent on the amount of STM4463; even, without STM4463, there was no transcript band for upper promoter, indicating that STM4463 acts on the upper promoter region during its regulation of ADI expression.

Bacterial DNA-binding proteins of CRP/Fnr family regulate the expression of specific genes in response to distinct external signal (110). The CRP protein of *E. coli* is the best-characterized member of the family. Genes in the identified ADI clusters are often transcribed as an operon and the expression of the ADI operon is regulated by a regulatory protein of the CRP/Fnr family (127). In the PE results and sequence analysis, there was a complete CBS in the upper promoter (Fig. 9). Therefore, I tried to estimate the regulation of CRP as another regulator for the ADI expression. Therefore, I tried to estimate the regulation of CRP as another regulator for the ADI expression. In the *crp* single mutant, the effect of ADI was abruptly decreased both in the qRT-PCR and β-galactosidase assay. CRP

protein mediates catabolism of other carbon sources via cAMP. The concentration of cAMP is determined by the availability of glucose. When glucose is transported, the phosphate group from enzyme III^{glc}-P is rapidly transferred to glucose so the concentration of enzyme III^{glc}-P remains low. Under these conditions, adenylate cyclase has low enzymatic activity, thus the concentration of cAMP remains low (168, 176). Adding of glucose up to 10 mM decreased the expression of ADI only when CRP protein existed (Fig. 13) confirming the CRP regulation again. One interesting result is that the ADI regulation by STM4463 was dependent on CRP. When I deleted *crp* gene, the induction of *STM4463* on the plasmid (p4463) failed to up-regulate the ADI expression in all transcriptional analysis (Fig. 14). From these results, I hypothesized that there were complex interactions between CRP and STM4463. Therefore, I tried to purify both proteins and wanted to test protein-DNA interaction and protein-protein interaction. Firstly, I purified CRP protein and confirmed that CRP directly bound to the upper promoter, which has a CBS at -35 region (Fig. 11). However, I failed to obtain a pure form of STM4463 protein because of its insolubility. If I could purify *STM4463*, it will be clearer on the interaction between two different but same type of regulator.

In the results, I also found that the patterns of *STM4463* regulation were similar to that of *STM4467*: both anaerobicity and addition of L-arginine

increased the expression of *STM4463* (Fig. 6A). Moreover, glucose inhibited the *STM4463* expression and there was no transcription of *STM4463* in the *crp* mutant (Fig. 15). If the expression of *STM4467* was dependent strictly on the *STM4463*, these signals might be sensed by STM4463 firstly. Therefore, the regulation of *STM4463* would be more important for the ADI expression in different conditions. Recently, it has been known that a transcriptional regulator, ArgR (STM4463 homolog) was under control of CRP in nitrogen metabolism in *E. coli* (181). Therefore, CRP regulation might be related to the induction of ADI by L-arginine.

Because of the CRP regulation on the *STM4463*, I needed to assess the binding of CRP to the *STM4463* promoter. Expectedly, CRP protein specifically bound to the promoter region of *STM4463* (a possible binding sequence, TGTGA-N_6-TCGCC in Fig. 15). These results represent a new regulation of CRP. CRP activates both *STM4467* and *STM4463* via a direct binding to their promoter. Especially for *STM4467*, CRP mediates the regulation of *STM4463*. In my knowledge, there is no report about the coordinated regulation by CRP until now.

To elucidate another effector protein for ADI regulation, I tested some regulators: *rcsB*, *argI*, and *fis*. RcsB and RcsC act as the effector and the sensor, respectively, of a two-component regulatory system by stimulating capsule synthesis from colonic acid synthesis *cps* genes (187). The *argI* gene

encoding ornithine carbamoyltransferase subunit I is located upstream of ADI operon. The factor-for-inversion stimulation protein (Fis) is a histone-like DNA binding protein involved in nucleoid organization and modulation of many DNA transactions, including transcription in enteric bacteria (66, 202). When I constructed deletion mutants for those genes and assessed the transcription of *STM4467*, only *fis* gene deletion changed the expression level of ADI (Fig. 18A and data not shown for other genes). Interestingly, this negative regulation by Fis worked well only with STM4463 (Fig. 18A). Understandably, Fis had a down-regulation on the expression of *STM4463* and therefore it could be said that ADI was regulated by Fis via STM4463 (Fig. 18B).

In *E. coli*, ArcA (Aerobic Respiratory Control) is one of the main transcriptional regulators involved in the metabolic shift from anaerobic to aerobic conditions and controlling the enzymatic defenses of bacteria against reactive oxygen (80). ArcA is a cytosolic response regulator of a two-component regulatory system, ArcA/ArcB. ArcB is a transmembrane histidine kinase sensor transferring a phosphoryl group to ArcA. Activated ArcA induces or represses a large number of regulons, which have been thoroughly characterized in *E. coli* (151, 171). The intracellular level of the functional ArcA regulator, phosphorylated ArcA (ArcA-P), is sensitively regulated by the oxidation/reduction status of the cell. Under anaerobic

conditions, ArcB autophosphorylates and then transphosphorylates AcrA, which then binds to the target promoter, thereby exerting regulatory effect on the target genes (44, 102). Recently, a broad analysis on the ArcA regulon in *S*. Typhimurium has been done by microarray (57). In this analysis, there is a clue for the ADI regulation by anaerobicity. Fis was highly repressed by AcrA in anaerobic condition. Moreover, they presented that ArcA activates STM4463, without any concrete explanation (57). In my study, I elucidated that Fis repressed the expression of STM4463. Therefore, I could explain that the activation of STM4463 by ArcA might result from the negative regulation of repressor, Fis by ArcA. Therefore, I constructed *arcA* deletion mutant and could find that the expressions of *STM4467* and *STM4463* were abruptly decreased at an anaerobic condition (Fig. 20A). These results support the regulation of ADI via activator, STM4463 by a global transcriptional factor ArcA for a relevant expression of ADI in anaerobic condition.

Polyamines are small polycationic amines ubiquitous in all living organisms. In bacteria, the predominant polyamines, putrescine and spermidine, have been implicated in a variety of functions including intercellular signaling, stress resistance and RNA and protein synthesis (39, 188). In this study, putrescine and spermidine activated the expression of ADI (Fig. 19). Between two polyamines, spermidine was more effective for

the induction of ADI indicating that spermidine is a signal and putrescine might affect after converting to spermidine. Moreover, two polyamines were related to the AcrA regulation. Without AcrA, putrescine and spermidine could not increase the expression of ADI (Fig. 20B). In *E. coli*, it has been known that polyamines stimulate ArcA synthesis (167). Therefore, it is possible that two polyamines also act as signal for the activation of ArcA and then, ArcA stimulates the expression of ADI in *S*. Typhimurium.

Although there was no direct clue for the interaction of STM4463 on the ADI promoter, I could finally make a mechanism of ADI regulation in *S*. Typhimurium from all these results (Fig. 21). In the normal culture condition, *Salmonella* express ADI at a very low level. Although, this expression arises from both upper (+1') and bottom promoter (+1) of ADI operon, two promoters are equally week for their acting on the ADI expression. Several environmental signals like anaerobicity, polyamines, and L-arginine will enhance the expression of *STM4463* firstly. In this regulation, CRP directly binds to the CBS in the promoter of *STM4463* activating its expression. Moreover, another regulator, Fis acts on the *STM4463* like as a repressor. Subsequently, the ADI regulator, STM4463, continues its assignment: the activation of ADI expression. According to several clues and analysis, I reached this conclusion that STM4463 is a derepressor. In the transcriptional analysis, ADI could be expressed

abruptly high level when STM4463 was overexpressed. However, STM4463 could not activate the ADI expression without CRP. STM4463 itself does not work on the promoter directly. Moreover, there was no interaction between STM4463 and CRP in bacterial two-hybrid analysis (data not shown). In other words, STM4463 does not induce the binding of RNAP to the promoter. Instead, there might be an unknown repressor in the ADI promoter. STM4463 will pull the repressor apart from the promoter as a derepressor, and then CRP will help RNAP bind to the promoter as an activator resulting in great expression of ADI. When I induced the *crp in trans*, this could not increase the expression of ADI as much as STM4463 overexpression (data not shown). This makes sense that CRP induces the proper interaction of RNAP to the ADI promoter (upper), but unknown repressor blocks the way of progress of RNAP. STM4463 acts on the repressor removing from the blocking, and then CRP-induced RNAP keeps on walking on the promoter expressing ADI transcript.

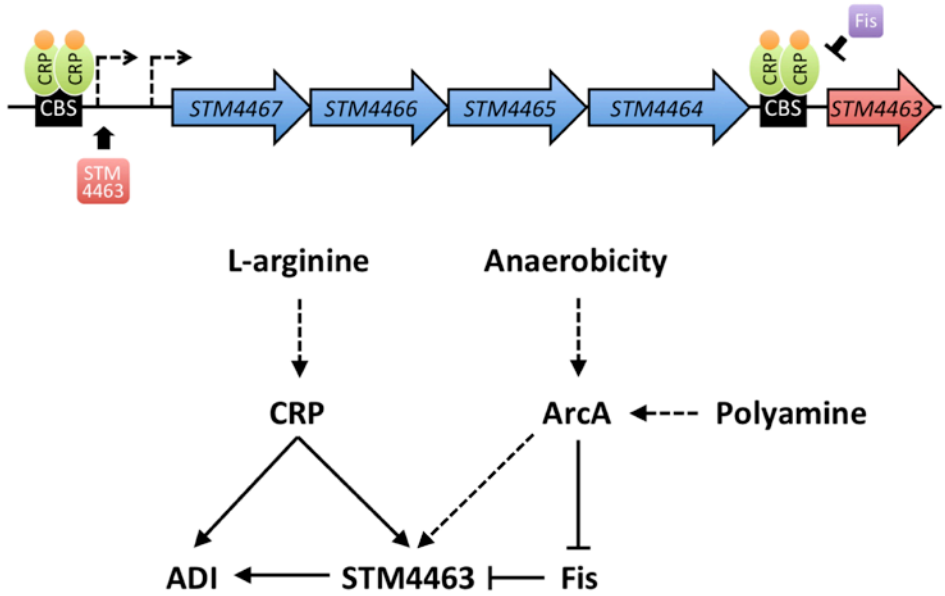

Figure 21. A schematic model of ADI regulation in *S.* Typhimurium.

PART II:

A Role of ADI in virulence of *S.* Typhimurium

Introduction

A facultative intracellular lifestyle is common among pathogenic bacteria. The intracellular life on one hand protects bacteria from a variety of immune responses of the host organisms and on the other hand, allows the utilization of host cell molecules limited in the host organisms. Bacterial pathogens have evolved two main categories of intracellular life. Members of one group have the ability to lyse the vacuole and escape into the host cell cytoplasm. *Listeria monocytogenes* and *Shigella* spp. are the best-studied pathogens in this group. A benefit of the cytoplasm is the direct access to metabolites and various nutrients of host cell. The other group of intracellular bacteria has evolved various strategies to persist and replicate within membrane-bound compartments, and *Salmonella* belongs to this group. *S.* Typhimurium can survive and efficiently replicate in a unique membrane-bound compartment, SCV, actively modifying the biogenesis of this vacuole throughout intracellular life. Within the SCV, a large number of bacterial factors are required for successful intracellular pathogenesis, and recent observations showed that the intracellular pathogen can actively manipulate the host cell in order to maintain the parasitophorous vacuole, to avoid antimicrobial activities of the host cell and to acquire nutrients for

intracellular replication (2, 53, 84, 144). Intracellular life of *Salmonella* is dependent on a large number of virulence traits, but the function of the T3SS encoded by SPI2 is of central importance. Although more than 20 effector proteins have been identified as translocated by the SPI2-T3SS, the molecular function and contribution to intracellular live is only known for a few of these proteins. Previous studies revealed that purine, pyrimidine and amino acid auxotroph of *S*. Typhimurium are unable to survive inside macrophages (64, 94). In addition, *S*. Typhimurium appeared to activate an alternative metabolic pathway for utilization of carbon sources during growth inside macrophages (56). These findings demonstrate that bacterial metabolism is a crucial determinant for their successful pathogenesis (42).

In addition to the metabolic function, the ADI system is also employed to protect some bacteria from stressful conditions. In oral streptococci and *Streptococcus pyogenes*, the ADI system helps the bacteria to resist against acidity by generating ammonia and thus neutralizing the pH (36, 49). Moreover, though it is rare, the ADI system plays roles in bacterial pathogenesis. ADI was necessary for *S. pyogenes* to invade into and survive inside epithelial cells (49). In *P. aeruginosa*, ADI pathway increased in cystic fibrosis (CF) isolates from end-stage disease and thus seemed to be additional biomarkers for the anaerobic CF lung adaptation (93). And, in the case of *Listeria monocytogenes*, the lack of ADI impaired its survival in

the spleen during mouse infection (170). An ADI-associated regulator, ArgR is not only essential for ADI expression, but also necessary for the biological fitness of *Streptococcus suis* (71).

In the present study, I investigated the role of the ADI system in *S*. Typhimurium pathogenesis. I found that a *S*. Typhimurium strain lacking the *STM4467*-ecoded ADI is defective for the ability of replication inside macrophages and attenuated for virulence in mice. I also revealed that the *STM4463*-encoded regulator contributes to *S*. Typhimurium virulence by up-regulating expression of the ADI gene cluster within macrophages.

Materials and Methods

Bacterial strains, and growth condition

The bacterial strains and plasmids used in this study are listed in Table 1. *S*. Typhimurium strains were derived from the strain 14028s. Phage P22-mediated transductions were performed as described previously (96). Bacteria were grown at 37°C in LB medium. Ampicillin, chloramphenicol, kanamycin and IPTG were used at 50 μg/ml, 25 μg/ml, 50 μg/ml, and 0.5 mM, respectively.

Construction of strains

The *S*. Typhimurium strain CH102, which is deleted for the *STM4467* gene, was constructed using the one-step gene inactivation method (48). The Km^r cassette from the plasmid pKD13 (48) was amplified using primers STM67-lamb-F (5′-ACTCCTTCTTTATTCTTGTAATTATGTAAAAGGTATAATGT GTAGGCTGGAGCTGCTTCG-3′) and STM67-lamb-R (5′-CGCGACGAC CAGTGTGCGTTTGTTTTCCATAACGTCTCCTATTCCGGGGATCCGTCG ACC-3′). The resulting PCR product was integrated into the *STM4467* region in the strain 14028s, and the Km^r cassette was subsequently removed using plasmid pCP20 (48). The CH201 strain is deleted for the *STM4463*

gene. For its construction, the Cm^r cassette of pKD3 (48) was amplified using primers STM63-lamb-F (5′-CGTTGATATCAATAATAAAGATAAG GTGCATTTATGAAGGTGTAGGCTGGAGCTGCTTCG-3′) and STM63-lamb-R (5′-ATTAATGCATGATTTACTCATCGCAAACGGTTCTTATGAA ATATGAATATCCTCCTTAGTTC-3′) and was integrated into the *STM4463* region in the strain 14028s. Deletion of the corresponding genes was verified by colony PCR. The CH110 strain, which carries a transcriptional *STM4467-lacZ* fusion, was constructed as described previously (55). The *lacZY* genes were introduced into the FRT site in the strain CH102 using plasmid pCE70 (134).

Construction of plasmids

The plasmid p4467 expresses the *STM4467* gene from its own promoter. For its construction, the *STM4467* gene was amplified using PCR with primers STM4467-pACYC-F (5′-TTGTTTTTTGAAGCTTTCTGACCC-3′) and STM4467-pACYC-R (5′-ACGACCAGCATGCGTTTGTTTT-3′) and chromosomal DNA from strain the 14028s as a template. The product was introduced between the HindIII and SphI restriction sites of pACYC184 (38). Plasmid pPM4463, which expresses the *STM4463* gene from its own promoter, was constructed. The *STM4463* gene was amplified using primers STM4463-pACYC-F (5′-GAAAGTCTGAATTCCGGCCTCTC-3′)

and STM4463-pACYC-R (5′-TTTACTCATCGCATGCGGTTCTTATG-3′). The PCR product was introduced between the HindIII and SphI restriction sites of pACYC184 (38). The sequences of the *STM4467*- and *STM4463*-coding regions on the recombinant plasmids were verified by nucleotide sequencing.

Cell culture

J774A.1 (ATCC TIB-67™), a murine macrophage-like cell line, was maintained in DMEM supplemented with 10% FBS, penicillin (50 U/ml) and streptomycin (50 U/ml) at 37°C under 5% CO_2. Cell cultures were replaced after passage #15.

Gentamicin protection assay

The experiment was conducted as described previously (42). J774A.1 macrophage cells were grown in DMEM supplemented with 10% FBS, penicillin (50 U/ml) and streptomycin (50 U/ml). Prior to bacterial infection, monolayer of 1×10^5 J774A.1 cells was prepared in a 24-well tissue culture plate and incubated in DMEM-10% FBS without antibiotics at 37°C for 1 h under 5% CO_2. A bacterial culture grown to stationary phase with aeration was applied onto the cell monolayer at a multiplicity of infection (MOI) of 10. After 1 h incubation, the wells were washed three times with pre-

warmed PBS to remove extracellular bacteria and then incubated for 1 h with the pre-warmed medium supplemented with 100 μg/ml of gentamicin to kill extracellular bacteria. Afterward, the wells were washed three times with PBS, lysed in 1% Triton X-100 for 30 min, and then diluted in PBS. A dilution of the suspension was plated on LB agar medium to enumerate the colony-forming units (CFUs).

Mouse virulence assay

Bacterial cells grown overnight in LB medium were pelleted, washed and suspended in PBS. Eight-week-old C3H/HeN female mice were used to assess the virulence of *S.* Typhimurium strains. Approximately 10^4 bacterial cells in 200 μl of PBS were injected intraperitoneally into groups of mice (5 mice/group), and the survival of the mice was recorded over 3 weeks. To analyze bacterial colonization in organs, the mice were sacrificed at 5 days after infection, and the spleens and livers were removed aseptically. The organs were homogenized in 1 ml of ice-cold PBS and serially diluted. Bacterial loads were determined by plating the diluents on LB agar plates.

Determination of nitrile concentration

J774A.1 macrophage cells were infected with bacteria as described above in triplicate. Supernatants were harvested at 18 h after infection. The nitrite concentration was measured using the Griess assay (76). Briefly, 50 µl of culture supernatants were mixed with an equal volume of Griess reagent (Promega). Absorbance was measured after 10 min at 550 nm in an ELISA microreader (SUNRISE-BASIC, TECAN). A $NaNO_2$ was used to establish the standard nitrite concentration in the supernatants.

RNA isolation and qRT-PCR analysis

For RNA extraction from *S.* Typhimurium growing inside J774A.1 macrophage cells, infection experiment was conducted as described above except for the increased volume of macrophage cell cultures (50 ml in 75 Cm^2 T-flask). At 1 h, 6 h and 18 h after infection, macrophage monolayers were washed, lysed in 1% Triton X-100 and centrifuged at 1,000 rpm for 5 min to pellet the lysed macrophage cells. From the supernatant containing intracellular bacteria, RNA was extracted by using RNeasy Mini Kit (QIAGEN). The RNA samples were then treated with RNase-free DNase (Ambion), and cDNA was synthesized using Omniscript reverse transcription reagents (QIAGEN) and random hexamers (Invitrogen). Quantification of cDNA was carried out using 2X iQ SYBR Green Supermix

(Bio-Rad), and real-time amplification of the PCR products was performed using the iCycler iQ real-time detection system (Bio-Rad). The calculated threshold cycle (C_t) corresponding to a target gene was normalized by the C_t of the control *rpoD* gene. The sigma factor *rpoD* gene was chosen as a control because no significant variation of *rpoD* expression was observed inside macrophages (63). The sequences of primers used in the qRT-PCR analysis were listed in Table 4.

Statistical analysis

Statistical analyses were conducted using the GraphPad Prism program (version 5.0). Survival curves of animal experiments were analyzed by the log-rank test, and all other results were analyzed by the unpaired *t*-test. Data were represented as mean ± standard deviation. A P value of <0.05 was considered statistically significant.

Ethics statement

This study was carried out according to the recommended protocol for the care and use of laboratory animals from the Institute of Laboratory Animal Resource in Seoul National University based on the Korean Animal Protection Law and Korea Food and Drug Administration regulation on the laboratory animals. The protocol was approved by the Committee on

the Ethics of animal experiments of Seoul National University (Institutional Animal Care and Use Committee permit number: SNU-120616-1).

Results

The *STM4467* gene contributes to *Salmonella* virulence

ADI is necessary for *S. pyogenes* invade into and survive inside epithelial cells (49). In *L. monocytogenes*, a mutant that lacked ADI survived less than wild-type in the spleen during a mouse infection (170). These findings suggested a role for ADI in bacterial pathogenesis.

To explore whether the *STM4467*-encoded ADI could contribute to *Salmonella* virulence, I initially compared the replication abilities of the wild-type and *STM4467* deletion strains within murine macrophages. The gentamicin protection assay revealed that the number of the *STM4467* deletion mutant within the macrophages was only ~30% with respect to the wild-type at 18 h post-infection (Fig. 22A). This result was not due to differences in the phagocytosis of the two strains because intracellular numbers of the two strains were similar at an earlier time point (i.e., 1 h) after infection (Fig. 22A). The phenotypic defect of the *STM4467* deletion strain was due to the function of STM4467 because expression of the *STM4467* gene from a plasmid enabled the *STM4467* deletion mutant to replicate within macrophages at a level similar to that of the wild-type strain (Fig. 22A).

Intramacrophage survival is necessary for *Salmonella* to systematically infect mammalian hosts. Thus, I reasoned that the *STM4467* deletion mutant might be attenuated for virulence in mice. To test this hypothesis, I injected *Salmonella* into groups of 5 mice via an intraperitoneal route. As illustrated in Fig. 13B, all of the mice inoculated with the wild-type strain died within 10 days, whereas 90% of mice that received the *STM4467* mutant survived over 3 weeks post-infection. I further verified the virulence phenotype of the *STM4467* deletion mutant by determining numbers of bacterial cells in organs of mice. In both the liver and spleen, the numbers of the *STM4467* deletion mutant were ~10-fold smaller than those of the wild-type strain at 5 days post-infection (Fig. 22C). This phenotypic difference was due to the function of STM4467 because the *STM4467* deletion strain carrying the STM4467 expression plasmid was able to colonize the liver and spleen as efficient as the wild-type strain (Fig. 22C). Taken together, these results suggest that in the absence of *STM4467*-encoded ADI activity, *S*. Typhimurium fails to avoid killing by macrophages and thus is attenuated for virulence.

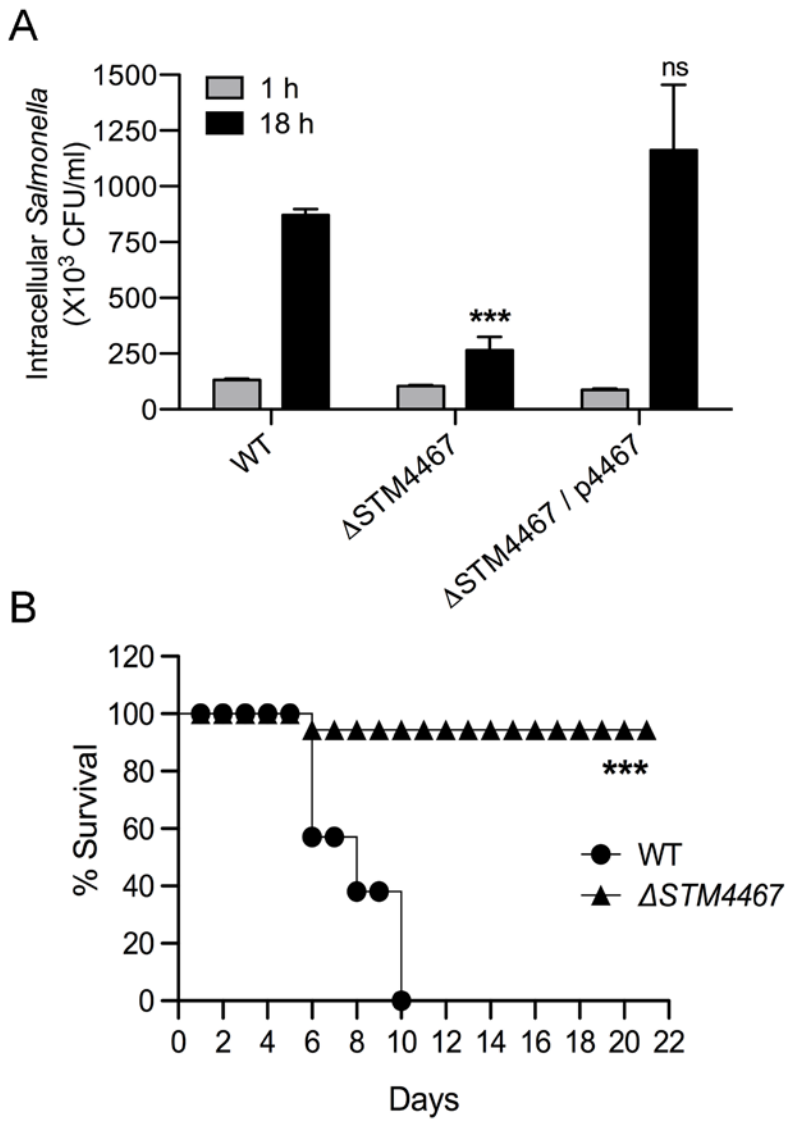
A
Intracellular Salmonella
(X10^3 CFU/ml)
1500
1250
1000
750
500
250
0
1 h
18 h
***
ns
WT
ΔSTM4467
ΔSTM4467 / p4467
B
% Survival
120
100
80
60
40
20
0
***
WT
ΔSTM4467
0 2 4 6 8 10 12 14 16 18 20 22
Days

C

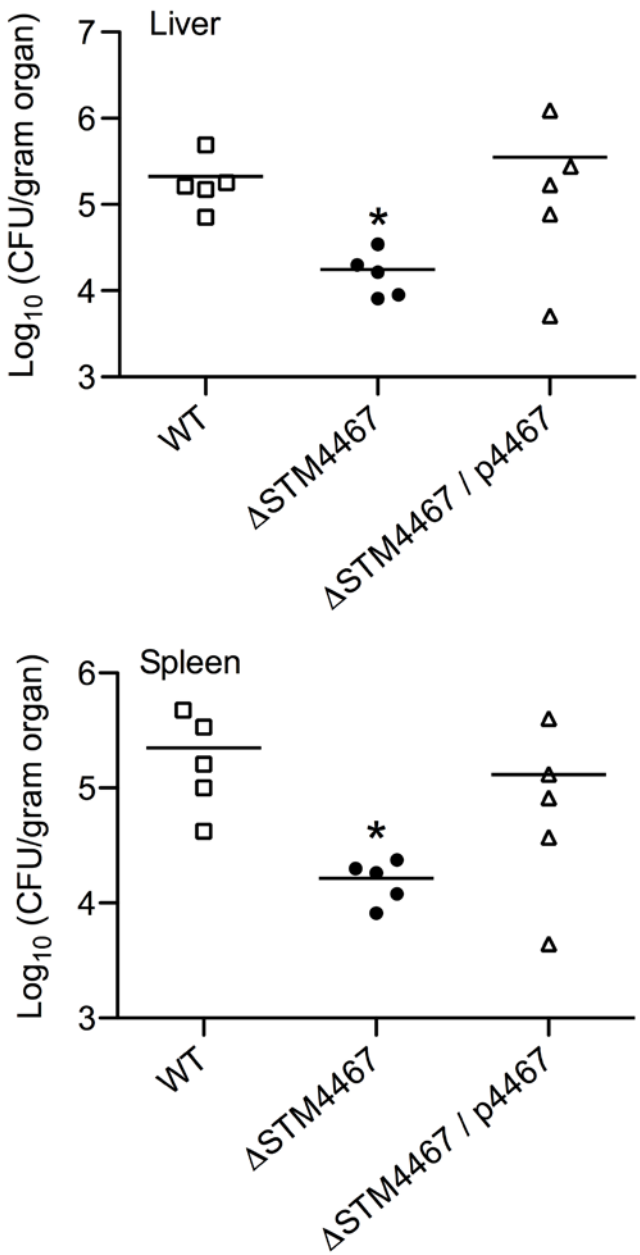
Liver
Log10 (CFU/gram organ)
7
6
5
4
3
*
WT
ΔSTM4467
ΔSTM4467 / p4467
Spleen
Log10 (CFU/gram organ)
6
5
4
3
*
WT
ΔSTM4467
ΔSTM4467 / p4467

Figure 22. The *STM4467* gene is necessary for *S.* Typhimurium virulence. (A) J774A.1 macrophage cells were infected with the wild-type (WT) strain (14028s), the *STM4467* deletion mutant (CH102), or strain CH102 harboring the p4467 plasmid (*ΔSTM4467*/p4467). The numbers of intracellular bacteria were determined at 1 and 18 h after infection by using the gentamicin protection assay. Means and standard deviations from at least three independent experiments are shown. Triple asterisks indicated that the numbers of bacteria were significantly different ($P < 0.001$) from those of the WT strain at 18 h postinfection; no, not significantly different. (B) Groups of C3H/HeN mice (5 mice/group) were injected intraperitoneally with ~ 10^4 cells of the WT strain or the *STM4467* deletion mutant. The survival of the mice was monitored daily for 3 weeks. The results of one of two independent experiments ($P < 0.001$), which yielded similar results, are shown. (C) Groups of C3H/HeN mice (5 mice/group) were infected with the WT strain, the *STM4467* deletion mutant, or strain CH102 harboring the p4467 plasmid as described for panel B. At 5 days after infection, the numbers of bacteria in the liver and spleen were determined. An asterisk indicates that the numbers of bacteria were significantly different ($P < 0.05$) from those of the WT strain.

Expression of the ADI pathway genes is enhanced inside macrophages

When pathogenic bacteria are growing within host cells, expression of genes important for their viability is often induced. Therefore, I hypothesized that expression of the *STM4467* gene might increase when *Salmonella* cells are inside macrophages. To test this hypothesis, I isolated RNA from wild-type *Salmonella* grown within macrophages and determined transcription levels of genes by conducting qRT-PCR. I found that *STM4467* transcription was enhanced in *Salmonella* growing inside macrophages: the *STM4467* mRNA levels increased by ~ 4-fold at 18 h compared to those at 1 h after bacterial entry into macrophages (Fig. 23A). Consistent with notions that the ADI system genes constitute an operon producing a polycistronic mRNA (18, 77), transcription levels of the *STM4466* and *STM4465* genes respectively encoding putative CK and OTC were also elevated at 18 h after phagocytosis (Fig. 23A).

In response to environmental cues inside phagosome, *Salmonella* expresses series of genes from *Salmonella* pathogenicity island 2 (SPI2), which mediates its survival within macrophages (83, 111). Therefore, induction of the SPI2 gene *ssaG* under our experimental setting (Fig. 23A) reflects that up-regulation of the ADI pathway could occur in response to environmental cues inside phagosome. It is noteworthy that induction of

the ADI pathway was observed only at 18 h after phagocytosis (Fig. 23A), the timing of which was slower than that of the SPI2 gene occurring at 6 h after bacterial entry into macrophages (Fig. 23A) (43). Thus, given that the environment within *Salmonella*-containing phagosome is dynamically changed, expression of the ADI system might be important at later stage of infection than the onset of expression of the SPI2 genes.

STM4463 regulator is necessary for *Salmonella* to express the ADI gene cluster and replicate inside macrophages

As the STM4463 protein appeared to enhance ADI expression (Fig. 8), I reasoned that the STM4463 regulator might be responsible for intramacrophage induction of the ADI system. To test this possibility, I examined transcription of the *STM4467*, *STM4466* and *STM4465* genes within macrophages. qRT-PCR analysis revealed that in contrast to the wild-type strain, the *STM4463* deletion mutant failed to induce expression of these three genes at 18 h after phagocytosis (Fig. 23B). The failure of the *STM4463* mutant to induce the ADI gene cluster is not due to a general expression defect because the intra-phagosomal induction of the SPI2 gene *ssaG* was unaffected by the *STM4463* deletion (Fig. 23B).

I then hypothesized that the STM4463 regulator could contribute to *Salmonella* virulence by activating ADI expression within macrophages. Indeed, the lack of STM4463 impaired *Salmonella*'s ability to replicate inside macrophages. The intracellular numbers of *STM4463*-deleted *Salmonella* were ~3-fold smaller than those of the wild-type strain at 18 h after phagocytosis (Fig. 24). This defective phenotype was due to the function of STM4463 because the replication ability of the *STM4463* deletion mutant was recovered by expression of the *STM4463* gene from a plasmid (Fig. 24). Numbers of the both wild-type and *STM4463* deletion strains inside

macrophages were similar at 1 h after infection, showing that the STM4463 regulator did not interfere with phagocytosis.

In the wild-type strain, transcription levels of the *STM4463* gene increased ~2-fold at 18 h after phagocytosis (Fig. 23A), concurrently with ADI pathway induction (Fig. 23A). In addition, the induction of the STM4463 regulator greatly increased the expression of the *STM4467* gene (Fig. 8). Therefore, although the precise mechanism of how STM4463 expression is controlled within macrophages is presently unclear, I propose that levels of the STM4463 regulator are promoted by unknown signals present inside the phagosome, which in turn activate expression of the ADI system.

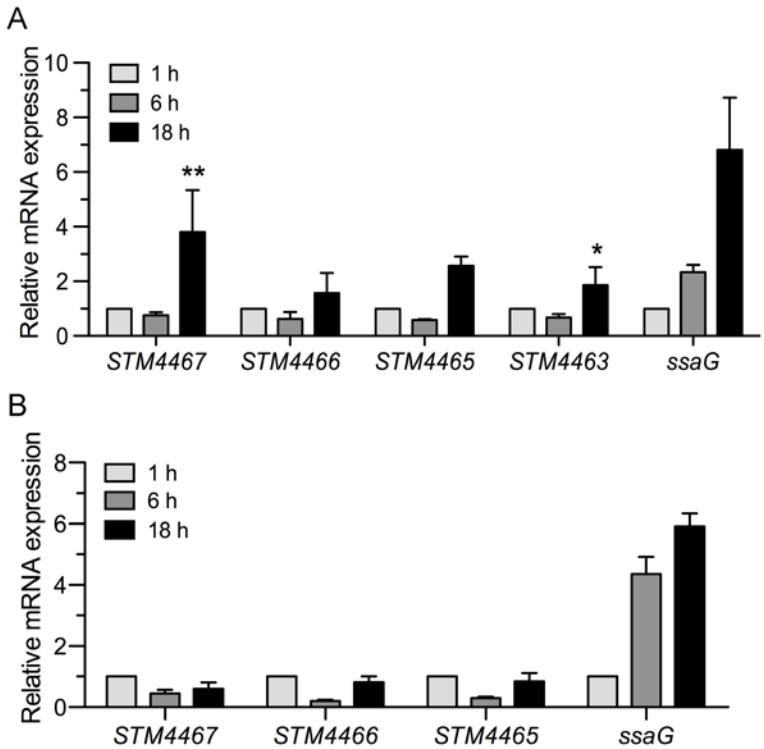

Figure 23. Expression of the ADI system is enhanced inside macrophages in an STM4463-dependent manner. The transcription levels of the *STM4467*, *STM4466*, *STM4465*, *STM4463*, and *ssaG* genes in *S.* Typhimurium growing inside macrophages were determined via qRT-PCR. J774A.1 macrophages were infected with the wild-type (14028s) (A) or the *STM4463* deletion strain (CH201) (B), and bacterial RNA was isolated at 1 h, 6 h, and 18 h after infection. To obtain the relative mRNA expression values on the y axis, the mRNA levels of each gene were divided by those of the *rpoD* gene, which were further normalized by the transcription levels displayed at 1 h after infection. Means and standard deviations from three independent experiments are shown. Asterisks indicate significant differences (**, $P < 0.01$; *, $P < 0.05$) in mRNA levels between the 1-h and 18-h samples.

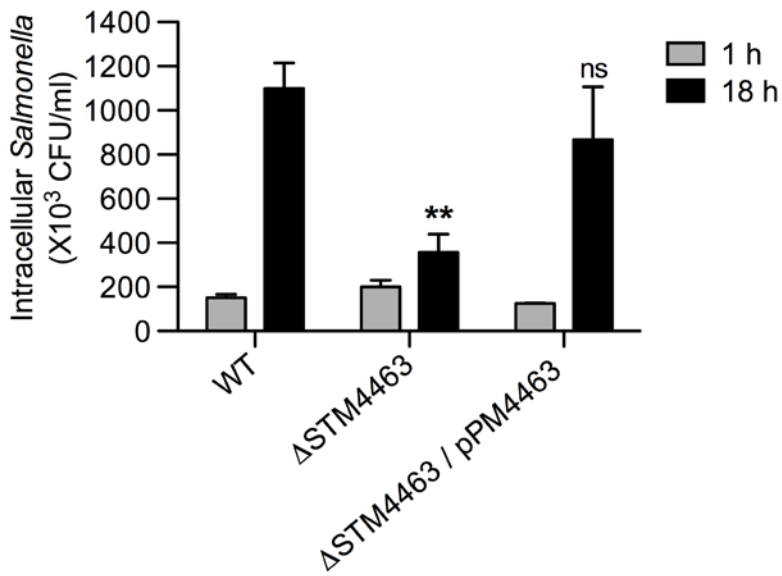

Figure 24. The STM4463 regulator is necessary for *S.* Typhimurium replication inside macrophages. J774A.1 macrophages were infected with the wild-type (WT) strain (14028s), an *STM4463* mutant (CH201), or strain CH201 carrying plasmid pPM4463 (*ΔSTM4463*/pPM4463). The numbers of intracellular bacteria were determined at 1 h and 18 h after infection. Means and standard deviations from at least three independent experiments are shown. Asterisks indicate that the numbers of bacteria are significantly different (**, $P < 0.01$) from those of the WT strain at 18 h post infection; ns, not significantly different.

STM4467 does not affect levels of nitric oxide production inside macrophages

After phagocytosis, bacterial cells are killed inside phagosome by actions of microbicidal products (68, 81). Of these antimicrobials, nitric oxide (NO) is synthesized from arginine by NO synthase (NOS), and the availability of arginine is one of the rate-limiting factors in cellular NO production (7, 62, 144). *S*. Typhimurium seems to have a means to control host arginine metabolism by which it can avoid NO toxicity. On the basis of these notions, I hypothesized that the enhanced ADI activity within phagosome might reduce NO levels by consuming arginine, which helps *Salmonella* to avoid NO-mediated killing by macrophages. To test this idea, I determined NO levels in macrophages with or without *Salmonella* infection. The result showed that infection by wild-type *Salmonella* dramatically increased NO levels in macrophages (Fig. 25), which is in good agreement with the notion that NOS activity is inducible upon bacterial infection (90). I found that the levels of NO production stimulated by *STM4467*-deleted *Salmonella* were comparable to those by wild-type (Fig. 25). Therefore, this result suggests that the *STM4467*-encoded ADI activity contributes to *Salmonella*'s intramacrophage survival via an alternative mechanism unrelated with NO production.

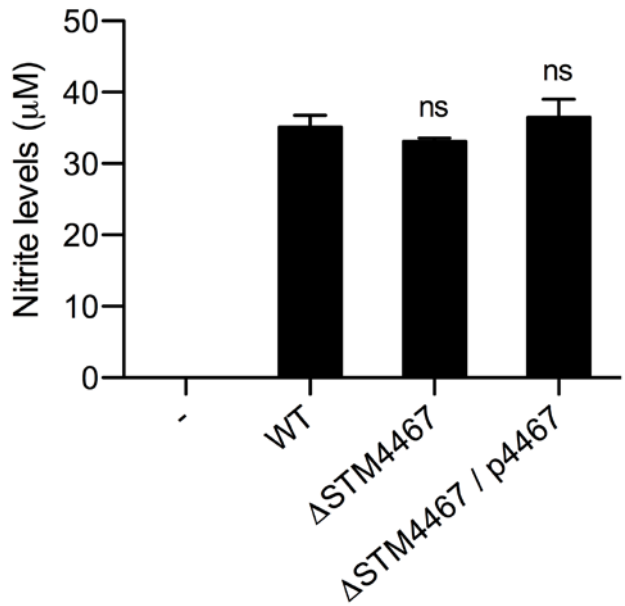

Figure 25. The *STM4467*-encoded ADI has no effect on NO_2^- generation by macrophages. J774A.1 macrophages were infected with the wild-type (WT) strain (14028s), an *STM4467* deletion mutant (CH102, *ΔSTM4467*), or strain CH102 harboring plasmid p4467 (*ΔSTM4467*/p4467). At 18 h after infection, levels of NO_2^- production in the supernatants of macrophages were determined by using the Griess reaction. Note that NO_2^- was nearly absent from macrophages without (-) *S*. Typhimurium infection. Means and standard deviations from three independent experiments are shown. "ns" indicates that the nitrite levels of bacteria are not significantly different from those of the WT strain.

Discussion

In other bacteria, ADI pathway has been associated with growth in specific environment and pathogenesis. Studies have shown that an *arcA* homologue in various streptococcal species is associated with reduced invasion and intracellular growth (170), and it has been postulated that the ADI pathway may contribute to the pathogenic nature of this bacterium (203). To assess ability of survival/replication of *Salmonella* inside macrophages, I conducted macrophage survival assay with the macrophage-like cell line J774A.1 as described in the methods. At the screening step to find target gene, only *STM4467* deletion resulted in decrease of survival ability of *Salmonella* within macrophage. Contrary to this, a deletion of other six genes showed the wild-type level of growth (data not shown), leading me to further studying about the effect of ADI pathway on the *Salmonella* pathogenesis. Return to the ADI, I assessed the expression level and pattern of the ADI gene in the macrophage during infection. The validity of expression of the ADI gene in the macrophage was supported by a study, which showed the proteome of *S*. Typhimurium (185). They presented that the highest up-regulated protein under *in vivo*-mimicking conditions appeared to be product from a predicted ORF

designated *STM4467* (185) suggesting several hypotheses for the role of ADI in *Salmonella* virulence.

Interestingly, all ADI genes were highly expressed within macrophages but its pattern was different with SPI-2 gene, *ssaG* (Fig. 23). However, there was a dip between 1 and 6 h within cells in the WT and *STM4463* deletion backgrounds in the qRT-PCR: The mRNA levels of the ADI genes and *STM4463* gene decreased at 6 after phagocytosis (Fig. 23). The decrease of expression of these genes cannot be explained by STM4463 regulation because the same decrease still existed in the *STM4463* deletion mutant. I would like to reason that this phenomenon might result from another regulatory effect on the arginine metabolism. This hypothesis could be supported by reports that expression of ADI genes is under the control of glucose catabolite repression in several bacteria such as *Streptococcus gordonii* (52), *Streptococcus suis* (79), *Enterococcus faecalis* (17) and *Lactobacillus sake* (211).

Along with the ADI genes, the regulator, *STM4463* was also increased in its expression during infection. In the transcriptional assay, *STM4463* controlled the regulation of ADI expression from the sensing of the signal for ADI expression to highly effective activation (Fig. 5, 6, 7, and 9). From these results, it is possible that STM4463 activates ADI expression within the macrophage during *Salmonella* infection. Expectedly, *STM4463* deletion

mutant failed to induce expression of ADI genes in the macrophage without the alteration of SPI-2 gene, *ssaG* (Fig. 23B). Moreover, the deletion of *STM4463* also had an effect of the *Salmonella* survival in the macrophage (Fig. 24). Therefore, a possible line of regulation and phenotypic contribution from the positive regulator, *STM4463* to the ADI genes was formed. However, there is a possibility that the failure of expression of the ADI gene cluster partially contributes to the defective survival of the *STM4463* mutant within macrophages. Because, the STM4463 regulator repressed expression of the fimbrial operon *std*, which appeared necessary for full *Salmonella* virulence in mice (40). The effect of *STM4463* and *std* mutations on *Salmonella* virulence was assessed by bacterial colonization in organs of mice that were infected via an oral route (40). But it remains unknown whether STM4463 regulation of the *std* operon could affect *Salmonella*'s survival inside macrophages. I could conclude that the regulator, STM4463 has more broad effects on the *Salmonella's* pathogenesis including an important role for ADI pathway in this study.

In part I, the most effective condition for the activation of ADI expression was an anaerobic condition. The low oxygen enhanced the expression of STM4463 resulting in activation of ADI (Fig. 6). Phagocytes use specific oxygen-derived antimicrobial effector molecules in sequential fashion to inhibit or kill intracellular *Salmonella*. Molecular oxygen is relatively inert

but can be reduced enzymatically to superoxide, a cytotoxic precursor of oxygen radicals (12, 13, 198). Similarly, nitric oxide synthases use oxygen to produce nitric oxide. Moreover, there is a common feature, hypoxia (low oxygen tension), in tumors, wounds, and inflamed or infected tissues (23, 100). The oxygen tension in healthy tissues is generally 20-70 mm Hg (2.5-9% oxygen), but much lower levels (<1% oxygen) are present in wounds and tissue foci of infection (150, 210). The hypoxia-inducible transcriptional factor (HIF-1α) is a major regulator to low oxygen stress (45, 150, 210). The influence of low oxygen tension on macrophage responses to microorganisms has been studied (118, 147). Bacterial products such as LPS and peptidoglycan can activate TLRs and NF-κB signaling to increase the transcription of *Hif1a*. Increased levels of HIF are observed in macrophages stimulated by various bacterial species, including *S. aureus*, *P. aeruginosa*, and *S*. Typhimurium (45, 160, 161), suggesting that HIF serves a general role in bacterial infection. Consequently, when infected by *Salmonella*, macrophage reduces oxygen concentration inside the phagosome by several innate immune functions. Therefore, this reduction of oxygen inside macrophage might be an important signal for the induction of ADI expression in *Salmonella* during infection.

Polyamines; putrescine, spermidine, and spermine, play a regulatory role in a variety of cellular activities (157, 158, 179). In the cell proliferation,

activity of ornithine decarboxylase (ODC), a rate-limiting enzyme in polyamine biosynthesis, is increased, and then polyamines were accumulated (89, 159). However, the role of polyamine is not restricted to proliferation. In macrophage-like cell line, ODC activity was induced by LPS (191, 209) and specific inhibitors of polyamine biosynthesis prevented its accumulation indicating that polyamines are associated with functional activation of macrophages (135). It also has been shown that polyamines play a role in virulence of several intracellular bacteria including *Francisella tularensis*, *Legionella pneumophila*, and *Shigella* spp. (16, 35, 148, 169). Recently a study has shown that polyamines are essential for virulence of *S*. Typhimurium. Polyamines specifically stimulate the expression of both SPI1 and SPI2 genes, indicating that they function as a signal for the control of the virulence gene expression in *S*. Typhimurium (103). Moreover, the expression of polyamine uptake genes is up regulated in *S*. Typhimurium during infection of mammalian cell (56, 87). These reports indicate that polyamines are environmental signals for *Salmonella* during infection. In this study, I also found that polyamine was another inducing signal for ADI expression in *S*. Typhimurium (Fig. 19). At this point of view, polyamines could be a signal for the expression of ADI within macrophage during *Salmonella* infection.

In eukaryotic cells, L-arginine is the substrate of several enzymes, among which the nitric oxide synthases (7, 144). One particular NOS, the inducible NOS is inducible by bacterial LPS, outer membrane proteins or cytokines in a wide range of tissues and cells (130, 204). Therefore, if L-arginine, the primary substrate for iNOS is limiting, only small amounts of NO will be produced, suggesting that the scavenging of L-arginine by the ADI pathway could be a mechanism to avoid accumulation of NO and survive within macrophage. This competition for substrate was already reported for other pathogens (75, 119). However, when I tested nitric oxide production in the macrophage infected by *STM4467* mutant, there was no difference compared to wild-type (Fig. 25). Instead, recent study reported that *Salmonella* up-regulates host arginase II in RAW264.7 macrophages blocking the NO production (115).

PART III

: Identification of the infection mechanism of *Salmonella* phage, iEPS5

Introduction

Bacteriophage infection is initiated by binding of the virion to a specific receptor located on the host surface. The attachment of phages to their host involves a strong interaction between a phage receptor binding protein (RBP) and one of the surface components (117). Some phages use a single, central fiber as their receptor recognition element or adhesion; others use a cluster of 3, 6, or 12 fibers associated with the tail structure. Adsorption may involve multiple steps, such as reversible binding by fibers responsible for initial host recognition and proper baseplate positioning, followed by irreversible binding of a different tail protein to a secondary receptor molecule. The molecular mechanisms by which bacteriophages deliver their genome into the host are far from being elucidated. Following attachment of the phage onto the host surface, a 'signal' is propagated along the tail to the capsid in which the genome is packed. The DNA is then released through the portal pore located at one vertex of the capsid and transported base pair after base pair into the host cytoplasm, leaving the empty phage particle attached to the surface.

Generally, bacteriophages have been found to infect a single bacterial strain only, or related strains from the same species (98, 120, 164). Therefore, the choice of host by phages was considered to be specific event during

their life cycles. The susceptibility of a bacterium to bacteriophage infection is primarily dependent on whether or not the phage can attach to specific attachment sites, receptors, on the cell (98, 120). Representative surface components for receptor are membrane proteins, for example, OmpA (T-even-like phages), FhuA (T5), BtuB (EPS7), and LamB (phage λ) (95, 143, 164). In addition to membrane proteins, a large proportion of phages require lipopolysaccharide (LPS) as their receptor (101, 121, 163), reflecting the dominance of this molecule on the Gram-negative bacteria surface. Another macromolecular structure that is known to bind phages is the flagellum. Phage χ1 (VIII.113) was a first flagellatropic phage was identified in 1936, having a very broad host range in enteric strains (54). Since then, phages of both Gram-negative and Gram-positive bacteria have been shown to require the flagellum, including the coliphage Chi (174) and PBS1 (70, 106), which is specific for motile strains. It is a well-known mechanism for infection of flagellatropic phage, Chi that it attaches to flagellar filaments using its tail fiber and flagellar rotation drives Chi translocation in like manner of a nut on a bolt (174, 177).

The bacterial flagellum is a 20-nm-thick and 10 to 15-μm-long helical filament that protrudes from the cell body. The major function of the flagellum is to enable swimming and chemotaxis in liquid media and swarming on surfaces. *Salmonella* has 6-8 flagella per cell, distributed

around the cell surface (peritrichous arrangement). Each flagellum is a complex structure made of ~ 25 different proteins, each protein present in multiple copies from a few to several thousand. The flagellum can be divided into three major components: a basal body (engine) by which it is anchored in the cell envelope, an external hook (universal joint), which connects the basal body and the filament (propeller) (41, 192).

The basal body has two parts – a moving rotor and a stationary stator, which together constitute the motor. The hook is a curved structure that serves as a flexible coupler between the basal body and the filament, enabling the synchronous rotation of the multiple flagella. While the hook is flexible, the filament is rigid in order to execute its propeller function. The filament is several cell lengths long, composed of thousands of subunits of a single protein (either FliC or FljB) that is capped at its tip by a scaffold protein. The filament is firmly anchored to the basal body, resisting a pulling force of ~60 pN, which is estimated to be at least a 100 times more than the tensile stress experienced by the filament during swimming (47). Flagellum rotation is driven by a transmembrane proton current (PMF or proton motive force) of rotary motor at speeds reaching up to 18,000 rpm (192). The integral-membrane proteins MotA and MotB form the ion-conducting stator complex (19, 108, 123, 146), which are necessary for motor rotation but not for flagellum assembly. The rotor can switch

between clockwise (CW) and counterclockwise (CCW) directions, as defined by an observer looking down the filament toward the cell body. Both rotation and switching are controlled by the FliG protein in the C ring. The other two proteins in the C ring - FliM and FliN - influence switching by binding the phosphorylated form of CheY (CheY-P), a response regulator of the chemotaxis system. CheY-P binding stabilizes the CW conformation; changing the orientation of FliG relative to MotA in such a way that the force exerted by MotA on FliG changes sign (19). This change of rotation is controlled by a chemotactic signal-transduction system that monitors chemical environmental cues. The length of the rod is 25 nm and the hook 55 nm. Two key players - FliK and FlhB - determine the rod-hook length and the switch to late secretion. FliK was first implicated in length control when null mutations in *fliK* were found to produce uncontrolled hook elongation or polyhooks. These mutants failed to make the switch to late of filament secretion, and were non-motile.

In this study, I isolated a novel bacteriophage iEPS5 infecting *Salmonella* specifically. To characterize this phage, morphological and genomic analyses were performed, and *in vitro* adsorption assay and one-step growth curve analysis were conducted for analysis of adsorption rate, latent period and burst size. In addition, random library screening and several flagella and chemotaxis mutants identified the receptor of iEPS5,

flagellar filaments, suggesting a new infection mechanism of flagellatropic bacteriophage.

Table 7. The bacterial strains and plasmids used in PART III

Strain or plasmid	Description	Reference or source [a]
***S.* Typhimurium**		
SL1344	Wild-type	NCTC
CH501	*ΔfliR*	This study
CH502	*ΔflgK*	This study
CH503	*ΔfliA*	This study
CH504	*ΔmotA*	This study
CH505	*ΔcheY*	This study
CH506	*ΔfliK*	This study
CH507	*ΔfliC*	This study
CH508	*ΔfljB*	This study
CH509	*ΔfliC* / *ΔfljB*	This study
CH511	*ΔfliR* / pACYC-*fliR*	This study
CH512	*ΔflgK* / pACYC-*flgK*	This study
CH514	*ΔmotA* / pUHE-*motA*	This study
CH515	*ΔcheY* / pUHE-*cheY*	This study
CH516	*ΔfliK* / pUHE-*fliK*	This study
SJW2811	*ΔfliG* (169-171) / CW-biased	(206)
SJW3076	*ΔcheY* to *cheZ* / CCW-biased	(193)
E. coli		
DH5α	*supE44 hsdR17 recA1 gyrA96 thi-1 relA1*	(82)
EC100D™	*pir*$^{+}$	Epicentre
Plasmid		
pUHE21-2*lacI*^{q}	rep$_{pMBI}$ Ap^{r} *lacI*^{q}	(184)
pACYC184	rep$_{p15A}$ Cm^{r} Tet^{r}	(38)
pKD13	repR$_{6K\gamma}$ Ap^{r}-FRT Km^{r}-FRT	(48)
pKD46	rep$_{pSC101(Ts)}$ Ap^{r} P$_{araBAD}$ γ β *exo*	(48)
pCP20	rep$_{pSC101(Ts)}$ Ap^{r} Cm^{r} *cI*857 λ P$_{R}$*flp*	(48)
pACYC-*fliR*	rep$_{p15A}$ Cm^{r} Tet^{r} *fliR*	This study
pACYC-*flgK*	rep$_{p15A}$ Cm^{r} Tet^{r} *flgK*	This study
pUHE-*motA*	rep$_{pMBI}$ Ap^{r} *lacI*^{q} *motA*	This study
pUHE-*cheY*	rep$_{pMBI}$ Ap^{r} *lacI*^{q} *cheY*	This study
pUHE-*fliK*	rep$_{pMBI}$ Ap^{r} *lacI*^{q} *fliK*	This study

[a] NCTC, National Collection of Type Cultures

Table 8. Oligonucleotides used for the construction of stains and plasmids in PART III

Primer name	Sequence (5′ → 3′)	Purpose
fliR-lamb-F	ATTACGTGCGCACTCTGTTCAGCAATTTACCTTATATCA TCGGATAAACAGAACG*TGTAGGCTGGAGCTGCTTCG*	λ Red deletion of *fliR*
fliR-lamb-R	TTTAAAATTTATTTTCGGATAAACCTTAGTAAAACAGGA TAAAAATTATGGGTTA*ATTCCGGGGATCCGTCGACC*	
flgK-lamb-F	GCCGATAACAACGAGTATTGAAGGATTAAA AGGAACCATC*TGTAGGCTGGAGCTGCTTCG*	λ Red deletion of *flgK*
flgK-lamb-R	TACATCATCTGGGTACTGATACGCATGTCA TCCTTCTCCT*ATTCCGGGGATCCGTCGACC*	
motA-lamb-F	CTGCGCATCCTGTCATAGTCAACAGCGGAA GGATGATGTC*TGTAGGCTGGAGCTGCTTCG*	λ Red deletion of *motA*
motA-lamb-R	CTGCGGCGTTTTACGACGACAATGGGATGA GCCTGATTTT*ATTCCGGGGATCCGTCGACC*	
cheY-lamb-F	TGGCGAAAATCAGTGCCGGACAGGCGATACGTATTTG AACCAGGAGTAGTATTTT*TGTAGGCTGGAGCTGCTTCG*	λ Red deletion of *cheY*
cheY-lamb-R	TCCTGCTGAGCCTTCATCAGCAGGCTTGATAGATGGTT GCATCATCATCGCATCC*ATTCCGGGGATCCGTCGACC*	
fliK-lamb-F	TCTGGCGCTCCTGGCGGGCGCGTTAGGCGC AGACGGCGCA*TGTAGGCTGGAGCTGCTTCG*	λ Red deletion of *fliK*
fliK-lamb-R	GCCGCTTTCCGCCAACTGGGTGCGCAACAT GGGCAGGGCG*ATTCCGGGGATCCGTCGACC*	
fliR-pACYC-F	TCCAGCAATTAAGCTTATATCATCG	Complementation of *fliR* gene in pACYC184
fliR-pACYC-R	ATATCCTGGTGCATGCTTTTTAAAA	
flgK-pACYC-F	ACGAGTATTGAAAGCTTAAAAGGAAC	Complementation of *flgK* gene in pACYC184
flgK-pACYC-R	ACTGATACGCATGCCATCCTTC	
motA-pUHE-F	CCCGACTGCGAATTCTGTCATAGT	Overexpression of *motA* gene in pUHE21-2*lacI*^{q}
motA-pUHE-R	GGGGACTCCGGATCCAAATCC	
cheY-pUHE-F	GCGATACGAATTCGAACCAGG	Overexpression of *cheY* gene in pUHE21-2*lacI*^{q}
cheY-pUHE-R	TTGATAGATGGATCCATCATCATC	
fliK-pUHE-F	CGTGCAGCAATGAGGAATTCCGA	Overexpression of *fliK* gene in pUHE21-2*lacI*^{q}
fliK-pUHE-R	GGATAATCATGGATCCTCTGGCG	

Materials and methods

Bacterial strains and growth conditions

The bacterial strains and plasmids used in this study are listed in Table 7. *S*. Typhimurium strains were derived from strain SL1344. P22-mediated transductions were performed as described previously (96). Bacteria were grown at 37°C in LB medium in aerobic condition. Ampicillin, chloramphenicol, kanamycin, and IPTG were used at 50 μg/ml, 25 μg/ml, 50 μg/ml, and up to 2 mM, respectively.

Construction of strains

The *S.* Typhimurium strain CH504, which is deleted for the *motA* gene, was constructed using the one-step gene inactivation method (48). The Km^r cassette from plasmid pKD13 was amplified using primers *motA*-lamb-F and *motA*-lamb-R. Primer *motA*-lamb-F (5′-CTGCGCATCCTGTCATAGTC AACAGCGGAAGGATGATGTCTGTAGGCTGGAGCTGCTTCG-3′) carries the sequence immediately upstream of the start codon of the *motA* gene following the priming site 1 sequence of pKD13 (48). Primer *motA*-lamb-R (5′- CTGCGGCGTTTTACGACGACAATGGGATGAGCCTGATTT

TATTCCGGGGATCCGTCGACC -3′) harbors the sequence immediately downstream of the stop codon of the *motA* gene linked to the priming site 4 sequence of pKD13 (48). The resulting PCR product was integrated into the *motA* region in strain SL1344 from which the Km^r cassette was removed using plasmid pCP20 (48). Deletion of the corresponding genes was verified by colony PCR. The strains CH501, 502, 505, and CH506 deleted for *fliR*, *flgK*, *cheY*, and *fliK* respectively were constructed by using the same strategy. The primers used for construction of strains were listed on Table 8.

Construction of plasmids

For complementation of mutant phenotypes, several vectors were constructed. To construct plasmid pUHE-*motA* in which the MotA protein is expressed from the p*lac* promoter, the *motA* gene was amplified by PCR using primers *motA*-pUHE-F (5′- CCCGACTGCGAATTCTGTCATAGT -3′) and *motA*-pUHE-R (5′- GGGGACTCCGGATCCAAATCC -3′), and chromosomal DNA from strain SL1344 as a template. The product was introduced between the EcoRI and BamHI restriction sites of pUHE21-2$lacI^q$ (184). Same vector and strategy was used for constructing pUHE-*cheY* and pUHE-*fliK*. Plasmid pACYC-*flgK*, which encodes the FlgK protein with its own promoter, was constructed for complementation of *flgK* deletion mutant. The *flgK* gene was amplified by PCR using primers *flgK*-pACYC-F

(5′- ACGAGTATTGAAAGCTTAAAAGGAAC -3′) and *flgK*-pACYC-R (5′-ACTGATACGCATGCCATCCTTC -3′), and chromosomal DNA from strain SL1344 as a template. The product was introduced between the HindIII and SphI restriction sites of pACYC184 (38). The *fliR* gene was also cloned to pACYC184 vector for complementation. Sequences of the *motA*, *cheY*, *fliK*, *fliR*, and *flgK* coding regions on the recombinant plasmids were confirmed by nucleotide sequencing. The primers used for construction of plasmids are listed on Table 8.

Propagation of bacteriophage

Phage was propagated in accordance with standard protocols for phage λ (173). Individual plaque was picked and eluted with sodium chloride-magnesium sulfate (SM) buffer (50 mM Tris (pH 7.5), 100 mM NaCl, and 10 mM $MgSO_4$). After re-picking and re-plating twice, phage was inoculated into exponentially-growing SL1344 at the multiplicity of infection (MOI) of 1 and incubated for 3 h at 37°C. Cell debris was removed by centrifugation (8,000 x g for 20 min at 4°C) and phage was precipitated overnight by adding 10% polyethylene glycol (PEG) 6000, followed by a CsCl density-gradient ultracentrifugation (60,000 x g for 4 h at 4°C). The CsCl-purified phage suspension was dialyzed using SM buffer and stored at 4°C.

Bacteriophage host range

Forty-five strains were used to test host range of iEPS5. A hundred micro liter of each test bacterial culture (O/N, overnight) was added to 5 ml of molten LB top agar (0.4% agar) and the mixture was overlaid on the LB bottom agar (1.5% agar) plates. After solidification of top agar, 10 μl of each serially diluted iEPS5 phage suspension was spotted on the overlaid plates and these plates were incubated at 37°C for 18 h. The sensitivity of test bacteria to iEPS5 phage was determined by degrees of clarity of the spots.

Transmission electron microscopy

Bacteriophages were put on carbon-coated copper grids and negatively stained with 2% aqueous uranyl acetate (pH 4.0) (Fisher Scientific). Transmission electron microscopy (TEM) was carried out using an energy filtering transmission electron microscope (LIBRA 120, Carl Zeiss) at 80 kV accelerating voltage at the National Institute of Agricultural Science and Technology (Suwon, Korea).

One-step growth curve

When the OD_{600} of the culture of the same reference strain reaches to 1.0, 50 ml of the culture was harvested. iEPS5 phage was added at a MOI of 0.01 and allowed to be adsorbed for 5 min at room temperature. To remove

the excessive phage, the mixture was centrifuged and the supernatant was discarded. And then the cell pellet was suspended with the same volume of fresh LB broth medium and the suspended culture was further incubated aerobically at 37°C. Two sets of samples were collected every 5 min for 1 h. These two sets of samples were immediately diluted and plated for phage titration. However, before the titration, the second set of samples was treated with 1% chloroform (final concentration) to release intracellular phages in order to determine the eclipse period before phage titration. Based on PFU number per ml, latent period, eclipse period, and burst size were determined.

Complete nucleotide sequencing and bioinformatics

Phage genomic DNA was prepared as described elsewhere (173). A Genome Sequencer 20 System (454 Life Science Corp.) was initially used for whole genome sequencing at Macrogen Inc., Korea. In order to reduce the contigs, a shotgun library was prepared with randomly sheared DNA using Hydroshear (part no. JHSH000000-1, Gene machines). DNA fragments of desired sizes (1–3 kb) were cloned into pCR4Blunt-TOPO vector (Invitrogen, CA) and DNA sequencing was performed using the Applied Biosystems BigDye v3.0 and an ABI Prism 3730 XL DNA analyzer. Finally, primer walking filled sequence gaps. The complete genome was

assembled using the seqman ii sequence analysis software (DNASTAR Inc., Madison, WI). The open reading frames (ORFs) were identified with the ORF Finder at the National Center of Bioinformatics site (http://www.ncbi.nlm.nih.gov/gorf) and GenMark.hmm prokaryotic version 2.5 (http://opal.biology.gatech.edu/GeneMark/genemark_prok_gms_plus.cgi). Sequence manipulations were performed using CLC Genomics workbench version 3.6.1. This work was performed by the aid of colleague (H. Shin).

Random mutagenesis and identification of phage receptor

For screening of phage receptor in the host bacteria, SL1344 was subjected to random insertion mutagenesis by using Tn5-based EZ:Tn transposon system (Epicentre, Madison, WI) according to the manufacturer's instructions. The transposon construct was released from pMOD3 by restriction digestion with PvuII, separated in 1% agarose gels, and gel purified using Promega gel extraction kit (Promega, Madison, WI). The complexes were electroporated into host cell and transformants were selected on LB agar plates containing kanamycin (50 μg/ml). The resulting colonies were individually cultured and preserved in LB broth containing 15% (v/v) glycerol at -80°C. Using these random mutant libraries, phage receptor was identified by dotting assay. Each random mutant was

overlaid on the 24-well plate containing 500 μl of 1.5% bottom agar. Then, 7 μl of the 10^6 PFU/ml phage, which was an enough titer for identifying infection was dotted on each well and incubated for 8 h at 37°C.

Determination of transposon insertion site

To localize Tn insertion site, chromosomal DNA was extracted from candidate clones, which showed resistant to iEPS5. After self-ligation of PvuII-digested mutant genomic DNA, a portion of the ligation mixture was electroporated to EC100D™ *pir*$^+$, and the transformant was rescued on LB agar plates containing kanamycin (50 μg/ml). The self-ligated vector was recovered by plasmid prep kit (QIAGEN) and sequenced with Tn-specific primers provided by the manufacturer (pMOD™<MCS> Forward Sequencing Primer; 5'-GCCAACGACTACGCACTAGCCAAC-3' and pMOD™<MCS> Reverse Sequencing Primer; 5'-GAGCCAATATGCGAGA ACACCCGAGAA-3'). PCR product was sequenced which was then BLAST-searched.

Motility assay

One micro liter of an overnight culture was spotted in the middle of a swim plate (LB, 0.3% agar) and allowed to dry for 1 h at room temperature. All plates were incubated at 37°C for 8 h or as noted otherwise.

Adsorption assay

To investigate adsorption of phage to various *Salmonella* strains, phage-binding assay was carried out. Host bacteria were cultivated in LB medium overnight. The cells were inoculated into 8 ml LB medium and incubated at 37°C to adjust a final concentration at 10^8 CFU/ml. After 2 h incubation, phage was infected with a 0.01 MOI. Every minute, the samples were collected and the bacterial cells were removed by centrifugation at 16,000 x g for 1 min and filtration using 0.22 μm pore size filters (Millipore). Finally, PFU from the collected supernatant samples (not adsorbed phage) was determined by serial dilution and standard plate counting using reference strain. The phage titer at time 0 was defined as 100%.

Preparation and purification of flagellin complexes

Purification of flagellar filament was performed as described by Aizawa *et al*. (88). Bacterial cells were grown aerobically at 37°C in LB broth (typically 1 liter). Cells were harvested in late exponential phase, centrifuged, suspended in 100 ml of ice-cold sucrose solution (0.5 M sucrose, 0.1 M Tris, pH 8.0), and dispersed by gentle stirring. To the suspension, 5 ml of lysozyme solution (2 mg/ml in distilled water) and 10 ml of 0.1 M EDTA (pH 7.5) was added. Then, the mixture was incubated on ice with gentle stirring. Although most of the cells were converted into spheroplasts

within 10 min, the solution was incubated for 40 min to ensure complete digestion of the peptidoglycan layer. Addition of 10 ml of 10% Trion X-100 lysed the resulting spheroplast. After complete lysis, 10 ml of 0.1 M $MgSO_4$ was added to the lysate, and the mixture was incubated at 30°C until the viscosity of the solution had decreased greatly (in 30 min), indicating that the cellular DNA had been degraded by the endogenous DNase. Remained cells and cell debris were removed by centrifugation at 4,000 x g for 10 min and the pH of the supernatant raised with 5 N NaOH. As the solution approached at pH 11, it became translucent suggesting that outer membrane structures had disintegrated. The lysate was subjected to high-speed centrifugation (60,000 x g for 60 min in polyallomer tubes, Beckman), and the pellets were suspended in alkaline solution (0.1 M KCl-KOH, 0.5 M sucrose, 0.1% Triton X-100, pH 11), re-centrifuged, and re-suspended in TET buffer (10 mM Tris, 5 mM EDTA, 0.1% Triton X-100, pH 8.0). The solution was diluted to 90 ml with TET buffer, and 36 g of CsCl was added to make a gradient in solution. The mixture was then centrifuged (55,000 x g for 16 h at 15°C). The flagella formed a thick band about ¾ of the way down the tube. The flagellar fraction was collected with syringe and dialyzed against TET buffer.

Phage staining and epifluorescence microscopy

Phage was labeled by using SYBR Gold (Invitrogen) as described (113). The SYBR-gold stock solution (10,000 x) was diluted with TE (10 mM Tris, 1 mM EDTA, pH 7.5) buffer. Phage lysate (about 10^{11} PFU/ml) was used for staining with 5x (final concentration) SYBR-Gold solution for 20 min in the dark at room temperature. Phage solution was diluted with SM buffer and was filtrated through Amicon Ultra-15 10,000 MWCO centrifugal filters (Millipore) at 1,500 x g for 90 min at 25°C to remove free SYBR-Gold particles. SYBR-Gold labeled phage was added to cells at a MOI of about 100 and incubated with shaking in the dark for different times (up to 1 h). Subsequently, a 1 ml sample was taken and centrifuged (4,000 x g for 5 min). The pellet was washed with motility solution (0.01 M KPO_4, 0.067 M NaCl, 10^{-4} M EDTA (pH 7.0)) and re-suspended in a small volume of motility solution for microscopy observation (Axio Imager.A1 upright microscope, Carl Zeiss).

Results

Isolation and characterization of iEPS5

The overall aim of this study was to assess the interaction between bacteriophage and its host bacteria during infection. I initially isolate a phage, iEPS5 infecting *S*. Typhimurium SL1344 from sewage samples. TEM analysis revealed that it belongs to *Siphoviridae* family featuring an isometric capsid (59 ± 2 nm) and non-contractile tail (216 ± 3 nm) (Fig. 26). At the end of tail, there was a tail fiber involved in the binding of the phage to the bacterial cell (98). The plaque morphology of iEPS5 was turbid and small on the agar plate and the lysis activity in the broth culture was relatively low (data not shown). iEPS5 had a narrow host ranges restricted to several strains of *Salmonella* (Table 9). All *S*. Typhimurium type strains and four of the nine *S*. Typhimurium isolates tested were sensitive to iEPS5. However, iEPS5 could not infect other Gram-negative bacteria including *E. coli* and Gram-positive bacteria indicating that iEPS5 is a *Salmonella*-specific phage. This host-specificity of iEPS5 would be worth identifying the phage-host interaction.

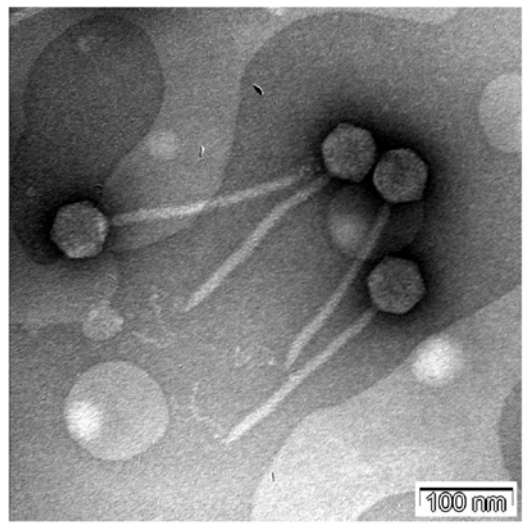

Phage	Family	Size (nm)	
		Head	Tail
iEPS5	*Siphoviridae*	216 ± 3	59 ± 2

Figure 26. Morphology of iEPS5 in TEM analysis. Electron microscopic image of phage iEPS5 negatively stained with 0.2% uranyl acetate. Scale bar, 100 nm.

Table 9. The host range of iEPS5

Bacterial isolate	Plaque[a]	Bacterial strain	Plaque[a]
***S.* Typhimurium**		***E. coli***	
SL1344	T	MG1655	-
UK1	T	DH5α	-
14028s	I	DH10B	-
LT2	T		
DT104	T	***E. coli* O157:H7**	
ATCC 19586	C	ATCC 35150	-
ATCC 43147	T	ATCC 43888	-
		ATCC 43890	-
***S.* Typhimurium isolate**		ATCC 43894	-
3068	T	ATCC 43895	-
S. T 1	-	O157:NM 3204-92	-
S. T 2	-	O157:NM H-0482	-
S. T 3	-		
S. T 4	T	***Salmonella***	
S. T 5	-	*S.* Typhi Ty 2-b	-
S. T 6	T	*S.* Paratyphi A IB 211	TT
S. T 8	I	*S.* Paratyphi B IB 231	-
S. T 10	T	*S.* Paratyphi C IB 216	-
***S.* Enteritidis**		*S.* Dublin IB 2973	-
ATCC 13078	-		
***S.* Enteritidis isolate**			
S. E 4	TT	**Other Gram positive bacteria**	
		Enterococcus faecalis ATCC 29212	-
Other Gram negative bacteria		*Staphylococcus aureus* ATCC 29213	-
Shigella flexineri 2a strain 2457T	-	*Staphylococcus epidermis* ATCC 35983	-
Shigella boydii IB 2474	-	*Bacillus subtilis* ATCC 23857	-
Vibrio fischeri ES-114 ATCC 700601	-	*Bacillus cereus* ATCC 14579	-
Pseudomonas aeruginosa ATCC 27853	-	*Listeria monocytogenes* ATCC 19114	-
Cronobacter sakazakii ATCC 29544	-	*Listeria innocua* I	-

[a] C, Clear plaque; T, Turbid plaque; TT, Very turbid plaque; I, Inhibition zone; -, non-specific

General features of iEPS5 genome

The iEPS5 genome comprises 59,254 bp with an overall G+C content of 56.31%, which is higher than that of *Salmonella* (52%) (133). As determined by the blast search, dot-plot analysis (data not shown) and gene annotation of putative ORFs, iEPS5 genome is highly similar to that of *Burkholderia* phage BcepNazgul (NC_005091). The genome of iEPS5 had 75 ORFs and tended to be clustered into functional modules (Fig. 27 and Table 10). The structural group was the most obvious and could be divided into three submodules: packaging, head structure and tail morphogenesis. The terminase of bacteriophage, constituted by a large (ORF64) and a small (ORF65) subunit, is essential for the initiation of DNA packaging. The head morphogenesis module was clustered in the region from ORF59 to ORF63 containing capsid protein, prohead protease ClpP, and portal protein which is required for DNA entering to the capsid and also used as a marker of phage diversity. The tail module appeared to extend from ORF38 to ORF53. A large number of genes encoding tail assembly protein and their homologies with other different phages indicate that iEPS5 has unusual tail. The other two modules, those are usually related to DNA replication, modification and expression. But these modules had lower identities to known phage genes compared to structural modules.

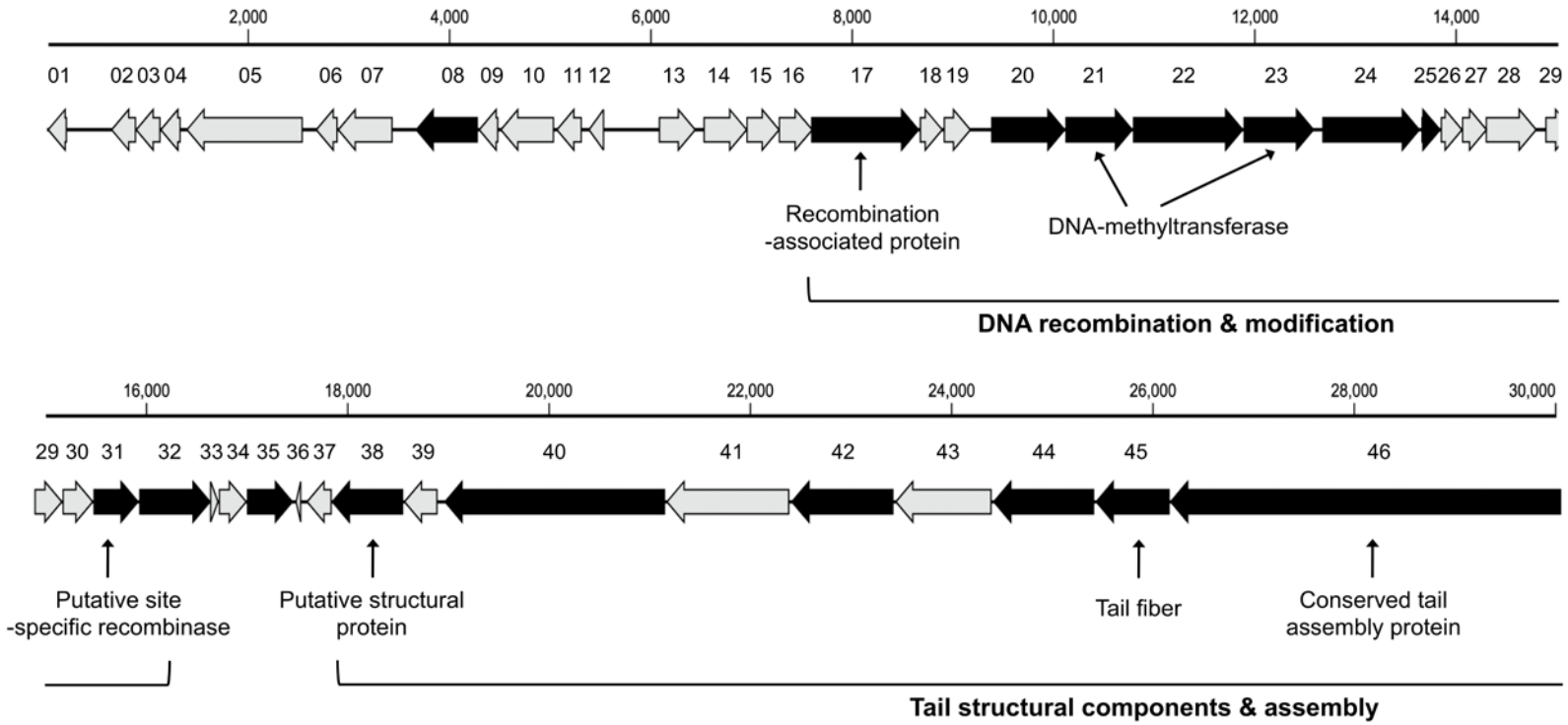

Figure 27. Schematic representation of the iEPS5 genome

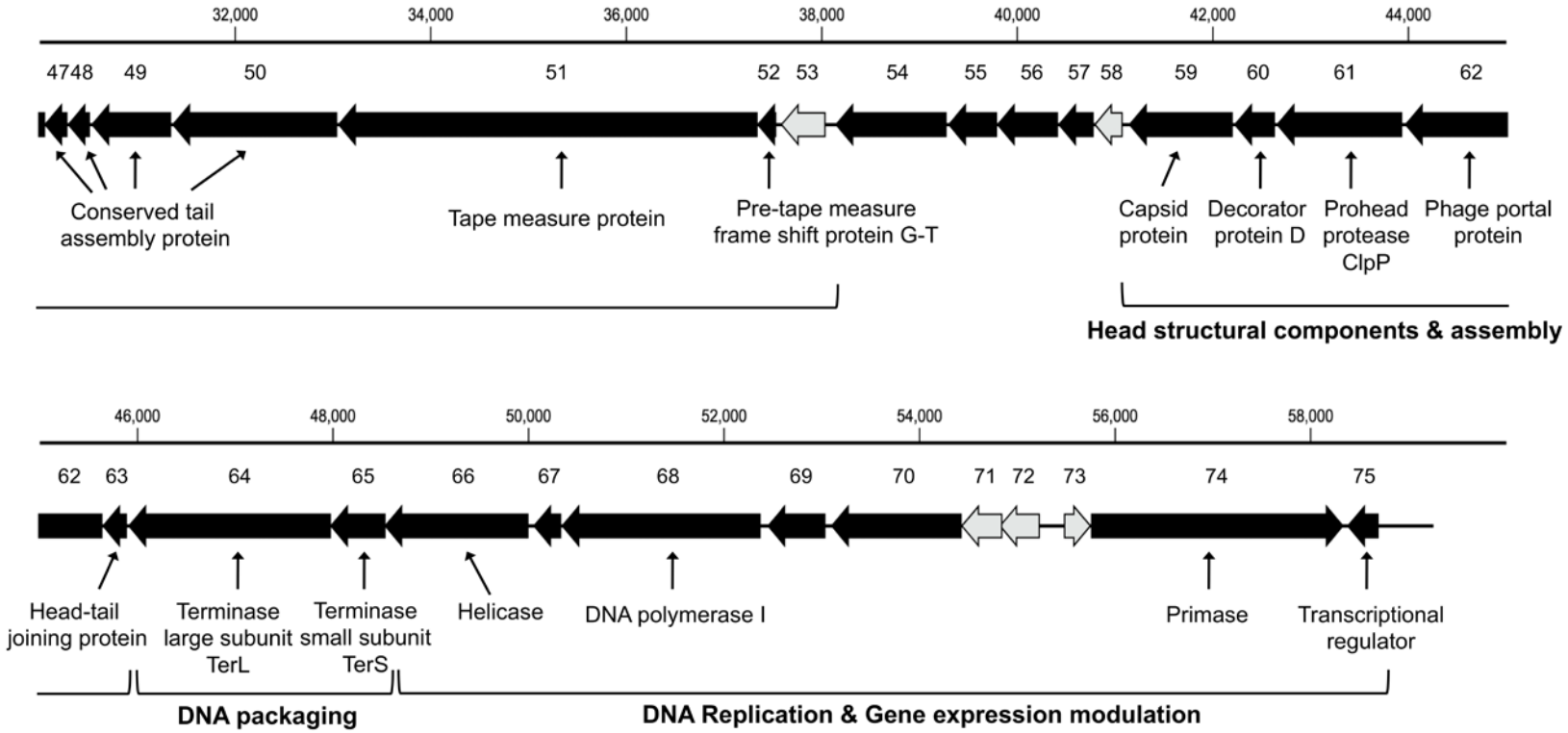

Figure 27. Schematic representation of the iEPS5 genome (continued)

Table 10. Features of bacteriophage iEPS5 ORFs, gene products, and functional assignments

ORF	Gene Strand	Left end	Right end	Length (nt)	No. amino acids	Size (kDa)	pI	Predictive function	Best hit	e value	No. amino acids	Accession no.
01	-	3	200	198	66	7.3	9.09	-	No significant hit	-	-	-
02	-	635	886	252	84	9.6	11.5	-	No significant hit	-	-	-
03	-	879	1130	252	84	9.4	10.7	-	No significant hit	-	-	-
04	-	1123	1329	207	69	7.5	6.8	-	No significant hit	-	-	-
05	-	1382	2542	1161	387	43.2	5.2	-	No significant hit	-	-	-
06	-	2668	2889	222	74	7.6	10.9	-	No significant hit	-	-	-
07	-	2886	3434	549	183	20.2	6.2	-	No significant hit	-	-	-
08	-	3660	4283	624	208	24.4	6.0	Conserved hypothetical protein	Bacteroides sp. D4	6E-12	197	ZP_04556224
09	-	4286	4486	201	67	7.8	11.1	-	No significant hit	-	-	-
10	-	4501	5040	540	180	20.2	9.8	-	No significant hit	-	-	-
11	-	5059	5316	258	86	9.5	6.4	-	No significant hit	-	-	-
12	-	5378	5536	159	53	5.7	11.8	-	No significant hit	-	-	-
13	+	6077	6448	372	124	13.7	9.5	-	No significant hit	-	-	-
14	+	6520	6960	441	147	16.7	5.2	-	No significant hit	-	-	-
15	+	6947	7282	336	112	12.4	9.7	-	No significant hit	-	-	-
16	+	7269	7610	342	114	12.5	5.4	-	No significant hit	-	-	-
17	+	7591	8667	1077	359	40.2	5.1	Recombination-associated protein	*Staphylococcus* phage SA1	0.0	358	ACZ55522
18	+	8670	8903	234	78	9.0	10.1	-	No significant hit	-	-	-
19	+	8908	9183	276	92	10.7	5.9	-	No significant hit	-	-	-

Table 10. Features of bacteriophage iEPS5 ORFs, gene products, and functional assignments (continued)

ORF	Gene Strand	Left end	Right end	Length (nt)	No. amino acids	Size (kDa)	pI	Predictive function	Best hit	e value	No. amino acids	Accession no.
20	+	9379	10119	741	247	27.8	5.2	Hypothetical protein	*Trypanosoma cruzi* strain CL Brener	4E-01	609	XP_819468
21	+	10116	10790	675	225	24.7	9.1	DNA-methyltransferase	*Eubacterium* rectale M104/1	4E-01	344	CBK93904
22	+	10787	11887	1101	367	40.8	6.0	Hypothetical protein	*Butyrivibrio proteoclasticus* B316		893	YP_003832575
23	+	11887	12591	705	235	26.8	9.2	DNA-methyltransferase	*Yersinia pseudotuberculosis* IP 32953	2E-37	291	YP_070324
24	+	12669	13643	975	325	37.0	5.5	Hypothetical protein	*Enterobacteria* phage Eco1230-10	3E-12	113	ADE87960
25	+	13654	13848	195	65	7.3	9.2	Hypothetical protein	*Haemophilus influenza* 6P18H1	2E-07	84	ZP_04464419
26	+	13845	14066	222	74	8.4	7.9	-	No significant hit	-	-	-
27	+	14056	14310	255	85	9.5	7.7	-	No significant hit	-	-	-
28	+	14292	14804	513	171	19.8	9.5	-	No significant hit	-	-	-
29	+	14885	15166	282	94	10.4	8.8	-	No significant hit	-	-	-
30	+	15163	15474	312	104	12.0	6.5	-	No significant hit	-	-	-

Table 10. Features of bacteriophage iEPS5 ORFs, gene products, and functional assignments (continued)

ORF	Gene Strand	Left end	Right end	Length (nt)	No. amino acids	Size (kDa)	pI	Predictive function	Best hit	e value	No. amino acids	Accession no.
31	+	15471	15923	453	151	17.1	9.7	Putative Site-specific recombinase	*Thiomonas* sp. 3As	2E-01	348	CAZ89169
32	+	15925	16638	714	238	27.4	9.7	Hypothetical protein	*Staphylococcus* phage SA1	3E-109	211	ACZ55544
33	+	16628	16717	90	30	3.3	11.8	-	No significant hit	-	-	-
34	+	16714	16998	285	95	11.1	7.5	-	No significant hit	-	-	-
35	+	16995	17456	462	154	17.3	5.5	Hypothetical protein	*Burkholderia ubonensis* Bu	7E-02	130	ZP_02378807
36	-	17457	17531	75	25	2.6	9.0	-	No significant hit	-	-	-
37	-	17587	17841	255	85	9.5	11.4	-	No significant hit	-	-	-
38	-	17838	18551	714	238	26.1	8.8	Putative structural protein	*Staphylococcus* phage SA1	7E-119	237	ACZ55542
39	-	18555	18893	339	113	12.5	6.0	-	No significant hit	-	-	-
40	-	18958	21153	2196	732	80.8	6.9	Hypothetical protein	*Staphylococcus* phage SA1	0.0	611	ACZ55502
41	-	21163	22389	1227	409	45.3	6.9	-	No significant hit	-	-	-
42	-	22404	23423	1020	340	37.0	6.2	Hypothetical protein	*Ralstonia* phage RSL1	2E-05	735	YP_001950063
43	-	23437	24399	963	321	34.8	5.3	-	No significant hit	-	-	-
44	-	24410	25417	1008	336	36.5	5.6	Hypothetical protein	*Plasmodium yoelii* str. 17XNL	7E-02	458	XP_730773

Table 10. Features of bacteriophage iEPS5 ORFs, gene products, and functional assignments (continued)

ORF	Gene Strand	Left end	Right end	Length (nt)	No. amino acids	Size (kDa)	pI	Predictive function	Best hit	e value	No. amino acids	Accession no.
45	-	25427	26167	741	247	27.2	5.0	Tail fiber protein	*Burkholderia* phage BcepNazgul	7E-08	1270	NP_918975
46	-	26167	30057	3891	1297	143.3	5.2	Conserved tail assembly protein	*Burkholderia* phage BcepNazgul	9E-145	741	NP_918976
47	-	30047	30286	240	80	9.1	9.3	Conserved tail assembly protein	*Pseudomonas* phage YuA	4E-01	68	YP_001595898
48	-	30286	30516	231	77	8.5	11.4	Conserved tail assembly protein	*Comamonas testosteroni* KF-1	3E-01	71	ZP_03543677
49	-	30528	31346	819	273	29.5	5.4	Conserved tail assembly protein	*Staphylococcus* phage SA1	8E-130	272	ACZ55535
50	-	31356	33044	1689	563	63.0	5.4	Conserved tail assembly protein	*Staphylococcus* phage SA1	0.0	562	ACZ55504
51	-	33050	37345	4296	1432	153.9	9.4	Tape measure protein	*Burkholderia* phage BcepNazgul	1E-59	830	NP_918983
52	-	37338	37535	198	66	7.6	10.7	Pre-tape measure frame shift Protein G-T	*Burkholderia* phage BcepNazgul	9E-06	243	NP_918998
53	-	37580	38041	462	154	17.0	6.0	-	No significant hit	-	-	-
54	-	38138	39277	1140	380	40.9	5.0	Hypothetical protein	*Staphylococcus* phage SA1	0.0	379	ACZ55519

Table 10. Features of bacteriophage iEPS5 ORFs, gene products, and functional assignments (continued)

ORF	Gene Strand	Left end	Right end	Length (nt)	No. amino acids	Size (kDa)	pI	Predictive function	Best hit	e value	No. amino acids	Accession no.
55	-	39291	39794	504	168	19.0	8.6	Hypothetical protein	*Burkholderia* phage BcepNazgul	5E-25	179	NP_918987
56	-	39791	40417	627	209	22.5	10.9	Hypothetical protein	*Staphylococcus* phage SA1	2E-93	208	ACZ55545
57	-	40417	40782	366	122	13.9	9.8	Hypothetical protein	*Burkholderia* phage BcepNazgul	2E-10	118	NP_918989
58	-	40785	41078	294	98	11	9.1	-	No significant hit	-	-	-
59	-	41140	42204	1065	355	40.1	6.8	Capsid protein	*Staphylococcus* phage SA1	0.0	354	ACZ55524
60	-	42217	42636	420	140	14.6	5.1	Decorator protein D	*Burkholderia* phage BcepNazgul	6E-10	131	NP_918992
61	-	42651	43937	1287	429	45.9	5.0	Prohead protease ClpP	*Staphylococcus* phage SA1	0.0	438	ACZ55516
62	-	43964	45643	1680	560	62.5	8.7	Phage portal protein	*Staphylococcus* phage SA1	0.0	559	ACZ55505
63	-	45640	45894	255	85	10.1	10.5	Head-tail joining protein	*Burkholderia* phage BcepNazgul	1E-06	76	NP_918996
64	-	45905	47980	2076	692	78.0	6.7	Terminase large subunit TerL	*Burkholderia* phage BcepNazgul	0.0	677	NP_918997

Table 10. Features of bacteriophage iEPS5 ORFs, gene products, and functional assignments (continued)

ORF	Gene Strand	Left end	Right end	Length (nt)	No. amino acids	Size (kDa)	pI	Predictive function	Best hit	e value	No. amino acids	Accession no.
65	-	47970	48539	570	190	21.5	9.9	Terminase small subunit TerS	*Burkholderia* phage BcepNazgul	1E-33	222	NP_918999
66	-	48526	50001	1476	492	56.5	5.9	Helicase	*Staphylococcus* phage SA1	0.0	491	ACZ55509
67	-	50048	50335	288	96	11.0	10.5	Conserved phage protein	Burkholderia phage BcepNazgul	3E-14	108	NP_919001
68	-	50337	52376	2040	680	77.4	8.6	DNA polymerase I	*Staphylococcus* phage SA1	0.0	645	ACZ55501
69	-	52443	53039	597	199	22.7	6.4	Conserved phage protein	*Staphylococcus* phage SA1	1E-86	198	ACZ55548
70	-	53094	54431	1338	446	50.6	5.4	Conserved phage protein	*Staphylococcus* phage SA1	0.0	445	ACZ55515
71	-	54424	54849	426	142	15.6	11.1	-	No significant hit	-	-	-
72	-	54815	55231	417	139	14.5	9.8	-	No significant hit	-	-	-
73	+	55474	55755	282	94	10.3	10.2	-	No significant hit	-	-	-
74	+	55752	58337	2586	862	98.6	5.6	Primase	*Staphylococcus* phage SA1	0.0	554	ACZ55506
75	-	58373	58696	324	108	12.7	84.8	Transcriptional regulator	*Desulfovibrio* sp. FW1012B	3E-3	110	ZP_06368734

Adsorption, latent period and burst size

Before studying on the interaction between phage and host bacteria, I clarified growth parameters of iEPS5 infection. To investigate *in vitro* adsorption ability of iEPS5 to the host bacteria, *S.* Typhimurium SL1344 was infected with iEPS5 at an MOI of 0.01. More than 50% of the phage was adsorbed in 5 min and at least 90% in 15 min onto the host bacteria (Fig. 28A). One-step growth curve analysis revealed that the eclipse and latent periods of iEPS5 were 15 and 30 min, respectively (Fig**.** 28B). The eclipse period was consistent with the *in vitro* adsorption assay result. The burst size was more than 100 PFU per infected host cell.

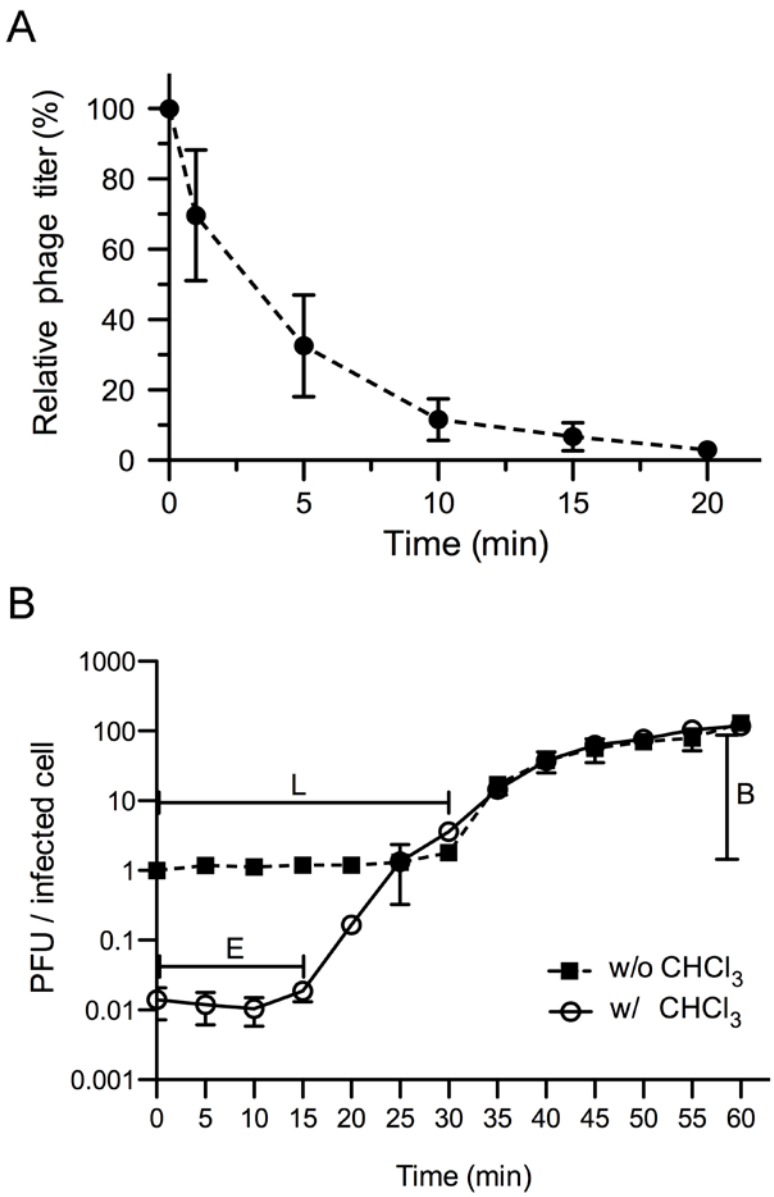
A
Relative phage titer (%)
100
80
60
40
20
0
0
5
10
15
20
Time (min)
B
PFU / infected cell
1000
100
10
1
0.1
0.01
0.001
L
E
B
w/o CHCl3
w/ CHCl3
0
5
10
15
20
25
30
35
40
45
50
55
60
Time (min)

Figure 28. The General steps of iEPS5 infection. (A) Exponentially growing cells were infected with iEPS5 (MOI, 0.01) and incubated at 37°C. After centrifugation and filtration, the phage titer in the filtrate was determined by standard overlay assay. The percentage of free phage particles was calculated as follows: (phage titer in the supernatant of iEPS5-infected bacterial suspension/phage titer in the supernatant of iEPS5-incubacted LB broth) x 100. The results are expressed as means and standard deviations of triplicate assays. (B) One-step growth curve analysis of *S.* Typhimurium SL1344 infected by iEPS5. E, eclipse period; L, latent period; B, burst size. Closed squares, non-chloroform-treated sample; opened circle, chloroform-treated sample. The error bars indicate standard deviations.

iEPS5 uses flagella as a receptor

To identify the receptor for iEPS5, transposon-mediated random library was constructed and resistant clones were screened. From 1,700 clones, I found five mutants resistant to iEPS5 infection (no plaque) and one mutant showing plaques with more turbidity (Table 11). Transposon insertion sites were determined by sequencing the transposon-chromosome boundaries, as described. All five resistant mutants were related to flagellar biosynthesis; flagellar biosynthesis sigma factor (*fliA*), flagellar export apparatus (*fliR*, *fliP*) and hook-filament junction (*flgK*) (Table 11). Flagellar specific sigma factor is responsible for transcription of class III flagellar genes, which include filament structure genes and genes of chemosensory pathway (155). Without the flagellar export apparatus, *Salmonella* still expresses flagellin monomers, but do not assemble functional flagella resulting in non-motile (61, 154). Hook-associated protein (HAP) is required for assembly of flagellin monomers into the outer filament of the flagellum by regulating the anti-sigma factor FlgM, which inhibits σ^{28} (FliA) prior to completion of the hook-basal body (HBB) structure. Therefore, *flgK* mutant is non-motile but secretes higher amounts of monomeric flagellin into the culture medium (8, 41). Expectedly, all five resistant mutants were non-motile on the swim plates due to the absence of flagella on their cell surfaces (Fig. 29).

Validity of the mutants described above, was further assessed with two representative mutants deleted in a *fliR* or a *flgK* gene by one-step gene inactivation method (48). The two mutants were non-motile (Fig. 30) and iEPS5 could not absorb to these two strains (Fig. 34). The motility and the sensitivity to iEPS5 of the *ΔfliR* and the *ΔflgK* strains were fully restored upon complementation with pACYC-*fliR* and pACYC-*flgK*, respectively (Fig. 30). From these results, I concluded that flagellum is a receptor of iEPS5.

Salmonella has two flagellar types and switches between two alternative, antigenic forms of its flagellin filament protein, either type B (FljB) or C (FliC) (11, 24). Two single deletion mutants (*ΔfliC* or *ΔfljB*) were motile (Fig. 29) and showed similar sensitivities to iEPS5 (data not shown), indicating that there is no preference of flagellar types used by iEPS5 as a receptor.

TEM analysis revealed a direct interaction between iEPS5 and flagella. After incubation of iEPS5 with its host bacteria followed by several washing to remove free phages, I could observe the phage bound to flagella. iEPS5 wrapped up the flagellar filament via its tail fiber (Fig. 31).

One more interesting mutant worth mentioning here is a mutant that has mutation in the *hnr* gene encoding a response regulator of RpoS (stationary phase specific sigma factor) (72, 91). Once, bound to Hnr, RpoS is transferred to the ClpXP protease, where it is unfolded and completely

degraded (91). Therefore, without Hnr, RpoS enhances its stability resulting in the reduction of flagellar expression (51). This regulation could explain a low motility of this mutant in the swim agar plate (Fig. 29) and the reduced motility resulted in producing a very turbid plaque by iEPS5.

Table 11. iEPS5 resistant isolates

Candidates	Sequencing results	Motility
3-B12	*fliR* : flagellar export apparatus	No
3-D2	*fliR* : flagellar export apparatus	No
6-H10	*hnr* : response regulator of RpoS	Reduced
12-B9	*flgK* : hook-filament junction protein	No
14-A7	*fliA*: flagellar biosynthesis sigma factor	No
15-D9	*fliP*: flagellar export apparatus	No

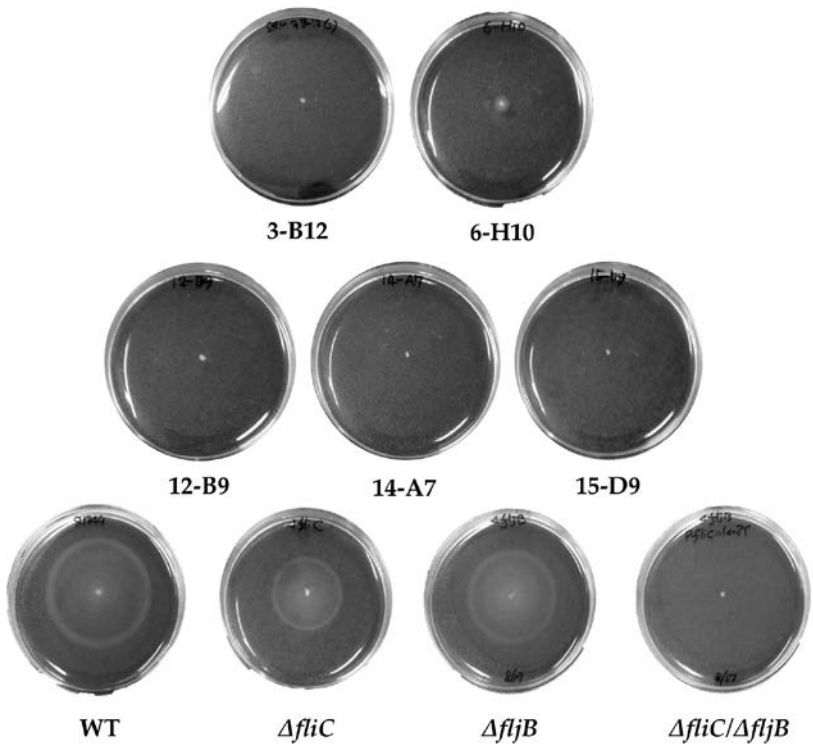

Figure 29. Motility assay of iEPS5 resistant isolates. Motility of six candidate mutants was assessed. One micro liter of an overnight culture of each candidate isolate was spotted in the middle of a swim plate (LB, 0.3% agar) and incubated at 37°C for 8 h. Wild-type, *ΔfliC*, *ΔfljB*, and *ΔfliC/ΔfljB* mutants were used for control.

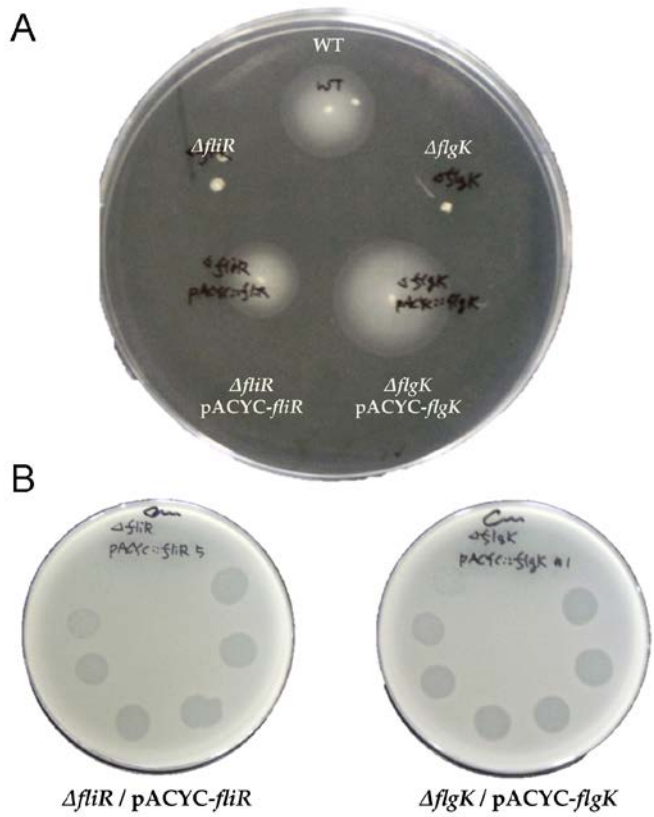

Figure 30. Motility and dotting assays of flagellar mutants and their complementation strains. (A) One micro liter of an overnight culture was spotted in the middle of a swim plate. All plates were incubated at 37°C for 6 h. (B) One hundred microliters of two complementation strain cultures was added to 5 ml of 0.4% LB agar, and the mixture was overlaid on 1.5% LB agar plates. Ten microliters of each serially diluted iEPS5 phage suspension from 10^2 to 10^{11} PFU/ml was spotted on the overlaid plates and incubated at 37°C. After incubation, the sensitivity of test bacteria to iEPS5 phage was determined by the degrees of clarity in the spots.

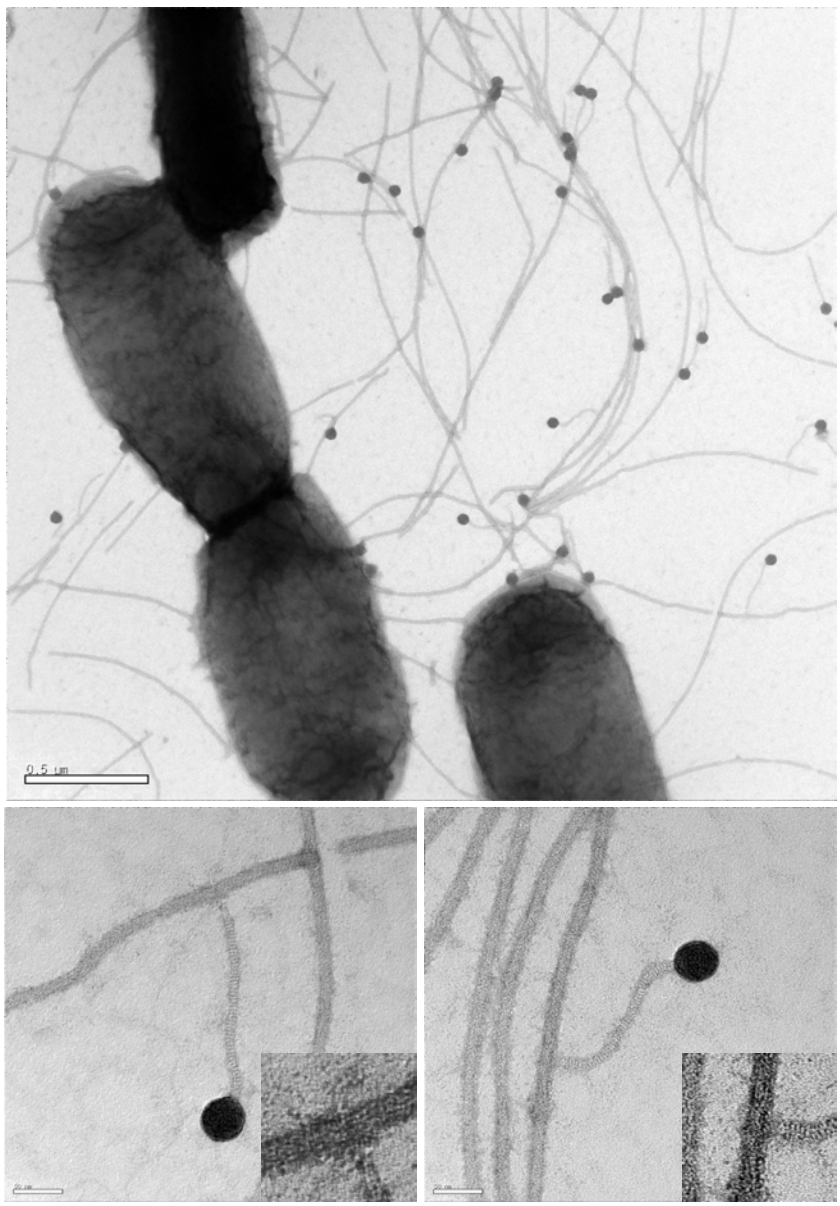

Figure 31. iEPS5 binds to flagellar filament via its tail fiber. Electron microscopic image of phage iEPS5 negatively stained with 0.2% uranyl acetate. Scale bars, 50 (down) and 500 nm (up).

Requirement of flagellar rotation

The most important role of flagella in the bacteria is a movement by rotating their flagellar filaments. It has been shown that flagellatropic phage Chi needs flagellar rotating CCW for successful infection (177). The requirement of flagellar rotation for iEPS5 infection was tested with *motA* mutant that assembled normal flagellar filament and basal body but could not rotate its flagella due to the absence of torque (146). As expected, iEPS5 could not absorb and infect to the paralyzed flagellar mutant (Fig. 32, 33, 34). Complementation of the mutant with a plasmid harboring the *motA* fused to the *lac* promoter could restore the motility and its sensitivity to iEPS5 in the presence of IPTG, indicating that motility of flagella is essential for iEPS5 infection (Fig. 33). Assessment with several diverse flagellar mutants with different motilities on the swim plate revealed that the infectivity of iEPS5 was reliant on the degrees of motility; iEPS5 presented low EOPs against the mutants showing low motility (Fig. 35).

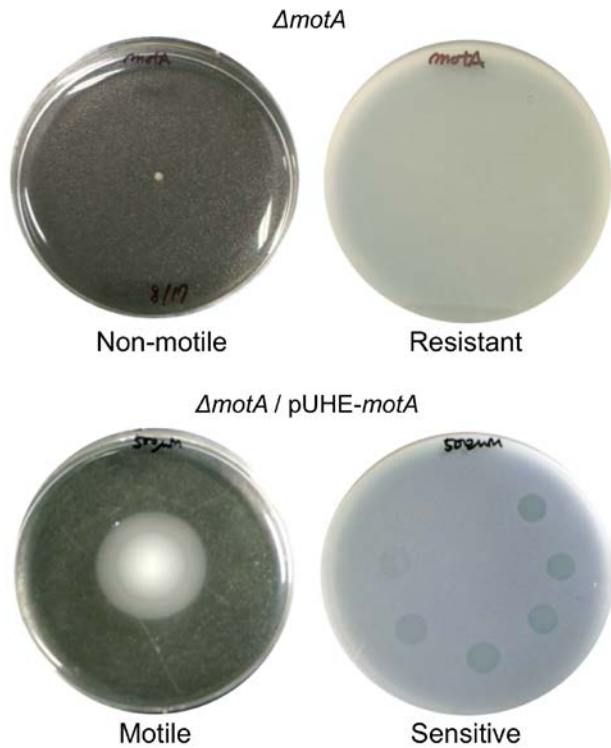

Figure 32. iEPS5 requires rotating flagella for its infection. Motility and dotting assay were performed using *motA* mutant and its complementation strain. In the complementation strain, 500 μM of IPTG was added to induce the expression.

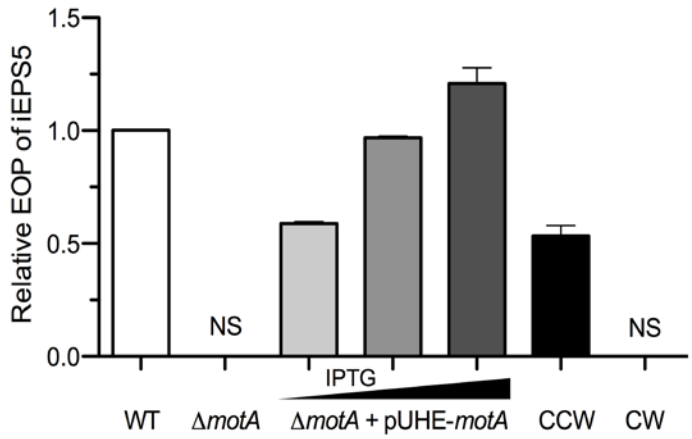

Figure 33. The EOPs of iEPS5 against flagellar rotation mutants of *Salmonella*. The plaque-forming ability of phage iEPS5 against each strain was measured as the efficiency of plating (EOP), which was set as 1 for wild-type. NS represents non-sensitivity of the host to iEPS5. CCW, SJW3076; CW, SJW2811.

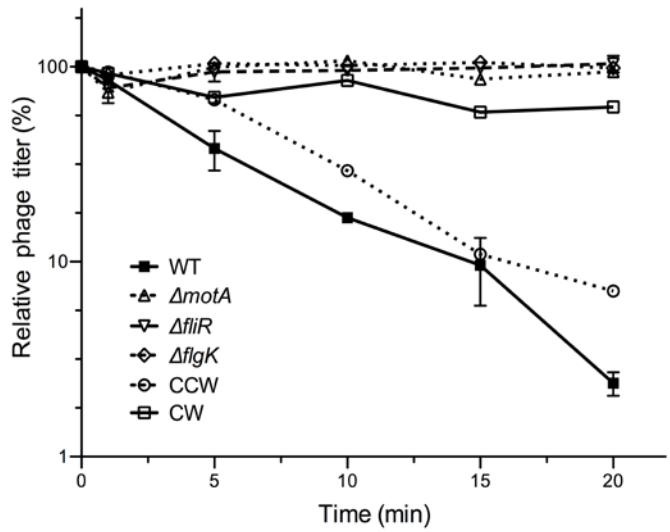

Figure 34. ***In vitro*** **adsorption assay of iEPS5 phage using plaque-counting method (1).** Each strain was infected by iEPS5 at MOI of 0.01. 100% relative titer of iEPS5 indicates the titer of iEPS5 at 0 min after infection. Each strain was designated by different symbols with lines: Closed square, wild-type; open triangle, *ΔmotA*; open inverted triangle, *ΔfliR*; open diamond, *ΔflgK*; open circle, SJW3076 (CCW-biased mutant); open square, SJW2811 (CW-biased mutant).

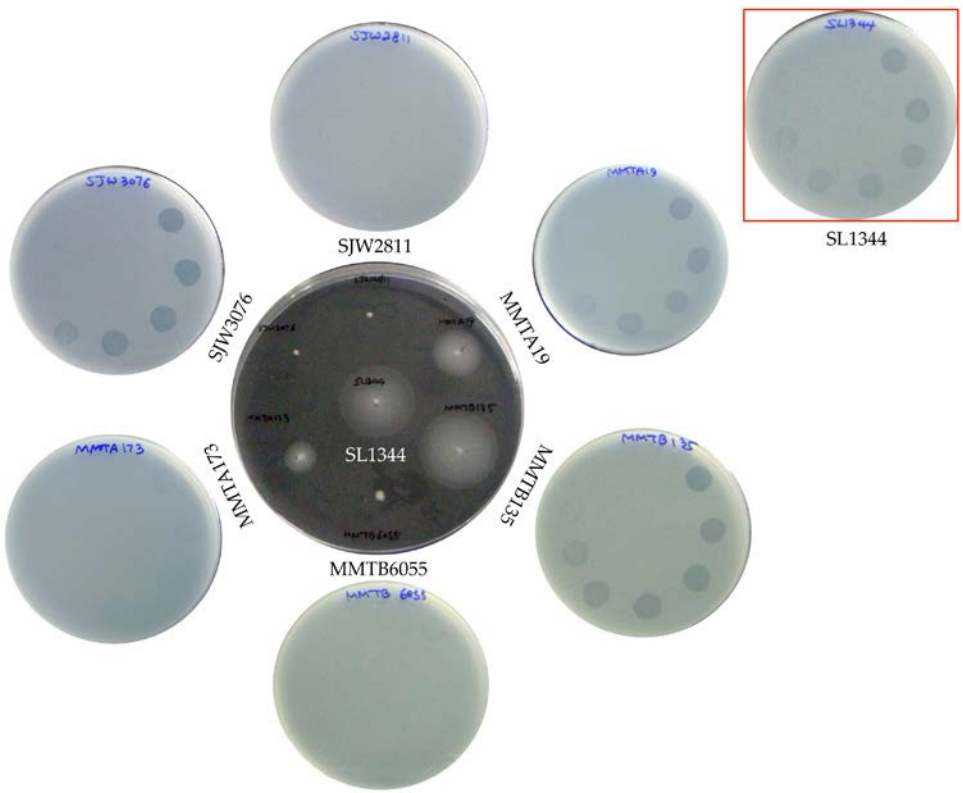

Figure 35. Requirement of motility for iEPS5 infection. Motility and dotting assay were performed using various mutants, which have different motile phenotypes. SJW2811 (extreme CW-biased), SJW3076 (CCW-biased), MMTA19 (slow *motA* mutant), MMTA173 (slow *motA* mutant), MMTB135 (slow *motB* mutant), MMTB6055 (slow *motB* mutant).

Purification of flagella and competitive adsorption

In previous results, the rotation of flagella was required for adequate adsorption and infection of iEPS5: paralyzed flagella of *motA* mutant could not be a receptor for phage. To confirm this result, I purified the flagella by using a purification method (6). Through several steps, I got a purified flagellar filament (Fig. 36 and Fig. 37A), and then performed a competitive adsorption assay using these purified flagella to verify whether iEPS5 could bind to non-rotating free form of flagella. As expected, the purified flagella did not inhibit iEPS5 bind to the rotating flagella of host bacterial cells (Fig. 37B). From these results I concluded that not just a flagellar filament, but functionally rotating flagellar filament is required for iEPS5 infection through proper adsorption to its receptor.

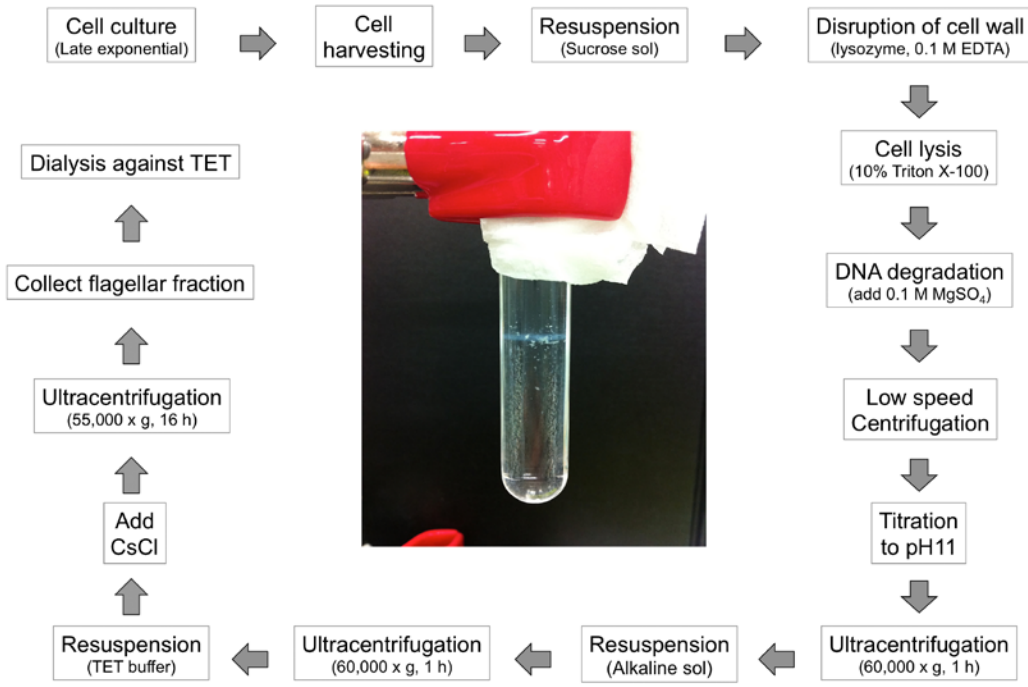

Figure 36. Purification of flagellar filament.

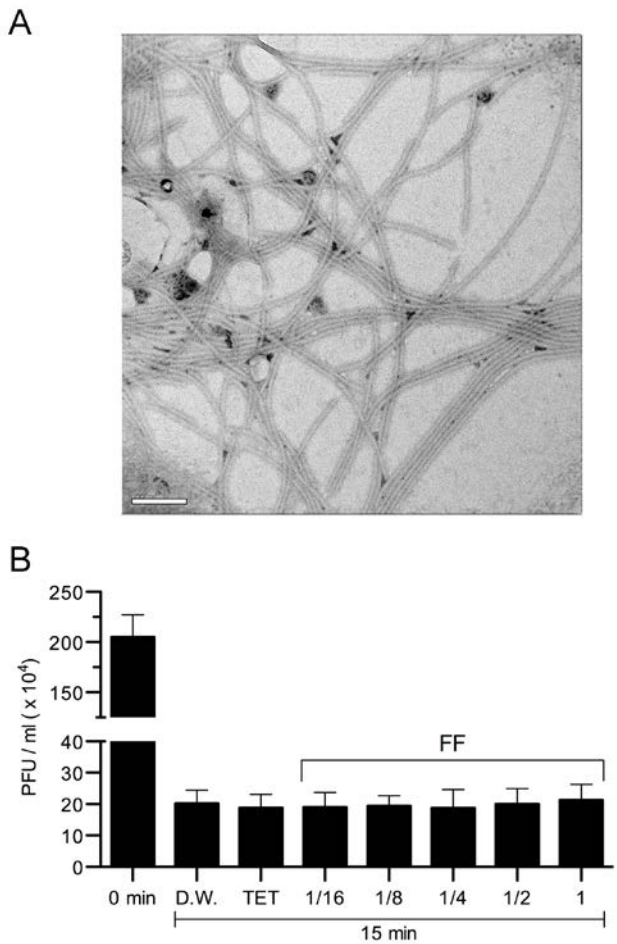

Figure 37. iEPS5 only interacts with functional flagella. (A) Transmission electron micrograph of purified flagella. Scale bar, 100 nm. (B) *In vitro* competitive adsorption assay of iEPS5 phage using purified flagella. Wild-type was infected by iEPS5 at MOI of 0.01 and incubated for 15 min. Two-fold diluted flagella fractions (1, 1/2, 1/4, 1/8, 1/16) were added to the culture. Each designation means: 0 min, wild-type with iEPS5 no incubation; DDW, wild-type with iEPS5 for 15 min incubation; TET, wild-type with iEPS5 in TET buffer for 15 min incubation; FF, wild-type with iEPS5 and flagella fraction for 15 min incubation.

Direction of flagellar rotation

Although iEPS5 can infect only motile strains of *Salmonella*, one exception was found with SJW3076 strain (Fig. 33). SJW3076 was highly sensitive to iEPS5 even though it is non-motile due to its CCW-biased rotation of flagella resulting from deletion of chemotaxis genes (deletion of *cheA* through *cheZ*) (126). These results imply that the direction of flagellar rotation might be critical for iEPS5 infection.

Bacterial chemotaxis is a migration toward favorable chemicals (attractants) and away from unfavorable ones (repellents) (131). Alternating flagellar rotation controls chemotaxis: smooth swimming from CCW rotation and tumbling from CW rotation (85). Switch from CCW to CW rotation of the flagella occurs as a result of binding of the phosphorylated CheY protein to the base of the flagellum (182) that the *cheY* deletion of *Salmonella* can make flagellar rotate CCW-biased. Similarly to SJW3076, *ΔcheY* mutant was also non-motile in the swim agar plate but highly sensitive to iEPS5 in spotting assay (data not shown) confirming the decisive factor for iEPS5 infection. The direction of flagella rotation can be changed from CCW-biased in the *ΔcheY* to CW-biased by overexpressing the *cheY* (166, 174). A plasmid harboring a *cheY* gene under control of *lac* promoter was introduced to the *ΔcheY* mutant and the EOPs of iEPS5 were measured with increasing amount of IPTG. Interestingly, the resistance of

the bacteria to iEPS5 was increased in an IPTG dependent manner. When I added 2 mM of IPTG, iEPS5 could not infect its host any more (Fig. 38 and Fig. 39).

Further experiments with another CCW-biased strain SJW3076, in which all of the chemotaxis genes (from *cheA* through *cheZ*) are deleted, and CW-biased strain SJW2811, in which *fliG* gene has deletion from amino acid residue 169 to 171 resulting in an extremely strong CW motor bias (193) also revealed that iEPS5 could adsorb to and infect only the CCW-biased SJW3076 (Fig. 33 and 34). These results indicate that iEPS5 infects the host bacteria using CCW-rotating flagella as a receptor and the direction of flagellar rotation is critical for iEPS5 infection strategy.

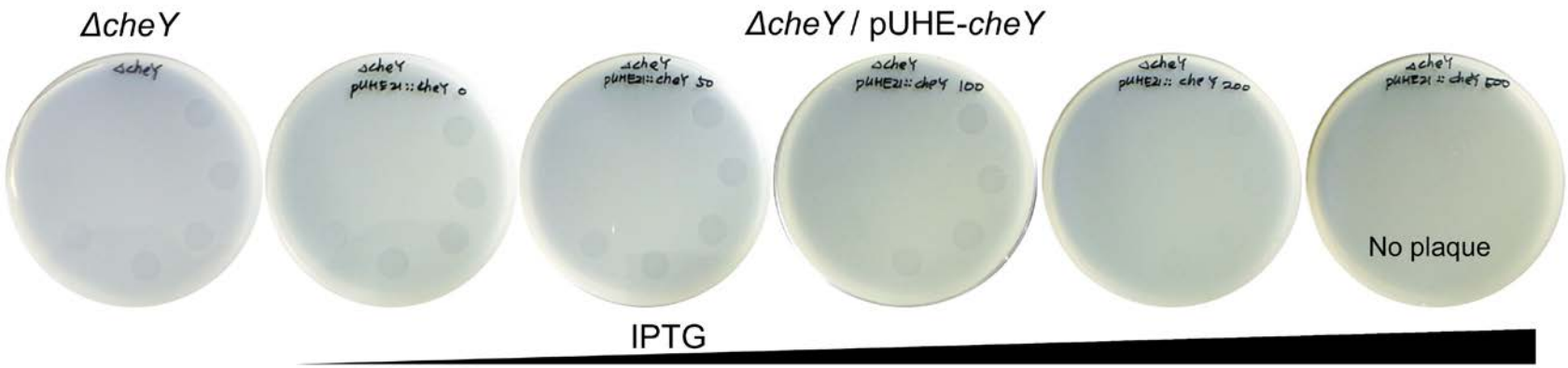

Figure 38. The direction of flagellar rotation is important for iEPS5 infection. The plaque-forming ability of phage iEPS5 against each strain was measured in *cheY* mutant and its complementation strain by dotting assay as described. The concentrations of IPTG are 0, 50, 100, 200, and 500 μM respectively.

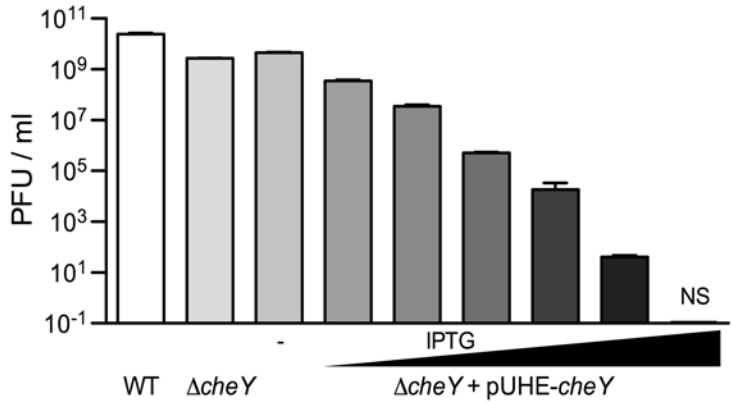

Figure 39. The EOPs of iEPS5 against flagellar rotation mutants of *Salmonella*. The plaque-forming ability of phage iEPS5 against each strain was measured as PFU/ml. NS represents non-sensitivity of the host to iEPS5. The concentrations of IPTG are 0, 100, 200, 500, 1,000, 1,500, and 2,000 μM respectively.

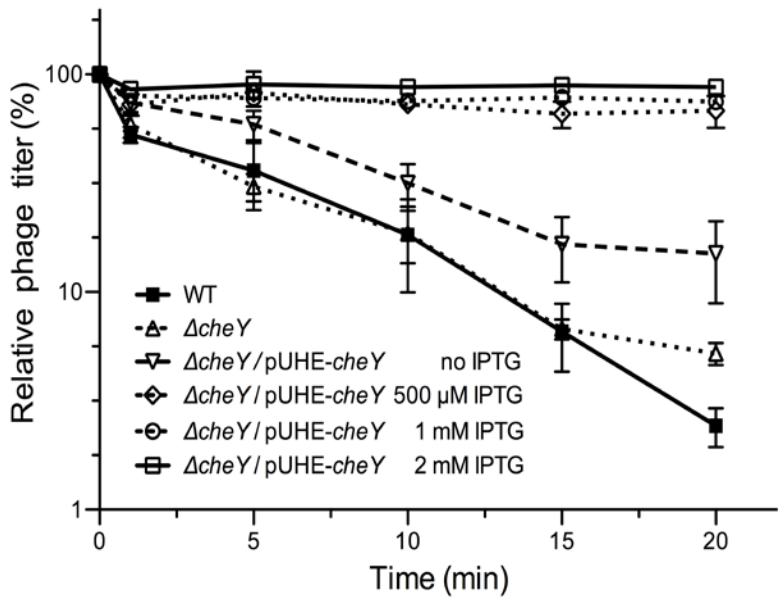

Figure 40. ***In vitro*** **adsorption assay of iEPS5 phage using plaque-counting method (2).** Each strain was infected by iEPS5 at MOI of 0.01. 100% relative titer of iEPS5 indicates the titer of iEPS5 at 0 min after infection. Each strain was designated by different symbols with lines: Closed square, wild-type; open triangle, *ΔcheY*; open inverted triangle, *ΔcheY*/pUHE-*cheY*; open diamond, *ΔcheY*/pUHE-*cheY* with 500 μM of IPTG; open circle, *ΔcheY*/pUHE-*cheY* with 1 mM of IPTG; open square, *ΔcheY*/pUHE-*cheY* with 2 mM of IPTG.

The importance of flagellar filament for iEPS5 infection

According to the "bolt and nut" model of Chi, hook structure is also important for flagellatropic phage infection: the phage must traverse the hook to reach down to the filament base (174). A molecular ruler, FliK, controls the length of the flagellar hook (normally ~55 nm). FliK measures hook length and catalyses the secretion-substrate specificity switch from rod-hook substrate specificity to late substrate secretion, which includes the filament subunits. It has been known that *fliK* mutant has a polyhook structure with wide length distribution up to about a micron in length but there is no flagellar filament in this strain (92, 141, 200).

To assess the iEPS5 infection to polyhook strain, I constructed *fliK* deletion mutant and identified the exact polyhook structure in electron microscopy (Fig. 41). Interestingly, iEPS5 could not infect the polyhook strain in dotting assay, even in a high titer concentration (data not shown). Moreover, iEPS5 did not bind to the *fliK* mutant *in vitro* adsorption assay. These resistances of polyhook strain to iEPS5 were recovered when introducing the complementation plasmid (Fig. 42).

To differentiate the infection mechanism of iEPS5 from Chi, I performed the phage challenge assay using different flagellar type strains: wild-type, normal hook with intact flagellar filament; *fliK* mutant, polyhook without flagellar filament; *ΔfliC/ΔfljB*, normal hook without flagellar filament;

ΔmotA, paralyzed normal flagella. The iEPS5 could be only propagated against wild-type, which have normal rotating flagella. The titer of iEPS5 in the polyhook strain was remained as same as the results of other resistant strains (*ΔmotA* and *ΔfliC*/*ΔfljB*) (Fig. 43A). Purportedly (174), Chi was propagated against *fliK* mutant, although the efficiency of infection was lower than in the wild-type (Fig. 43B).

In the TEM analysis, I got a picture, which could explain the importance of flagellar filament for iEPS5 infection. In the mixture of iEPS5 and *fliK* mutant, phages could not bind to the polyhook structure by using their tail fiber (Fig. 41). In this time, I also repeated the TEM analysis using a mixture of iEPS5 and wild-type and found that the head of phages bound to the flagellar filament showed brighter than that of free phages around the host, indicating the injection of phage DNA genome leaving the phage with empty head (Fig. 44). From these results, I hypothesized that flagellar filament could be a receptor for adsorption but also a DNA infection site after binding of phage.

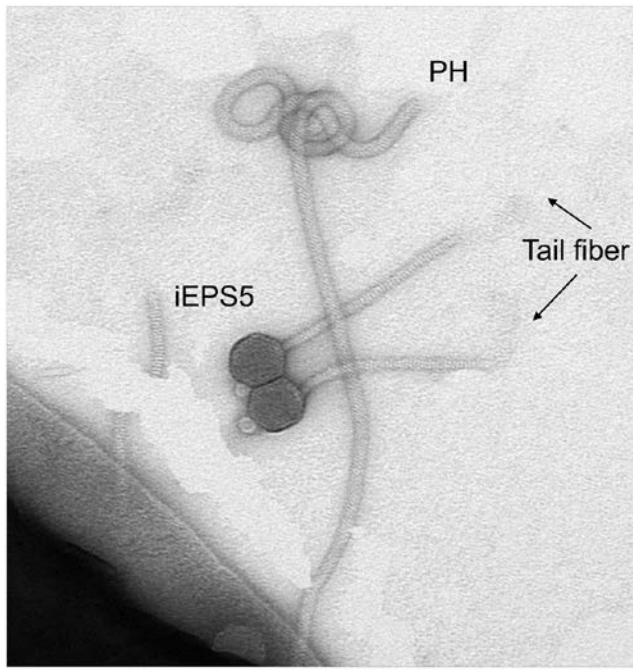

Figure 41. Confirmation of polyhook structure of *ΔfilK* and unbound form of iEPS5 in TEM analysis. Polyhook structure and unbound form of phage. Transmission electron micrograph of iEPS5 and polyhook strain (CH506, *ΔfilK*). Arrows designate phage, tail fiber, and polyhook (PH).

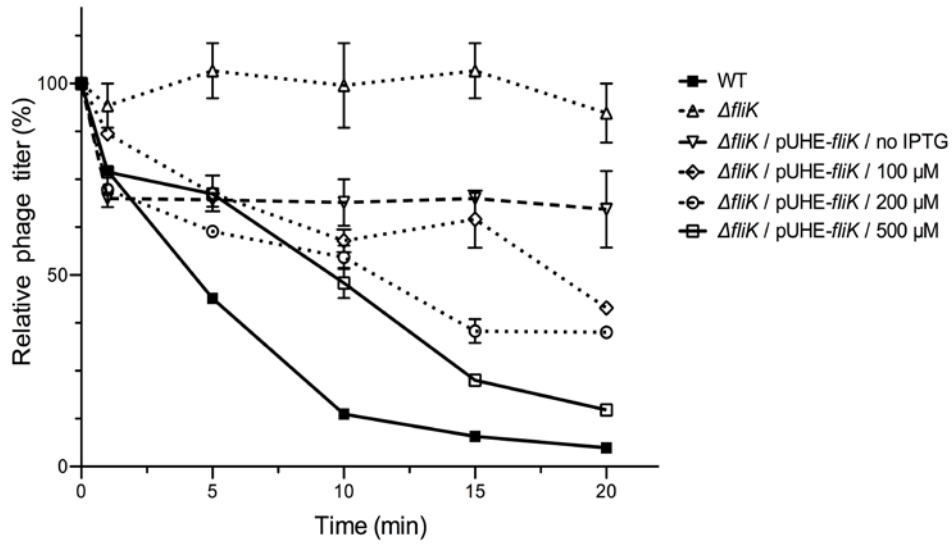

Figure 42. ***In vitro*** **adsorption assay of iEPS5 phage using plaque-counting method (3).** Exponentially growing cells were infected with iEPS5 (MOI, 0.01) and incubated at 37°C. After centrifugation and filtration, the phage titer in the filtrate was determined by standard overlay assay. The percentage of free phage particles was calculated as follows: (phage titer in the supernatant of iEPS5-infected bacterial suspension/phage titer in the supernatant of iEPS5-incubacted at 0 min) x 100. The results are expressed as means and standard deviations of triplicate assays. The concentrations of IPTG are 0, 100, 200, and 500 μM, respectively. Each strain was designated by different symbols with lines: Closed square, wild-type; open triangle, *ΔfliK*; open inverted triangle, *ΔfliK*/pUHE-*fliK*; open diamond, *ΔfliK*/pUHE-*fliK* with 100 μM of IPTG; open circle, *ΔfliK*/pUHE-*fliK* with 200 μM of IPTG; open square, *ΔfliK*/pUHE-*fliK* with 500 μM of IPTG.

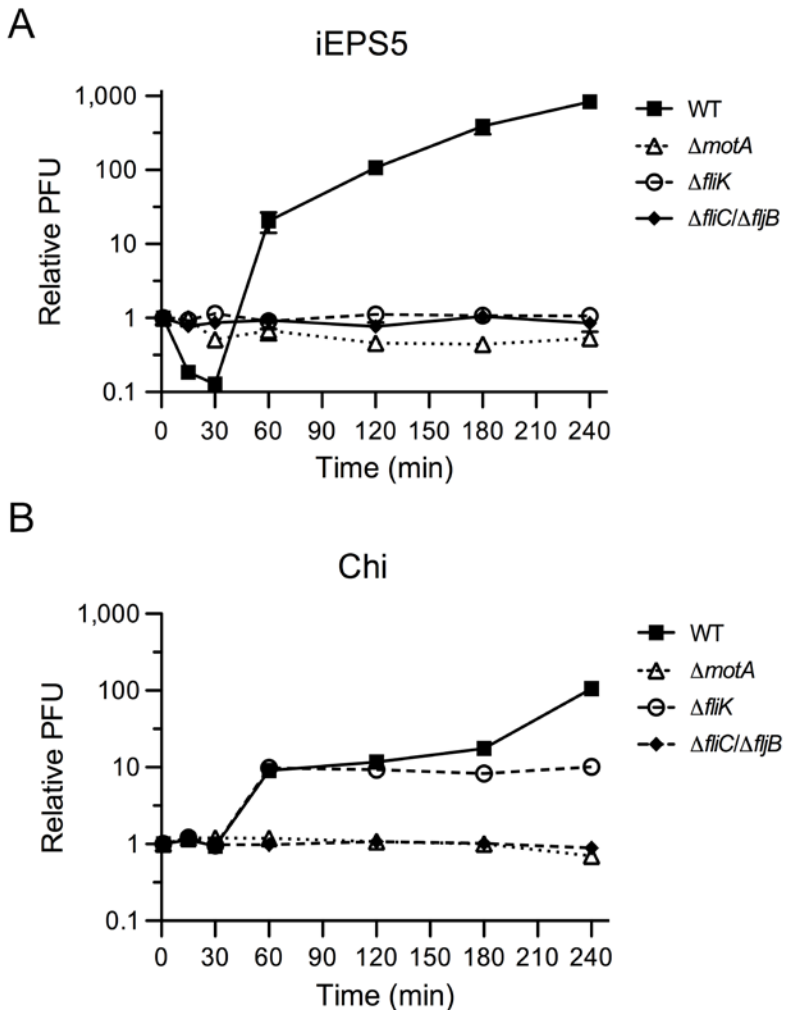

Figure 43. Phage challenge assay. Bacterial challenge assay with iEPS5 (A) and Chi (B) to diverse flagellar types: normal flagella (SL1344, WT), non-motile flagella (CH504, *ΔmotA*), normal hook without filament (CH509, *ΔfliC*/*ΔfljB*), and polyhook without filament (CH506, *ΔfliK*). Each phage was added at an MOI of 0.1 to the bacterial culture after 1.5 h incubation (time point, 0).

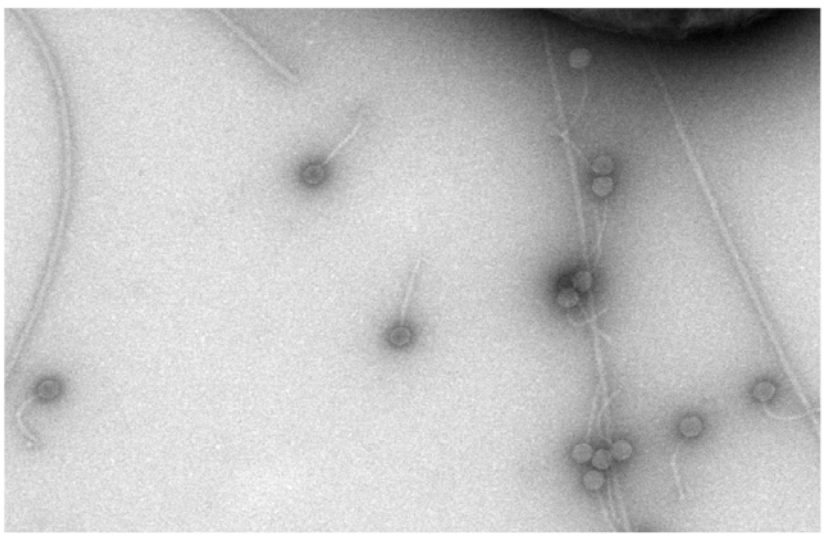

Figure 44. Flagellar filament-associated iEPS5 appeared an empty head structure. Electron microscopic image of mixture of wild-type and iEPS5 negatively stained with 0.2% uranyl acetate.

Flagellar filament might be the DNA-injection site of iEPS5

In order to elucidate the differences in infection processes between Chi and iEPS5, I tried to find a method for detection of phage DNA path during infection in the microscope. Among several DNA staining materials, SYBR-gold was selected for its ability to penetrate the phage capsid (113, 145, 205). SYBR-gold is an unsymmetrical cyanine dye that binds to RNA, ssDNA, and dsDNA (145). Phages inject its DNA into host bacteria only when they remain bound to their specific receptor on the bacterial surface. Binding a fluorophore such as SYBR-gold to the phage DNA does not alter the phage infection process. Moreover, after injection inside the host, the fluorophore bound to the phage DNA keeps its fluorescence (145).

The SYBR-gold-labeled iEPS5 was mixed with the host bacteria and incubated for 1 h at the same condition used for *in vitro* adsorption assay. When viewed under an epifluorescence microscope, the fluorescent phages were seen as a small spot corresponding to individual phage particles that were stained because of the diffusion of SYBR-gold through the capsids. Interestingly, from 1 to 20 min after infection, some flagella had fluorescence (GF), but that fluorescence seemed to move to the cytosol of the bacteria (Fig. 45). These observations suggest that the SYBR-gold-labeled phage DNA may travel through the flagella to the inside bacteria because the only fluorescent material, SYBR-gold, can move solely with

DNA, the genome of iEPS5. At 1 h after infection, several bacteria fluoresced because the SYBR-gold-labeled iEPS5 genome was inside their cytosol (Fig. 45). The presence of fluorescent flagellar filament probably resulting from the flagellar filled with the SYBR-gold-labeled iEPS5 DNA suggests that flagella itself could be a passage for injection of phage genome during infection. These observations were not seen with Chi, indicating different infection process between Chi and iEPS5.

These sequential displays of phage infection have not been reported before in the flagellatropic phage. Compared to the flagella-bound form of phage showed as a fluorescent dot (Fig. 46), these flagella filled with GF implied that flagella itself could be a passage for transportation of phage genome during infection. Flagellin is a 20-nm-thick; a 10 to 15-μm-long hollow tube and has a narrow channel with a diameter of 2.5~3.0 nm (41, 124). The size of DNA is ~2 nm in diameter. Therefore, the flagellin channel could be a pathway for phage DNA. Mechanism of DNA injection through flagella filament should be elucidated for better understanding of phage DNA injection.

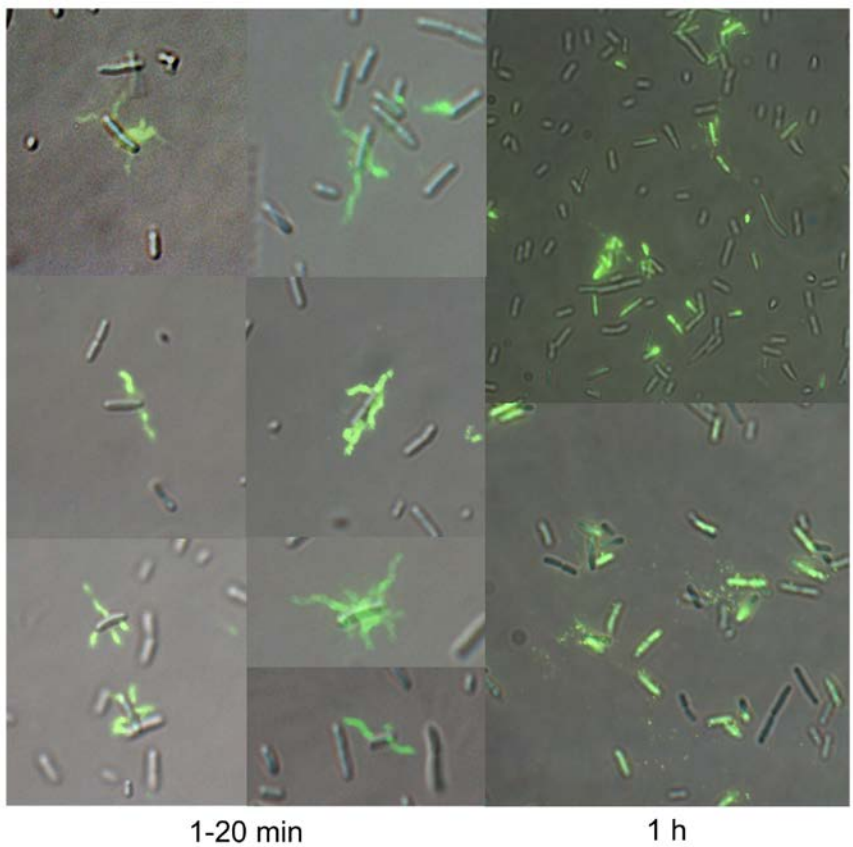

Figure 45. Visualization of bacterial cells carrying the specific gene transferred by SYBR-gold-labeled iEPS5 (1). Magnification = 1,000X.

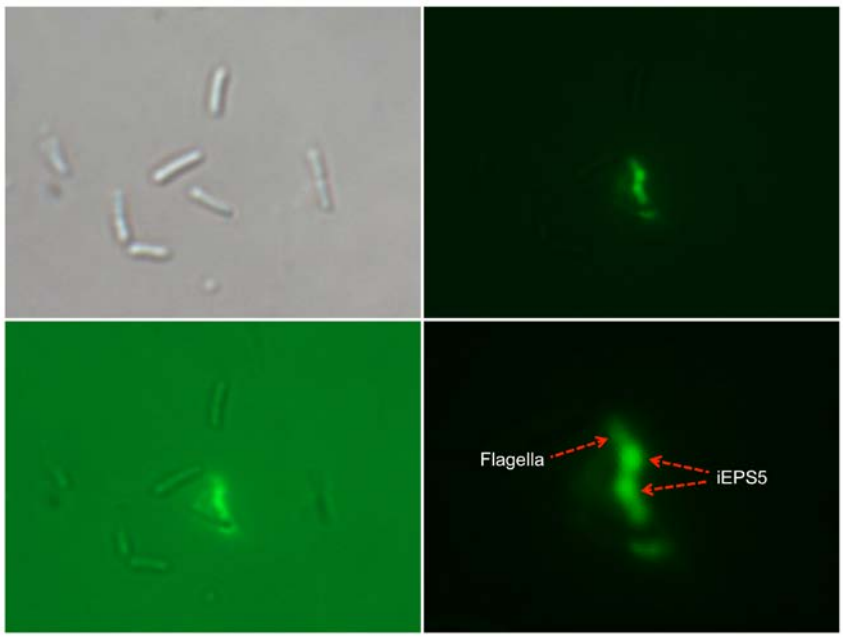

Figure 46. Visualization of bacterial cells carrying the specific gene transferred by SYBR-gold-labeled iEPS5 (2). The image at right down side is an enlarged picture indicating a flagellum filled with SYBR-gold-labeled DNA and flagella-bound phages with arrow, respectively. Magnification = 1,000X.

Discussion

The first step in the infection process is the adsorption of the phage to the bacterial cell, which is mediated by the tail fibers or by some analogous structure on those phages (120). The tail fibers attach to specific receptors on the bacterial cell and the host specificity of the phage is usually determined by the type of tail fibers that a phage has. The nature of the bacterial receptor varies for different bacteria as explained in introduction. These receptors are on the bacteria for other purposes and phages have evolved to use these receptors for infection.

In this study, a novel phage, iEPS5, of the *Siphoviridae* family was isolated. Genome sequencing of iEPS5 and its narrow host range suggested that iEPS5 has a specific receptor for its infection. In the genome, iEPS5 has a gene encoding tail fiber, which is related to phage adsorption. Tail fiber was also identified in the TEM analysis. Along with these results, a variety of lines of evidence support the hypothesis that iEPS5 is flagellatropic. First, all resistant mutants were related to flagellar biosynthesis and its assembly from the random mutant library screening. Most of the structural components of the flagellum of *Salmonella* are exported through a flagellum-specific pathway, which is a member of the family of type III secretary pathway (41, 124). FliR and FliP are embedded in a patch of

membrane in the central pore of the MS ring as export apparatus, therefore, the mutants could not assembled functional flagellar filament (61, 154). The hook-associated protein (HAP), FlgK has roles both in flagellar biosynthesis and assembly by regulating the anti-sigma factor, FlgM, which inhibits σ^{28} (FliA) prior to completion of the hook-basal body (HBB) structure (8). Therefore, the *flgK* mutant has been known to produce an intermediate structure that is unable to assemble the HAPs or filament but is able to secrete FlgM, FliC, and FliD (109). Finally, the flagellar specific sigma factor, FliA is an important regulator for activating class 3 promoters, leading to late flagellar gene expression (124). In conclusion, all these mutants have no flagellar filament assembled, but a fully formed HBB complex in their membranes. From these observations, it can be inferred that flagellin could be the site of viral adsorption and that iEPS5 does not bind to the basal body in a way that would allow infection. Also I assessed the sensitivity of flagellin mutant to iEPS5 infection because *Salmonella* Typhimurium has two types of flagellin genes (*fliC* and *fljB*) under control of flagellar phase variation (24). Each single mutant, which lacks of *fliC* or *fljB* respectively, was motile on the agar plate and sensitive to iEPS5, but, double mutant (*ΔfliC*/*ΔfljB*) was non-motile and resistant to phage infection supporting that both types of flagellar filament are the binding sites of iEPS5 for infection (data not shown).

The most important role of flagella in the bacteria is a movement by rotating their flagellar filaments. The flagellar motor consists of five proteins: MotA and MotB, which function as the stator and conduct the passage of protons to drive flagellar rotation, and the three switch proteins that are part of the rotor, FliG, FliM, and FliN. The passage of protons through MotA and MotB channels causes a conformational change in MotA (the power stroke) and direct interactions of MotA with the carboxyl terminus of FliG turning a ring of FliG molecules (123, 124). iEPS5 expectedly could not infect *motA* mutant that has paralyzed flagella. In both of TEM analysis and adsorption assay, *motA* mutant could not bind to the non-rotating flagella suggesting that not just a flagellar filament, but functionally rotating flagellin is required for iEPS5 infection through proper adsorption to its receptor.

Chemotaxis, the ability of some bacteria to sense and respond to their chemical environment by moving toward attractants and away from repellents, has under the ability to regulate the frequency with which their flagella switch between CW and CCW rotation (182). CCW rotation results in 'smooth swimming' of the bacterium in an approximately linear path, whereas the switch to CW rotation causes the bacterium to tumble (85). In this event, the CheY acts as a determinant of flagellar rotation for its direction. The phosphorylated CheY diffuses through the cytoplasm and

binds to an assembly of proteins called the 'switch' at the base of the flagellar motor. It is a binding event that results in the change of direction of the flagella from the default CCW to CW rotation (182). Therefore, *cheY* deleted mutant shows CCW-biased rotating flagella but the *cheY* over-expressing mutant characterizes CW-biased rotation in its flagella (174). Interestingly, iEPS5 could infect *cheY* mutant as wild-type, but when CheY increased in the cytoplasm, the EOP of iEPS5 was reduced gradually and finally iEPS5 could not infect fully CW-biased bacteria. Therefore, it is concluded that CCW-rotating flagella is required for proper binding and infection of iEPS5 to its host.

The flagellar filament is a supercoiled assembly of a single protein, flagellin, and is made of 11 protofilaments, which are longitudinal helical arrays of subunits (34, 125). Each protofilament can have one of two slightly different conformational states, L- and R-type (97, 172). Therefore, there can be 12 distinct polymorphic forms. This polymorphic supercoiling of the filament can be essential for bacterial taxis. In *Salmonella enterica*, flagellar motor rotates CCW for run, with several flagellar filaments in a left-handed helical shape forming a bundle and propelling its movement. The motor reverses its rotation and transforms the left-handed helical form to a right-handed one causing the bundle to fall apart (34, 125). The left-handed flagellar supercoil consists of 9L/2R (normal), and the right-handed

ones are 7L/4R (semicoil), 6L/5R (curly I), or 5L/6R (curly II), implying that the number of the R-type protofilaments need to be increased for transformation to the right-handed supercoils (34, 125, 129). In the bi-stable protofilament model predicts, the intersubunit repeat distances of the L- and R-type protofilaments were 52.7 Å and 51.9 Å, respectively (207). The difference of 0.8 Å would be responsible for the binding of iEPS5 to the flagellar filament. Therefore, I tested the infection ability of iEPS5 to the two different strains having 11L/0R (SJW1660) and 0L/11R (SJW1655) flagella, respectively. Unexpectedly, iEPS5 could infect both strains (data not shown) indicating that the difference of 0.8 Å between L- and R-type protofilaments is not crucial for phage infection.

A serially conducted experiment for identifying the receptor for iEPS5 revealed that iEPS5 infected to *Salmonella* by adsorption to the motile but only CCW-rotating flagellar filament on the cell surface. This infection mechanism of iEPS5 appears to be different from what is known about the mechanism of infection of the flagellatropic coliphage Chi, where attachment to the active flagellar filament is an intermediate step, improving the efficiency of infection (177). Phage Chi could infect both mutants lacking filaments and mutants with polyhooks supporting that its ultimate receptor is the basal body of flagellar assembles (174). Moreover, both CCW flagellar rotation and the correct structure of the helical grooves

on the flagellar surface are essential to infection by Chi in the manner of a nut on a bolt (174). Recently, two flagellar-dependent phages (ΦOT8 and ΦAT1) were identified and characterized by a group. Both phages could not bind to non-motile and non-flagellated bacteria (58, 59). In this study, iEPS5 could not infect the mutants lacking filament suggesting a possibility that it would inject its DNA into the flagellum. Flagellin is a 20-nm-thick; a10 to 15-μm-long hollow tube and has a narrow channel with a diameter of 2.5~3.0 nm (41, 124). Therefore, this channel of flagellin could be a pathway for phage DNA. To suggest this new infection mechanism for flagellatropic phage like iEPS5, it is remained to elucidate the injection of phage DNA to the flagellar filament.

REFERENCES

1. **Abedon, S. T.** 2009. Phage evolution and ecology. Adv. Appl. Microbiol. **67:**1-45.

2. **Abrahams, G. L., and M. Hensel.** 2006. Manipulating cellular transport and immune responses: dynamic interactions between intracellular *Salmonella enterica* and its host cells. Cell. Microbiol. **8:**728-737.

3. **Ackermann, H. W.** 2003. Bacteriophage observations and evolution. Res. Microbiol. **154:**245-251.

4. **Ackermann, H. W.** 2001. Frequency of morphological phage descriptions in the year 2000. Brief review. Arch. Virol. **146:**843-857.

5. **Ackermann, H. W.** 2009. Phage classification and characterization. Methods Mol. Biol. **501:**127-140.

6. **Aizawa, S. I., G. E. Dean, C. J. Jones, R. M. Macnab, and S. Yamaguchi.** 1985. Purification and characterization of the flagellar hook-basal body complex of *Salmonella typhimurium*. J. Bacteriol. **161:**836-849.

7. **Alderton, W. K., C. E. Cooper, and R. G. Knowles.** 2001. Nitric oxide synthases: structure, function and inhibition. Biochem. J. **357:**593-615.

8. **Aldridge, P., J. Karlinsey, and K. T. Hughes.** 2003. The type III secretion chaperone FlgN regulates flagellar assembly via a negative feedback loop containing its chaperone substrates FlgK and FlgL. Mol. Microbiol. **49:**1333-1345.

9. **Alekshun, M. N.** 2001. Beyond comparison--antibiotics from genome data? Nat. Biotechnol. **19:**1124-1125.

10. **Alpuchearanda, C. M., E. L. Racoosin, J. A. Swanson, and S. I. Miller.** 1994. *Salmonella* stimulate macrophage macropinocytosis and persist within spacious phagosomes. J. Exp. Med. **179:**601-608.

11. **Andrewes, F. W.** 1922. Studies in group-agglutination I The *salmonella* group and its antigenic structure. J. Pathol. Bacteriol. **25:**505-521.

12. **Babior, B. M.** 1999. NADPH oxidase: an update. Blood **93:**1464-1476.

13. **Babior, B. M.** 1995. The respiratory burst oxidase. Curr. Opin. Hematol. **2:**55-60.

14. **Bachrach, G., M. Leizerovici-Zigmond, A. Zlotkin, R. Naor, and D. Steinberg.** 2003. Bacteriophage isolation from human saliva. Lett. Appl. Microbiol. **36:**50-53.

15. **Bader, M. W., W. W. Navarre, W. Shiau, H. Nikaido, J. G. Frye, M. McClelland, F. C. Fang, and S. I. Miller.** 2003. Regulation of *Salmonella typhimurium* virulence gene expression by cationic antimicrobial peptides. Mol. Microbiol. **50:**219-230.

16. **Barbagallo, M., M. L. Di Martino, L. Marcocci, P. Pietrangeli, E. De Carolis, M. Casalino, B. Colonna, and G. Prosseda.** 2011. A new

piece of the Shigella Pathogenicity puzzle: spermidine accumulation by silencing of the speG gene [corrected]. PLoS one **6:**e27226.

17. **Barcelona-Andres, B., A. Marina, and V. Rubio.** 2002. Gene structure, organization, expression, and potential regulatory mechanisms of arginine catabolism in *Enterococcus faecalis*. J. Bacteriol. **184:**6289-6300.

18. **Baur, H., E. Luethi, V. Stalon, A. Mercenier, and D. Haas.** 1989. Sequence analysis and expression of the arginine-deiminase and carbamate-kinase genes of *Pseudomonas aeruginosa*. Eur. J. Biochem. **179:**53-60.

19. **Berg, H. C.** 2003. The rotary motor of bacterial flagella. Annu. Rev. Biochem. **72:**19-54.

20. **Bergh, O., K. Y. Borsheim, G. Bratbak, and M. Heldal.** 1989. High abundance of viruses found in aquatic environments. Nature **340:**467-468.

21. **Blanc-Potard, A. B., and E. A. Groisman.** 1997. The *Salmonella selC* locus contains a pathogenicity island mediating intramacrophage survival. EMBO J. **16:**5376-5385.

22. **Blaser, M. J., and L. S. Newman.** 1982. A review of human salmonellosis: I. Infective dose. Rev. Infect. Dis. **4:**1096-1106.

23. **Blouw, B., H. Q. Song, T. Tihan, J. Bosze, N. Ferrara, H. P. Gerber, R. S. Johnson, and G. Bergers.** 2003. The hypoxic response of tumors is dependent on their microenvironment. Cancer Cell **4:**133-146.

24. **Bonifield, H. R., and K. T. Hughes.** 2003. Flagellar phase variation in *Salmonella enterica* is mediated by a posttranscriptional control mechanism. J. Bacteriol. **185:**3567-3574.

25. **Boyde, T. R., and M. Rahmatullah.** 1980. Optimization of conditions for the colorimetric determination of citrulline, using diacetyl monoxime. Anal. Biochem. **107:**424-431.

26. **Breitbart, M., B. Felts, S. Kelley, J. M. Mahaffy, J. Nulton, P. Salamon, and F. Rohwer.** 2004. Diversity and population structure of a near-shore marine-sediment viral community. Proc. Biol. Sci. **271:**565-574.

27. **Brenner, F. W., R. G. Villar, F. J. Angulo, R. Tauxe, and B. Swaminathan.** 2000. *Salmonella* nomenclature. J. Clin. Microbiol. **38:**2465-2467.

28. **Brumell, J. H., D. L. Goosney, and B. B. Finlay.** 2002. SifA, a type III secreted effector of *Salmonella typhimurium*, directs *Salmonella*-induced filament (Sif) formation along microtubules. Traffic **3:**407-415.

29. **Brumell, J. H., and S. Grinstein.** 2004. *Salmonella* redirects phagosomal maturation. Curr. Opin. Microbiol. **7:**78-84.

30. **Brumell, J. H., P. Tang, S. D. Mills, and B. B. Finlay.** 2001. Characterization of *Salmonella*-induced filaments (Sifs) reveals a delayed interaction between *Salmonella*-containing vacuoles and late endocytic compartments. Traffic **2:**643-653.

31. **Buchmeier, N., A. Blanc-Potard, S. Ehrt, D. Piddington, L. Riley, and E. A. Groisman.** 2000. A parallel intraphagosomal survival strategy shared by *Mycobacterium tuberculosis* and *Salmonella enterica*. Mol. Microbiol. **35:**1375-1382.

32. **Buchwald, D. S., and M. J. Blaser.** 1984. A review of human salmonellosis: II. Duration of excretion following infection with nontyphi *Salmonella*. Rev. Infect. Dis. **6:**345-356.

33. **Bumann, D.** 2009. System-level analysis of *Salmonella* metabolism during infection. Curr. Opin. Microbiol. **12:**559-567.

34. **Calladine, C. R.** 1978. Change of waveform in bacterial flagella - role of mechanics at molecular level. J. Mol. Biol. **118:**457-479.

35. **Carlson, P. E., Jr., J. Horzempa, D. M. O'Dee, C. M. Robinson, P. Neophytou, A. Labrinidis, and G. J. Nau.** 2009. Global transcriptional response to spermine, a component of the intramacrophage environment, reveals regulation of *Francisella* gene expression through insertion sequence elements. J. Bacteriol. **191:**6855-6864.

36. **Casiano-Colon, A., and R. E. Marquis.** 1988. Role of the arginine deiminase system in protecting oral bacteria and an enzymatic basis for acid tolerance. Appl. Environ. Microbiol. **54:**1318-1324.

37. **Chalker, R. B., and M. J. Blaser.** 1988. A review of human salmonellosis: III. Magnitude of *Salmonella* infection in the United States. Rev. Infect. Dis. **10:**111-124.

38. **Chang, A. C., and S. N. Cohen.** 1978. Construction and characterization of amplifiable multicopy DNA cloning vehicles derived from the P15A cryptic miniplasmid. J. Bacteriol. **134:**1141-1156.

39. **Chattopadhyay, M. K., C. W. Tabor, and H. Tabor.** 2003. Polyamines protect Escherichia coli cells from the toxic effect of oxygen. Proc. Natl. Acad. Sci. U.S.A. **100:**2261-2265.

40. **Chessa, D., M. G. Winter, S. P. Nuccio, C. Tukel, and A. J. Baumler.** 2008. RosE represses Std fimbrial expression in *Salmonella enterica* serotype Typhimurium. Mol. Microbiol. **68:**573-587.

41. **Chevance, F. F., and K. T. Hughes.** 2008. Coordinating assembly of a bacterial macromolecular machine. Nat. Rev. Microbiol. **6:**455-465.

42. **Choi, J., D. Shin, H. Yoon, J. Kim, C. R. Lee, M. Kim, Y. J. Seok, and S. Ryu.** 2010. *Salmonella* pathogenicity island 2 expression negatively controlled by EIIA(Ntr)-SsrB interaction is required for *Salmonella* virulence. P. Natl. Acad. Sci. U.S.A. **107:**20506-20511.

43. **Cirillo, D. M., R. H. Valdivia, D. M. Monack, and S. Falkow.** 1998. Macrophage-dependent induction of the *Salmonella* pathogenicity island 2 type III secretion system and its role in intracellular survival. Mol. Microbiol. **30:**175-188.

44. **Compan, I., and D. Touati.** 1994. Anaerobic activation of *arcA* transcription in *Escherichia coli* - roles of Fnr and ArcA. Mol. Microbiol. **11:**955-964.

45. **Cramer, T., Y. Yamanishi, B. E. Clausen, I. Forster, R. Pawlinski, N. Mackman, V. H. Haase, R. Jaenisch, M. Corr, V. Nizet, G. S. Firestein, H. P. Gerber, N. Ferrara, and R. S. Johnson.** 2003. HIF-1 alpha is essential for myeloid cell-mediated inflammation. Cell **112:**645-657.

46. **d'Herelle, F.** 1917. An invisible antagonist microbe of dysentery bacillus. Cr. Hebd. Acad. Sci. **165:**373-375.

47. **Darnton, N. C., and H. C. Berg.** 2008. Bacterial flagella are firmly anchored. J. Bacteriol. **190:**8223-8224.

48. **Datsenko, K. A., and B. L. Wanner.** 2000. One-step inactivation of chromosomal genes in *Escherichia coli* K-12 using PCR products. P. Natl. Acad. Sci. U.S.A. **97:**6640-6645.

49. **Degnan, B. A., M. C. Fontaine, A. H. Doebereiner, J. J. Lee, P. Mastroeni, G. Dougan, J. A. Goodacre, and M. A. Kehoe.** 2000. Characterization of an isogenic mutant of *Streptococcus pyogenes* Manfredo lacking the ability to make streptococcal acid glycoprotein. Infect. Immun. **68:**2441-2448.

50. **Dimova, D., P. Weigel, M. Takahashi, F. Marc, G. D. Van Duyne, and V. Sakanyan.** 2000. Thermostability, oligomerization and DNA-binding properties of the regulatory protein ArgR from the hyperthermophilic bacterium *Thermotoga neapolitana*. Mol. Gen. Genet. **263:**119-130.

51. **Dong, T., R. Yu, and H. Schellhorn.** 2011. Antagonistic regulation of motility and transcriptome expression by RpoN and RpoS in *Escherichia coli*. Mol. Microbiol. **79:**375-386.

52. **Dong, Y., Y. Y. Chen, J. A. Snyder, and R. A. Burne.** 2002. Isolation and molecular analysis of the gene cluster for the arginine deiminase system from *Streptococcus gordonii* DL1. Appl. Environ. Microbiol. **68:**5549-5553.

53. **Drecktrah, D., L. A. Knodler, R. Ireland, and O. Steele-Mortimer.** 2006. The mechanism of *Salmonella* entry determines the vacuolar environment and intracellular gene expression. Traffic **7:**39-51.

54. **Edwards, S., and G. G. Meynell.** 1968. The widespred occurrence of enteric flagellar phages. J. Gen. Virol. **2:**443-444.

55. **Ellermeier, C. D., A. Janakiraman, and J. M. Slauch.** 2002. Construction of targeted single copy *lac* fusions using lambda Red and FLP-mediated site-specific recombination in bacteria. Gene **290:**153-161.

56. **Eriksson, S., S. Lucchini, A. Thompson, M. Rhen, and J. C. Hinton.** 2003. Unravelling the biology of macrophage infection by gene expression profiling of intracellular *Salmonella enterica*. Mol. Microbiol. **47:**103-118.

57. **Evans, M. R., R. C. Fink, A. Vazquez-Torres, S. Porwollik, J. Jones-Carson, M. McClelland, and H. M. Hassan.** 2011. Analysis of the ArcA regulon in anaerobically grown *Salmonella enterica* sv. Typhimurium. BMC Microbiol. **11:**58.

58. **Evans, T. J., M. A. Crow, N. R. Williamson, W. Orme, N. R. Thomson, E. Komitopoulou, and G. P. Salmond.** 2010. Characterization of a broad-host-range flagellum-dependent phage

that mediates high-efficiency generalized transduction in, and between, *Serratia* and *Pantoea*. Microbiology **156:**240-247.

59. **Evans, T. J., A. Trauner, E. Komitopoulou, and G. P. C. Salmond.** 2010. Exploitation of a new flagellatropic phage of *Erwinia* for positive selection of bacterial mutants attenuated in plant virulence: towards phage therapy. J. Appl. Microbiol. **108:**676-685.

60. **Ezaki, T., Y. Kawamura, and E. Yabuuchi.** 2000. Recognition of nomenclatural standing of *Salmonella typhi* (Approved Lists 1980), *Salmonella enteritidis* (Approved Lists 1980) and *Salmonella typhimurium* (Approved Lists 1980), and conservation of the specific epithets *enteritidis* and *typhimurium*. Request for an opinion. Int. J. Syst. Evol. Microbiol. **50 Pt 2:**945-947.

61. **Fan, F., K. Ohnishi, N. R. Francis, and R. M. Macnab.** 1997. The FliP and FliR proteins of *Salmonella typhimurium*, putative components of the type III flagellar export apparatus, are located in the flagellar basal body. Mol. Microbiol. **26:**1035-1046.

62. **Fang, F. C.** 2004. Antimicrobial reactive oxygen and nitrogen species: concepts and controversies. Nat. Rev. Microbiol. **2:**820-832.

63. **Faucher, S. P., S. Porwollik, C. M. Dozois, M. McClelland, and F. Daigle.** 2006. Transcriptome of *Salmonella enterica* serovar Typhi within macrophages revealed through the selective capture of transcribed sequences. P. Natl. Acad. Sci. U.S.A. **103:**1906-1911.

64. **Fields, P. I., R. V. Swanson, C. G. Haidaris, and F. Heffron.** 1986. Mutants of *Salmonella*-Typhimurium that cannot survive within the macrophage are avirulent. P. Natl. Acad. Sci. U.S.A. **83:**5189-5193.

65. **Figueira, R., and D. W. Holden.** 2012. Functions of the *Salmonella* pathogenicity island 2 (SPI-2) type III secretion system effectors. Microbiol-Sgm **158:**1147-1161.

66. **Finkel, S. E., and R. C. Johnson.** 1993. The Fis protein: it's not just for DNA inversion anymore. Mol. Microbiol. **7:**1023.

67. **Fischetti, V. A.** 2008. Bacteriophage lysins as effective antibacterials. Curr. Opin. Microbiol. **11:**393-400.

68. **Flannagan, R. S., G. Cosio, and S. Grinstein.** 2009. Antimicrobial mechanisms of phagocytes and bacterial evasion strategies. Nat. Rev. Microbiol. **7:**355-366.

69. **Francis, C. L., M. N. Starnbach, and S. Falkow.** 1992. Morphological and cytoskeletal changes in epithelial-cells occur immediately upon interaction with *Salmonella*-Typhimurium grown under low-oxygen conditions. Mol. Microbiol. **6:**3077-3087.

70. **Frankel, R. W., and T. M. Joys.** 1966. Adsorption specificity of bacteriophage PBS1. J. Bacteriol. **92:**388-&.

71. **Fulde, M., J. Willenborg, A. de Greeff, L. Benga, H. E. Smith, P. Valentin-Weigand, and R. Goethe.** 2011. ArgR is an essential local transcriptional regulator of the *arcABC* operon in *Streptococcus suis* and is crucial for biological fitness in an acidic environment. Microbiol-Sgm **157:**572-582.

72. **Galperin, M. Y.** 2006. Structural classification of bacterial response regulators: Diversity of output domains and domain combinations. J. Bacteriol. **188:**4169-4182.

73. **Garcia-del Portillo, F., J. W. Foster, and B. B. Finlay.** 1993. Role of acid tolerance response genes in *Salmonella typhimurium* virulence. Infect. Immun. **61:**4489-4492.

74. **Garmendia, J., C. R. Beuzon, J. Ruiz-Albert, and D. W. Holden.** 2003. The roles of SsrA-SsrB and OmpR-EnvZ in the regulation of genes encoding the *Salmonella typhimurium* SPI-2 type III secretion system. Microbiol-Sgm **149:**2385-2396.

75. **Gobert, A. P., D. J. McGee, M. Akhtar, G. L. Mendz, J. C. Newton, Y. Cheng, H. L. Mobley, and K. T. Wilson.** 2001. *Helicobacter pylori* arginase inhibits nitric oxide production by eukaryotic cells: a strategy for bacterial survival. P. Natl. Acad. Sci. U.S.A. **98:**13844-13849.

76. **Griess, P.** 1879. Bemerkungen zu der abhandlung der H.H. Weselsky und Benedikt "Ueber einige azoverbindungen.". Chem. Ber. **12:**426-428.

77. **Griswold, A., Y. Y. Chen, J. A. Snyder, and R. A. Burne.** 2004. Characterization of the arginine deiminase operon of *Streptococcus rattus* FA-1. Appl. Environ. Microbiol. **70:**1321-1327.

78. **Groisman, E. A., and H. Ochman.** 1997. How *Salmonella* became a pathogen. Trends Microbiol. **5:**343-349.

79. **Gruening, P., M. Fulde, P. Valentin-Weigand, and R. Goethe.** 2006. Structure, regulation, and putative function of the arginine deiminase system of *Streptococcus suis*. J. Bacteriol. **188:**361-369.

80. **Gunsalus, R. P., and S. J. Park.** 1994. Aerobic-anaerobic gene regulation in *Escherichia coli*: control by the ArcAB and Fnr regulons. Res. Microbiol. **145:**437-450.

81. **Hampton, M. B., A. J. Kettle, and C. C. Winterbourn.** 1998. Inside the neutrophil phagosome: oxidants, myeloperoxidase, and bacterial killing. Blood **92:**3007-3017.

82. **Hanaha, D.** 1985. in DNA Cloning: A practical approach.

83. **Hansen-Wester, I., and M. Hensel.** 2001. *Salmonella* pathogenicity islands encoding type III secretion systems. Microbes. Infect. **3:**549-559.

84. **Haraga, A., M. B. Ohlson, and S. I. Miller.** 2008. *Salmonellae* interplay with host cells. Nat. Rev. Microbiol. **6:**53-66.

85. **Harshey, R. M.** 2003. Bacterial motility on a surface: many ways to a common goal. Annu. Rev. Microbiol. **57:**249-273.

86. **Hausler, T.** 2006. Bug killers. Nat. Med. **12:**600-601.

87. **Hautefort, I., A. Thompson, S. Eriksson-Ygberg, M. L. Parker, S. Lucchini, V. Danino, R. J. Bongaerts, N. Ahmad, M. Rhen, and J. C. Hinton.** 2008. During infection of epithelial cells *Salmonella enterica* serovar Typhimurium undergoes a time-dependent transcriptional adaptation that results in simultaneous expression of three type 3 secretion systems. Cell. Microbiol. **10:**958-984.

88. **Hebrard, M., C. Kroger, S. K. Sivasankaran, K. Handler, and J. C. Hinton.** 2011. The challenge of relating gene expression to the

virulence of *Salmonella enterica* serovar Typhimurium. Curr. Opin. Biotechnol. **22:**200-210.

89. **Heby, O.** 1981. Role of polyamines in the control of cell proliferation and differentiation. Differentiation **19:**1-20.

90. **Henard, C. A., and A. Vazquez-Torres.** 2011. Nitric oxide and *Salmonella* pathogenesis. Front Microbiol. **2:**84.

91. **Hengge-Aronis, R.** 2002. Signal transduction and regulatory mechanisms involved in control of the sigma(S) (RpoS) subunit of RNA polymerase. Microbiol. Mol. Biol. Rev. **66:**373-395, table of contents.

92. **Hirano, T., S. Yamaguchi, K. Oosawa, and S. Aizawa.** 1994. Roles of FliK and FlhB in determination of flagellar hook length in *Salmonella typhimurium*. J. Bacteriol. **176:**5439-5449.

93. **Hoboth, C., R. Hoffmann, A. Eichner, C. Henke, S. Schmoldt, A. Imhof, J. Heesemann, and M. Hogardt.** 2009. Dynamics of adaptive microevolution of hypermutable *Pseudomonas aeruginosa* during chronic pulmonary infection in patients with cystic fibrosis. J. Infect. Dis. **200:**118-130.

94. **Hoiseth, S. K., and B. A. D. Stocker.** 1981. Aromatic-dependent *Salmonella*-Typhimurium are non-virulent and effective as live vaccines. Nature **291:**238-239.

95. **Hong, J., K. P. Kim, S. Heu, S. J. Lee, S. Adhya, and S. Ryu.** 2008. Identification of host receptor and receptor-binding module of a

newly sequenced T5-like phage EPS7. FEMS Microbiol. Lett. **289:**202-209.

96. **Hughes, K. T., and S. R. Maloy.** 2007. Advanced bacterial genetics : use of transposons and phage for genomic engineering. Academic Press, San Diego, Calif.

97. **Hyman, H. C., and S. Trachtenberg.** 1991. Point mutations that lock *Salmonella*-Typhimurium flagellar filaments in the straight right-handed and left-handed forms and their relation to filament superhelicity. J. Mol. Biol. **220:**79-88.

98. **Hyman, P., and S. T. Abedon.** 2010. Bacteriophage host range and bacterial resistance. Adv. Appl. Microbiol. **70:**217-248.

99. **Igarashi, K., and K. Kashiwagi.** 2010. Modulation of cellular function by polyamines. Int. J. Biochem. Cell Biol. **42:**39-51.

100. **Ikeda, E.** 2005. Cellular response to tissue hypoxia and its involvement in disease progression. Pathol. Int. **55:**603-610.

101. **Incardona, N. L., and L. Selvidge.** 1973. Mechanism of adsorption and eclipse of bacteriophage phi X174. II. Attachment and eclipse with isolated *Escherichia coli* cell wall lipopolysaccharide. J. Virol. **11:**775-782.

102. **Iuchi, S., and E. C. C. Lin.** 1993. Adaptation of *Escherichia coli* to redox environments by gene-expression. Mol. Microbiol. **9:**9-15.

103. **Jelsbak, L., L. E. Thomsen, I. Wallrodt, P. R. Jensen, and J. E. Olsen.** 2012. Polyamines are required for virulence in *Salmonella enterica* serovar Typhimurium. PLoS one **7:**e36149.

104. **Jessup, C. M., and S. E. Forde.** 2008. Ecology and evolution in microbial systems: the generation and maintenance of diversity in phage-host interactions. Res. Microbiol. **159:**382-389.

105. **Jones, B. D., N. Ghori, and S. Falkow.** 1994. *Salmonella*-Typhimurium initiates murine infection by penetrating and destroying the specialized epithelial M-cells of the Peyers-patches. J. Exp. Med. **180:**15-23.

106. **Joys, T. M.** 1965. Correlation between susceptibility to bacteriophage PBS1 and motility in *Bacillus subtilis*. J. Bacteriol. **90:**1575-&.

107. **Kingsley, R. A., A. D. Humphries, E. H. Weening, M. R. De Zoete, S. Winter, A. Papaconstantinopoulou, G. Dougan, and A. J. Baumler.** 2003. Molecular and phenotypic analysis of the CS54 island of *Salmonella enterica* serotype *typhimurium*: identification of intestinal colonization and persistence determinants. Infect. Immun. **71:**629-640.

108. **Kojima, S., K. Imada, M. Sakuma, Y. Sudo, C. Kojima, T. Minamino, M. Homma, and K. Namba.** 2009. Stator assembly and activation mechanism of the flagellar motor by the periplasmic region of MotB. Mol. Microbiol. **73:**710-718.

109. **Komoriya, K., N. Shibano, T. Higano, N. Azuma, S. Yamaguchi, and S. I. Aizawa.** 1999. Flagellar proteins and type III-exported virulence factors are the predominant proteins secreted into the culture media of *Salmonella typhimurium*. Mol. Microbiol. **34:**767-779.

110. **Korner, H., H. J. Sofia, and W. G. Zumft.** 2003. Phylogeny of the bacterial superfamily of Crp-Fnr transcription regulators: exploiting the metabolic spectrum by controlling alternative gene programs. FEMS Microbiol. Rev. **27:**559-592.

111. **Kuhle, V., and M. Hensel.** 2004. Cellular microbiology of intracellular *Salmonella enterica*: functions of the type III secretion system encoded by *Salmonella* pathogenicity island 2. Cell. Mol. Life Sci. **61:**2812-2826.

112. **Kukanich, K. S.** 2011. Update on *Salmonella* spp. contamination of pet food, treats, and nutritional products and safe feeding recommendations. J. Am. Vet. Med. Assoc. **238:**1430-1434.

113. **Kunisaki, H., and Y. Tanji.** 2010. Intercrossing of phage genomes in a phage cocktail and stable coexistence with *Escherichia coli* O157:H7 in anaerobic continuous culture. Appl. Microbiol. Biotechnol. **85:**1533-1540.

114. **Labrie, S. J., J. E. Samson, and S. Moineau.** 2010. Bacteriophage resistance mechanisms. Nat. Rev. Microbiol. **8:**317-327.

115. **Lahiri, A., P. Das, and D. Chakravortty.** 2008. Arginase modulates *Salmonella* induced nitric oxide production in RAW264.7 macrophages and is required for *Salmonella* pathogenesis in mice model of infection. Microbes. Infect. **10:**1166-1174.

116. **Lee, A. K., C. S. Detweiler, and S. Falkow.** 2000. OmpR regulates the two-component system SsrA-SsrB in *Salmonella* pathogenicity island 2. J. Bacteriol. **182:**771-781.

117. **Letellier, L., P. Boulanger, L. Plancon, P. Jacquot, and M. Santamaria.** 2004. Main features on tailed phage, host recognition and DNA uptake. Front. Biosci. **9:**1228-1339.

118. **Lewis, J. S., J. A. Lee, J. C. Underwood, A. L. Harris, and C. E. Lewis.** 1999. Macrophage responses to hypoxia: relevance to disease mechanisms. J. Leukoc. Biol. **66:**889-900.

119. **Li, Z., L. Kulakova, L. Li, A. Galkin, Z. Zhao, T. E. Nash, P. S. Mariano, O. Herzberg, and D. Dunaway-Mariano.** 2009. Mechanisms of catalysis and inhibition operative in the arginine deiminase from the human pathogen *Giardia lamblia*. Bioorg. Chem. **37:**149-161.

120. **Lindberg, A. A.** 1973. Bacteriophage receptors. Annu. Rev. Microbiol. **27:**205-241.

121. **Lindberg, A. A., and T. Holme.** 1969. Influence of O side chains on the attachment of the Felix O-1 bacteriophage to *Salmonella* bacteria. J. Bacteriol. **99:**513-519.

122. **Lu, C. D., H. Winteler, A. Abdelal, and D. Haas.** 1999. The ArgR regulatory protein, a helper to the anaerobic regulator ANR during transcriptional activation of the *arcD* promoter in *Pseudomonas aeruginosa*. J. Bacteriol. **181:**2459-2464.

123. **Macnab, R. M.** 1986. Proton-driven bacterial flagellar motor. Meth. Enzymol. **125:**563-581.

124. **Macnab, R. M.** 2004. Type III flagellar protein export and flagellar assembly. Biochim. Biophys. Acta **1694:**207-217.

125. **Macnab, R. M., and M. K. Ornston.** 1977. Normal to curly flagellar transitions and their role in bacterial tumbling - stabilization of an alternative quaternary structure by mechanical force. J. Mol. Biol. **112:**1-30.

126. **Magariyama, Y., S. Yamaguchi, and S. Aizawa.** 1990. Genetic and behavioral analysis of flagellar switch mutants of *Salmonella typhimurium*. J. Bacteriol. **172:**4359-4369.

127. **Maghnouj, A., T. F. de Sousa Cabral, V. Stalon, and C. Vander Wauven.** 1998. The *arcABDC* gene cluster, encoding the arginine deiminase pathway of *Bacillus licheniformis*, and its activation by the arginine repressor *argR*. J. Bacteriol. **180:**6468-6475.

128. **Makhlin, J., T. Kofman, I. Borovok, C. Kohler, S. Engelmann, G. Cohen, and Y. Aharonowitz.** 2007. *Staphylococcus aureus* ArcR controls expression of the arginine deiminase operon. J. Bacteriol. **189:**5976-5986.

129. **Maki-Yonekura, S., K. Yonekura, and K. Namba.** 2010. Conformational change of flagellin for polymorphic supercoiling of the flagellar filament. Nat. Struct. Mol. Biol. **17:**417-U450.

130. **Malladi, V., M. Puthenedam, P. H. Williams, and A. Balakrishnan.** 2004. Enteropathogenic *Escherichia coli* outer membrane proteins induce iNOS by activation of NF-kappaB and MAP kinases. Inflammation **28:**345-353.

131. **Mariconda, S., Q. Wang, and R. M. Harshey.** 2006. A mechanical role for the chemotaxis system in swarming motility. Mol. Microbiol. **60:**1590-1602.

132. **Mattey, M., and J. Spencer.** 2008. Bacteriophage therapy-cooked goose or phoenix rising? Curr. Opin. Biotechnol. **19:**608-612.

133. **McClelland, M., K. E. Sanderson, J. Spieth, S. W. Clifton, P. Latreille, L. Courtney, S. Porwollik, J. Ali, M. Dante, F. Du, S. Hou, D. Layman, S. Leonard, C. Nguyen, K. Scott, A. Holmes, N. Grewal, E. Mulvaney, E. Ryan, H. Sun, L. Florea, W. Miller, T. Stoneking, M. Nhan, R. Waterston, and R. K. Wilson.** 2001. Complete genome sequence of *Salmonella enterica* serovar Typhimurium LT2. Nature **413:**852-856.

134. **Merighi, M., C. D. Ellermeier, J. M. Slauch, and J. S. Gunn.** 2005. Resolvase-in vivo expression technology analysis of the *Salmonella enterica* serovar Typhimurium PhoP and PmrA regulons in BALB/c mice. J. Bacteriol. **187:**7407-7416.

135. **Messina, L., G. Spampinato, A. Arcidiacono, L. Malaguarnera, M. Pagano, B. Kaminska, L. Kaczmarek, and A. Messina.** 1992. Polyamine involvement in functional activation of human macrophages. J. Leukoc. Biol. **52:**585-587.

136. **Meynell, E.** 1964. The significance of bacteriophage in bacterial classification. a review. J. Gen. Microbiol. **36:**461-469.

137. **Miao, E. A., J. A. Freeman, and S. I. Miller.** 2002. Transcription of the SsrAB regulon is repressed by alkaline pH and is independent of PhoPQ and magnesium concentration. J. Bacteriol. **184:**1493-1497.

138. **Michetti, P., M. J. Mahan, J. M. Slauch, J. J. Mekalanos, and M. R. Neutra.** 1992. Monoclonal secretory immunoglobulin A protects

mice against oral challenge with the invasive pathogen *Salmonella typhimurium*. Infect. Immun. **60:**1786-1792.

139. **Miller, J. H.** 1972. Experiments in molecular genetics. Cold Spring Harbor Laboratory, Cold Spring Harbor, N.Y.

140. **Miller, S. I., A. M. Kukral, and J. J. Mekalanos.** 1989. A two-component regulatory system (*phoP phoQ*) controls *Salmonella typhimurium* virulence. P. Natl. Acad. Sci. U.S.A. **86:**5054-5058.

141. **Minamino, T., B. Gonzalez-Pedrajo, K. Yamaguchi, S. I. Aizawa, and R. M. Macnab.** 1999. FliK, the protein responsible for flagellar hook length control in *Salmonella*, is exported during hook assembly. Mol. Microbiol. **34:**295-304.

142. **Miroux, B., and J. E. Walker.** 1996. Over-production of proteins in *Escherichia coli*: Mutant hosts that allow synthesis of some membrane proteins and globular proteins at high levels. J. Mol. Biol. **260:**289-298.

143. **Mondigler, M., R. T. Vogele, and K. J. Heller.** 1995. Overproduced and purified receptor-binding protein Pb5 of bacteriophage-T5 binds to the T5 receptor protein FhuA. FEMS Microbiol. Lett. **130:**293-300.

144. **Mori, M., and T. Gotoh.** 2004. Arginine metabolic enzymes, nitric oxide and infection. J. Nutr. **134:**2820S-2825S; discussion 2853S.

145. **Mosier-Boss, P. A., S. H. Lieberman, J. M. Andrews, F. L. Rohwer, L. E. Wegley, and M. Breitbart.** 2003. Use of fluorescently labeled

phage in the detection and identification of bacterial species. Appl. Spectrosc. **57:**1138-1144.

146. **Muramoto, K., and R. M. Macnab.** 1998. Deletion analysis of MotA and MotB, components of the force-generating unit in the flagellar motor of *Salmonella*. Mol. Microbiol. **29:**1191-1202.

147. **Murdoch, C., M. Muthana, and C. E. Lewis.** 2005. Hypoxia regulates macrophage functions in inflammation. J. Immunol. **175:**6257-6263.

148. **Nasrallah, G. K., A. L. Riveroll, A. Chong, L. E. Murray, P. J. Lewis, and R. A. Garduno.** 2011. *Legionella pneumophila* requires polyamines for optimal intracellular growth. J. Bacteriol. **193:**4346-4360.

149. **Nishijyo, T., S. M. Park, C. D. Lu, Y. Itoh, and A. T. Abdelal.** 1998. Molecular characterization and regulation of an operon encoding a system for transport of arginine and ornithine and the ArgR regulatory protein in *Pseudomonas aeruginosa*. J. Bacteriol. **180:**5559-5566.

150. **Nizet, V., and R. S. Johnson.** 2009. Interdependence of hypoxic and innate immune responses. Nat. Rev. Immunol. **9:**609-617.

151. **Nystrom, T., C. Larsson, and L. Gustafsson.** 1996. Bacterial defense against aging: role of the Escherichia coli ArcA regulator in gene expression, readjusted energy flux and survival during stasis. Embo J. **15:**3219-3228.

152. **Ochman, H., F. C. Soncini, F. Solomon, and E. A. Groisman.** 1996. Identification of a pathogenicity island required for *Salmonella* survival in host cells. P. Natl. Acad. Sci. U.S.A. **93:**7800-7804.

153. **Ohl, M. E., and S. I. Miller.** 2001. *Salmonella*: a model for bacterial pathogenesis. Annu. Rev. Med. **52:**259-274.

154. **Ohnishi, K., F. Fan, G. J. Schoenhals, M. Kihara, and R. M. Macnab.** 1997. The FliO, FliP, FliQ, and FliR proteins of *Salmonella typhimurium*: putative components for flagellar assembly. J. Bacteriol. **179:**6092-6099.

155. **Ohnishi, K., K. Kutsukake, H. Suzuki, and T. Iino.** 1990. Gene *fliA* encodes an alternative sigma factor specific for flagellar operons in *Salmonella typhimurium*. Mol. Gen. Genet. **221:**139-147.

156. **Park, S. M., C. D. Lu, and A. T. Abdelal.** 1997. Purification and characterization of an arginine regulatory protein, ArgR, from *Pseudomonas aeruginosa* and its interactions with the control regions for the *car*, *argF*, and *aru* operons. J. Bacteriol. **179:**5309-5317.

157. **Pavlov, V., and O. Dimitrov.** 1996. [The catabolism of polyamines]. Molekuliarna meditsina = Molecular medicine / Nauchno sdruzhenie "Molekuliarna meditsina" **1:**16-21.

158. **Pegg, A. E.** 1986. Recent advances in the biochemistry of polyamines in eukaryotes. Biochem J. **234:**249-262.

159. **Pegg, A. E., L. M. Shantz, and C. S. Coleman.** 1995. Ornithine decarboxylase as a target for chemoprevention. J. Cell. Biochem. **22:**132-138.

160. **Peyssonnaux, C., P. Cejudo-Martin, A. Doedens, A. S. Zinkernagel, R. S. Johnson, and V. Nizet.** 2007. Cutting edge: Essential role of hypoxia inducible factor-1 alpha in development of lipopolysaccharide-induced sepsis. J. Immunol. **178:**7516-7519.

161. **Peyssonnaux, C., V. Datta, T. Cramer, A. Doedens, E. A. Theodorakis, R. L. Gallo, N. Hurtado-Ziola, V. Nizet, and R. S. Johnson.** 2005. HIF-1 alpha expression regulates the bactericidal capacity of phagocytes. J. Clin. Invest. **115:**1806-1815.

162. **Porwollik, S., E. F. Boyd, C. Choy, P. Cheng, L. Florea, E. Proctor, and M. McClelland.** 2004. Characterization of *Salmonella enterica* subspecies I genovars by use of microarrays. J. Bacteriol. **186:**5883-5898.

163. **Quirk, A. V., A. Sletten, and R. C. Hignett.** 1976. Properties of phage-receptor lipopolysaccharide from *Pseudomonas morsprunorum*. J. Gen. Microbiol. **96:**375-381.

164. **Rakhuba, D. V., E. I. Kolomiets, E. S. Dey, and G. I. Novik.** 2010. Bacteriophage receptors, mechanisms of phage adsorption and penetration into host cell. Pol. J. Microbiol. **59:**145-155.

165. **Ramsden, A. E., L. J. Mota, S. Munter, S. L. Shorte, and D. W. Holden.** 2007. The SPI-2 type III secretion system restricts motility of *Salmonella*-containing vacuoles. Cell. Microbiol. **9:**2517-2529.

166. **Ravid, S., P. Matsumura, and M. Eisenbach.** 1986. Restoration of flagellar clockwise rotation in bacterial envelopes by insertion of the chemotaxis protein CheY. P. Natl. Acad. Sci. U.S.A. **83:**7157-7161.

167. **Rhee, M. S., Y. S. Kim, S. Y. Park, M. H. Choi, B. M. Kim, S. U. Kang, K. J. Lee, and J. H. Lee.** 2002. Polyamine stimulation of *arcA* expression in *Escherichia coli*. J. Microbiol. **40:**305-312.

168. **Rhodius, V. A., D. M. West, C. L. Webster, S. J. W. Busby, and N. J. Savery.** 1997. Transcription activation at class II CRP-dependent promoters: The role of different activating regions. Nucleic Acids Res. **25:**326-332.

169. **Russo, B. C., J. Horzempa, D. M. O'Dee, D. M. Schmitt, M. J. Brown, P. E. Carlson, Jr., R. J. Xavier, and G. J. Nau.** 2011. A *Francisella tularensis* locus required for spermine responsiveness is necessary for virulence. Infect. Immun. **79:**3665-3676.

170. **Ryan, S., M. Begley, C. G. Gahan, and C. Hill.** 2009. Molecular characterization of the arginine deiminase system in *Listeria monocytogenes*: regulation and role in acid tolerance. Environ. Microbiol. **11:**432-445.

171. **Salmon, K. A., S. P. Hung, N. R. Steffen, R. Krupp, P. Baldi, G. W. Hatfield, and R. P. Gunsalus.** 2005. Global gene expression profiling in *Escherichia coli* K12: effects of oxygen availability and ArcA. J. Biol. Chem. **280:**15084-15096.

172. **Samatey, F. A., K. Imada, S. Nagashima, F. Vonderviszt, T. Kumasaka, M. Yamamoto, and K. Namba.** 2001. Structure of the bacterial flagellar protofilament and implications for a switch for supercoiling. Nature **410:**331-337.

173. **Sambrook, J., and W. D. Russell.** 2001. Molecular cloning: a laboratory manual, 3rd edition.

174. **Samuel, A. D., T. P. Pitta, W. S. Ryu, P. N. Danese, E. C. Leung, and H. C. Berg.** 1999. Flagellar determinants of bacterial sensitivity to chi-phage. P. Natl. Acad. Sci. U.S.A. **96:**9863-9866.

175. **Sanchez-Vargas, F. M., M. A. Abu-El-Haija, and O. G. Gomez-Duarte.** 2011. *Salmonella* infections: an update on epidemiology, management, and prevention. Travel. Med. Infect. Dis. **9:**263-277.

176. **Savery, N. J., G. S. Lloyd, M. Kainz, T. Gaal, W. Ross, R. H. Ebright, R. L. Gourse, and S. J. W. Busby.** 1998. Transcription activation at class II CRP-dependent promoters: identification of determinants in the C-terminal domain of the RNA polymerase alpha subunit. EMBO J. **17:**3439-3447.

177. **Schade, S. Z., J. Adler, and H. Ris.** 1967. How bacteriophage chi attacts motile bacteria. J. Vriol. **1:**599-609.

178. **Schlumberger, M. C., and W. D. Hardt.** 2006. *Salmonella* type III secretion effectors: pulling the host cell's strings. Curr. Opin. Microbiol. **9:**46-54.

179. **Seiler, N.** 2004. Catabolism of polyamines. Amino acids **26:**217-233.

180. **Selsted, M. E., S. I. Miller, A. H. Henschen, and A. J. Ouellette.** 1992. Enteric defensins: antibiotic peptide components of intestinal host defense. J. Cell. Biol. **118:**929-936.

181. **Shimada, T., N. Fujita, K. Yamamoto, and A. Ishihama.** 2011. Novel roles of cAMP receptor protein (CRP) in regulation of transport and metabolism of carbon sources. PLoS one **6:**e20081.

182. **Silversmith, R. E., and R. B. Bourret.** 1999. Throwing the switch in bacterial chemotaxis. Trends Microbiol. **7:**16-22.

183. **Skurnik, M., and E. Strauch.** 2006. Phage therapy: facts and fiction. Int. J. Med. Microbiol. **296:**5-14.

184. **Soncini, F. C., E. G. Vescovi, and E. A. Groisman.** 1995. Transcriptional autoregulation of the *Salmonella typhimurium phoPQ* operon. J. Bacteriol. **177:**4364-4371.

185. **Sonck, K. A., G. Kint, G. Schoofs, C. Vander Wauven, J. Vanderleyden, and S. C. De Keersmaecker.** 2009. The proteome of *Salmonella* Typhimurium grown under in vivo-mimicking conditions. Proteomics **9:**565-579.

186. **Stocker, B. A.** 1955. Bacteriophage and bacterial classification. J. Gen. Microbiol. **12:**375-381.

187. **Stout, V., and S. Gottesman.** 1990. RcsB and RcsC: a two-component regulator of capsule synthesis in Escherichia coli. J. Bacteriol. **172:**659-669.

188. **Sturgill, G., and P. N. Rather.** 2004. Evidence that putrescine acts as an extracellular signal required for swarming in *Proteus mirabilis*. Mol. Microbiol. **51:**437-446.

189. **Sulakvelidze, A., Z. Alavidze, and J. G. Morris, Jr.** 2001. Bacteriophage therapy. Antimicrob. Agents Chemother. **45:**649-659.

190. **Summers, W. C.** 2001. Bacteriophage therapy. Annu. Rev. Microbiol. **55:**437-451.

191. **Taffet, S. M., and M. K. Haddox.** 1985. Bacterial lipopolysaccharide induction of ornithine decarboxylase in the macrophage-like cell line RAW264: requirement of an inducible soluble factor. J. Cell. Physiol. **122:**215-220.

192. **Terauchi, T., S. Kojima, and M. Homma.** 2011. Structure and function of energy transduction protein complex of bacterial flagellar motor. Seikagaku **83:**822-833.

193. **Togashi, F., S. Yamaguchi, M. Kihara, S. I. Aizawa, and R. M. Macnab.** 1997. An extreme clockwise switch bias mutation in *fliG* of *Salmonella typhimurium* and its suppression by slow-motile mutations in *motA* and *motB*. J. Bacteriol. **179:**2994-3003.

194. **Tomljenovic-Berube, A. M., D. T. Mulder, M. D. Whiteside, F. S. Brinkman, and B. K. Coombes.** 2010. Identification of the regulatory logic controlling *Salmonella* pathoadaptation by the SsrA-SsrB two-component system. PLoS Genet. **6:**e1000875.

195. **Touz, M. C., A. S. Ropolo, M. R. Rivero, C. V. Vranych, J. T. Conrad, S. G. Svard, and T. E. Nash.** 2008. Arginine deiminase has multiple regulatory roles in the biology of *Giardia lamblia*. J. Cell. Sci. **121:**2930-2938.

196. **Twort, F. W.** 1915. An investigation on the nature of ultra-microscopic viruses. Lancet **2:**1241-1243.

197. **Valdez, Y., R. B. Ferreira, and B. B. Finlay.** 2009. Molecular mechanisms of *Salmonella* virulence and host resistance. Curr. Top. Microbiol. Immunol. **337:**93-127.

198. **Vazquez-Torres, A., and F. C. Fang.** 2001. Oxygen-dependent anti-*Salmonella* activity of macrophages. Trends Microbiol **9:**29-33.

199. **Vazquez-Torres, A., Y. Xu, J. Jones-Carson, D. W. Holden, S. M. Lucia, M. C. Dinauer, P. Mastroeni, and F. C. Fang.** 2000. *Salmonella* pathogenicity island 2-dependent evasion of the phagocyte NADPH oxidase. Science **287:**1655-1658.

200. **Waters, R. C., P. W. O'Toole, and K. A. Ryan.** 2007. The FliK protein and flagellar hook-length control. Protein Sci. **16:**769-780.

201. **Weber, C. J.** 2009. Update on *Salmonella* infection. Urologic nursing **29:**129-131.

202. **Wilson, R. L., S. J. Libby, A. M. Freet, J. D. Boddicker, T. F. Fahlen, and B. D. Jones.** 2001. Fis, a DNA nucleoid-associated protein, is involved in *Salmonella typhimurium* SPI-1 invasion gene expression. Mol. Microbiol. **39:**79-88.

203. **Winterhoff, N., R. Goethe, P. Gruening, M. Rohde, H. Kalisz, H. E. Smith, and P. Valentin-Weigand.** 2002. Identification and characterization of two temperature-induced surface-associated proteins of *Streptococcus suis* with high homologies to members of the Arginine Deiminase system of *Streptococcus pyogenes*. J. Bacteriol. **184:**6768-6776.

204. **Witthoft, T., L. Eckmann, J. M. Kim, and M. F. Kagnoff.** 1998. Enteroinvasive bacteria directly activate expression of iNOS and NO production in human colon epithelial cells. Am. J. Physiol. **275:**G564-571.

205. **Wu, D., D. Van Valen, Q. C. Hu, and R. Phillips.** 2010. Ion-dependent dynamics of DNA ejections for bacteriophage lambda. Biophys. J. **99:**1101-1109.

206. **Yamaguchi, S., S. Aizawa, M. Kihara, M. Isomura, C. J. Jones, and R. M. Macnab.** 1986. Genetic evidence for a switching and energy-transducing complex in the flagellar motor of *Salmonella typhimurium*. J. Bacteriol. **168:**1172-1179.

207. **Yamashita, I., K. Hasegawa, H. Suzuki, F. Vonderviszt, Y. Mimori-Kiyosue, and K. Namba.** 1998. Structure and switching of bacterial flagellar filaments studied by X-ray fiber diffraction (vol 5, pg 125, 1998). Nat. Struct. Biol. **5:**612-612.

208. **Yoon, H. J., J. E. McDermott, S. Porwollik, M. McClelland, and F. Heffron.** 2009. Coordinated regulation of virulence during systemic infection of *Salmonella enterica* serovar Typhimurium. PLoS Pathog. **5**.

209. **Zheng, S. A., C. M. McElwain, and S. M. Taffet.** 1991. Regulation of mouse ornithine decarboxylase gene expression in a macrophage-like cell line: synergistic induction by bacterial lipopolysaccharide and cAMP. Biochem. Biophys. Res. Commun. **175:**48-54.

210. **Zinkernagel, A. S., R. S. Johnson, and V. Nizet.** 2007. Hypoxia inducible factor (HIF) function in innate immunity and infection. J. Mol. Med-Jmm **85:**1339-1346.

211. **Zuniga, M., M. Champomier-Verges, M. Zagorec, and G. Perez-Martinez.** 1998. Structural and functional analysis of the gene

cluster encoding the enzymes of the arginine deiminase pathway of *Lactobacillus sake*. J. Bacteriol. **180:**4154-4159.

212. **Zuniga, M., G. Perez, and F. Gonzalez-Candelas.** 2002. Evolution of arginine deiminase (ADI) pathway genes. Mol. Phylogenet. Evol. **25:**429-444.

국문초록

Salmonella 는 설사, 복통, 구토 등 가벼운 증상부터 장티푸스와 같은 질환에 이르기까지 다양한 병을 일으키는 원인 균으로서, 동물에서 사람까지 다양한 숙주를 대상으로 감염된다. 이미 *Salmonella* 의 병원성 메커니즘에 대한 많은 연구가 진행되어왔지만, 아직까지 알려지지 않은 새로운 병원성 인자들에 대한 연구가 필요하다. 또한 직접적인 제어 방법으로서 그 중요성이 재조명 받고 있는 박테리오파지에 대한 연구 또한 *Salmonella* 를 제어하는데 기여를 할 것이다. 본 연구에서는 *Salmonella* 의 병원성과 관련된 새로운 인자를 규명하고 그 조절 메커니즘에 대한 연구를 수행하였으며, 박테리오파지의 새로운 감염 메커니즘에 대해 연구하였다. 본 저자는 *Salmonella* 가 숙주의 세포 내에서 살아남아 병을 일으키는데 중요한 역할을 할 것이라 예상되는 유전자를 *Mycobacterium tuberculosis* 와의 단백질 서열 상동성의 비교를 통해 확보하였다. 그 중 arginine deiminase 를 합성하는 유전자인 *STM4467* 을 선택하고 이를 대상으로 후속 연구를 진행하였다.

Arginine deiminase (ADI), ornithine carbamoyltransferase (OTC), 그리고 carbamate kinase (CK)는 ADI 시스템 구성하며, 혐기성의 조건에서

arginine 을 이용하여 에너지 (ATP)를 생성하는 역할을 하는 대사과정이다. 많은 박테리아에서 그 존재가 확인되었고, 역할과 기능들이 밝혀져 있지만, *Salmonella* Typhimurium 에서는 아직까지 그 기능에 대해 연구된 바가 없었다. 따라서 먼저 *STM4467* 유전자가 ADI 단백질을 합성하는 것을 확인하였으며, 기존에 알려진 발현 조건인 혐기성 조건과, 기질로서 과량으로 존재하는 arginine 에 의해 그 발현이 증가하였다.

분자 유전학적 수준에서 유전자 발현을 확인하기 위해 ADI 오페론을 분석하였다. *Salmonella* 의 ADI 오페론은 *STM4467*, *STM4466*, *STM4465*, *STM4464* 의 총 4 개의 유전자로 이루어졌으며, 프로모터에는 2 개의 전사시작 위치를 갖고 있었다. 그 중 CRP-binding site (CBS)를 포함하는 상위 프로모터가 CRP 와 STM4463 에 의해 조절을 받았다. STM4463 은 활성인자로서 ADI 의 발현을 증가시켰으며, CRP 에 의존적인 조절을 확인하였다. CRP 는 ADI 의 상위 프로모터에 직접적으로 결합하여 ADI 의 발현에 있어 RNA polymerase 가 결합을 하는데 중요한 역할을 하는 것으로 예상된다. CRP 는 ADI 뿐만 아니라 활성인자인 STM4463 의 발현을 DNA 에 직접 작용하여 조절하는 것을 확인하였다. ADI 의 발현 패턴이 STM4463 의

발현 패턴과 동일한 것을 통해 ADI 의 발현 조절은 STM4463 에 절대적으로 의존하는 것임을 알 수 있었다. 또한 DNA 결합 단백질인 Fis 가 STM4463 의 발현을 억제하는 조절함을 통해서 ADI 의 발현에 영향을 주는 것을 확인하였다. 이러한 전사조절은 상위 조절자인 ArcA 가 polyamine 을 signal 로 하여 그 활성이 증가고 이에 따라 Fis 를 억제함으로써 최종적으로 ADI 의 발현이 증가되는 것임을 알 수 있었다.

또한 *Salmonella* 에서 ADI 활성이 병원성에 중요한 역할을 하는 것을 확인하였다. *STM4467* 유전자가 결여된 균주는 대식세포 내에서 생존 및 성장을 할 수 없었고, 쥐에서도 그 병원성이 매우 감소되는 것을 알 수 있었다. 대식세포 내에서 ADI 유전자들의 발현이 STM4463 의 조절 하에 증가하는 것을 확인하였고, 따라서 *STM4463* 유전자가 결여된 균주도 ADI 의 발현이 증가할 수 없기 때문에 대식세포 내에서 생존 및 성장을 할 수 없었다. ADI 와 동일하게 arginine 을 기질로 하는 iNOS 와 경쟁을 통할 것으로 예상을 하였지만, *STM4467* 유전자가 결여된 균주는 대식세포 내에서 정상적인 nitric oxide 생산을 보였다.

Salmonella 를 숙주로 하는 박테리오파지인 iEPS5 를 분리하고 그 특성을 분석하였다. iEPS5 는 정이십면체의 머리와 비수축성 꼬리를 갖는 구조로서 *Siphoviridae* 에 속한다. 게놈 시퀀싱을 통해 59,254 bps 의 dsDNA 를 유전체로 갖고 있으며, 75 개의 ORF 를 확인하였다.

박테리오파지의 리셉터를 찾기 위해, iEPS5 에 저항성을 보이는 돌연변이 균주를 *Salmonella* random mutant library 에서 선별하였다. iEPS5 에 저항성을 보이는 돌연변이 균주들은 모두 편모를 합성하는 유전자에 돌연변이가 있었으며, 이를 통해 iEPS5 의 receptor 는 편모임을 알 수 있었다. 운동성에 중요한 유전자인 *motA* 가 결여된 균주를 통해 편모가 운동성을 가질 때에만 iEPS5 가 편모에 결합하여 감염을 일으키는 것을 확인하였다. 또한 chemotaxis 유전자가 결여된 돌연변이 균주 (*ΔcheY*, SJW2811, SJW3076)를 통해 iEPS5 는 반 시계방향 (CCW)으로 회전하는 편모에 특이적으로 부착하여 숙주에 감염하는 것을 알 수 있었다. 편모의 filament 가 없이 긴 hook 을 갖는 polyhook 균주 (*ΔfliK*)가 iEPS5 에 저항성을 나타내는 것을 통해 iEPS5 가 감염을 하는데 있어, 편모의 구조 중 filament 가 중요하다는 것을 유추할 수 있었다. 마지막으로 DNA 에 결합하는

형광물질로 박테리오파지의 DNA 를 염색하여 박테리오파지가 감염하여 DNA 가 이동하는 것을 확인하였고, 이를 통해 iEPS5 는 편모와 상호작용을 하여 결합을 하고, 결과적으로 DNA 를 편모의 filament 로 주입하여 감염을 일으키는 메커니즘을 제시할 수 있었다.

핵심어: 살모넬라 티피뮤리움(*Salmonella* Typhimurium), Arginine deiminase 기작, 병원성, 박테리오파지, 리셉터, 편모, 파지 생물학적 방제 (biocontrol)

학 번: 2007-21394